LA-DC — 11039

EANDC(US) - 134 A
INDC(USA) - 15 G
September, 1969

INDC-322

PREPRINT FROM

LOS ALAMOS SCIENTIFIC LABORATORY of the University of California

LOS ALAMOS • NEW MEXICO

NUCLEAR PHYSICS STUDIES WITH FAST NEUTRONS: A SURVEY

By

John C. Hopkins

UNITED STATES
ATOMIC ENERGY COMMISSION
CONTRACT W-7405-ENG. 36

90

LA-DC – 11039 September, 1969

PREPRINT FROM

LOS ALAMOS SCIENTIFIC LABORATORY
of the
University of California

LOS ALAMOS • NEW MEXICO

NUCLEAR PHYSICS STUDIES WITH FAST NEUTRONS:

A SURVEY

By

John C. Hopkins

UNITED STATES
ATOMIC ENERGY COMMISSION
CONTRACT W-7405-ENG. 36

NUCLEAR PHYSICS STUDIES WITH FAST NEUTRONS:

A SURVEY

John C. Hopkins

Los Alamos Scientific Laboratory, University of California

Los Alamos New Mexico

TABLE OF CONTENTS

NUCLEAR PHYSICS STUDIES WITH FAST NEUTRONS:

A SURVEY

John C. Hopkins

ABSTRACT

A survey of recent nuclear physics experiments with fast neutrons is presented. The survey is limited to those studies involving a neutron, with an energy greater than 0.5 MeV, in the entrance channel. Neutron capture is specifically excluded. The first part gives descriptions of 6 representative fast-neutron experimental techniques or facilities. In the second part, 11 specific fields are identified and reviewed. The fields are: (1) the nucleon-nucleon interaction, (2) total cross sections, (3) fluctuation phenomena, (4) elastic and inelastic scattering, (5) (n,2n) cross sections, (6) (n,charged particle) cross sections, (7) (n,xγ) cross sections, (8) polarization, (9) electromagnetic neutron-nucleus interactions, (10) fission, and (11) high-energy phenomena. The final section contains a few brief comments regarding the directions that fast-neutron physics research may take in the future.

NUCLEAR PHYSICS STUDIES WITH FAST NEUTRONS:

A SURVEY

John C. Hopkins

I. INTRODUCTION

This report is a survey of the field of fast-neutron experimental nuclear physics. The one subject that has been intentionally omitted is neutron capture. The investigations to be included involve reactions with a fast (E_n > 0.5 MeV) neutron in the entrance channel.

First, the experimental situation will be discussed. This section will explain how fast-neutron experiments are done now, using well-known and accepted methods. New procedures or state-of-the-art techniques will not be discussed. Following this, the various fields of endeavor will be surveyed. Eleven different specialties have been identified, and the aims, present status, and general direction of each will be covered.

There are two objectives: one is to provide the nuclear physicist, who is not engaged in fast-neutron physics, with a general review. The other is to supply a sufficiently complete bibliography to provide a starting point for further, more detailed study.

II. EXPERIMENTAL

The methods and techniques employed in fast-neutron experiments will now be discussed. Some level of understanding of the mechanics of actually doing experiments is necessary for an appreciation of the history and evolution of this particular field. First, the structure and mode of operation of a typical fast-neutron time-of-flight facility will be described in some detail. Following this, five other fast-neutron facilities will be described. This selection of examples covers the field of modern fast-neutron physics laboratories fairly well.

It should be emphasized that this discussion concerns typical techniques in use now, not state-of-the-art experiments. Some of the hardware and ideas are older than the physicists using them.

II-1. Los Alamos Van de Graaff and Tandem Time-of-Flight Facilities

Naturally the Los Alamos Scientific Laboratory (LASL) time-of-flight facilities have been chosen as the main example. They have two accelerators and two neutron areas.

One accelerator is a twenty-year-old 8-MeV Van de Graaff handmade by J. L. McKibben. The other is a 1963-vintage 15-MeV HVEC tandem. There is a Mobley beam-bunching system on the Van de Graaff (known locally as the "Vertical"), and a klystron bunching system on the tandem. The Vertical can be used to inject a negative beam into the tandem, with a resultant proton energy of $\sim$23 MeV. Under these conditions, however, there is no beam compression.

They have a wide variety of particles at their disposal, but since the subject under discussion is neutron physics, the remarks will be restricted to the hydrogen beams, i.e., protons, deuterons, and tritons.

With this brief summary, we will go back and examine some of the details.

Figure 1 shows schematically the time-of-flight area associated with the Vertical Van de Graaff. A 300-μA proton or deuteron beam from a McKibben duoplasmatron ion source is chopped in the high-voltage head. At the output of the machine there are 10-nsec long bursts every 500 nsec with an average beam current of 4 μA.

The 10-nsec long beam bursts are bunched in time by requiring that the leading edge of a burst take a longer flight path to the target than the middle of the burst, which in turn takes a longer path than the trailing edge. The geometry and sweeping voltages are adjusted to make all parts of the burst arrive at the target simultaneously. Of course, aberrations render the arrival not fully simultaneous. In this case, the usual spread of arrival times is 0.8 nsec. This time can be reduced somewhat at the expense of beam current. Average operation results in about 2.5 μamp on target at a 2-MHz rate. The Los Alamos system, as it originally existed, is described in some detail by Cranberg et al. (Cr 61).

There are many other ways to get pulsed beams. Grodzins, Rose, and Van de Graaff reviewed the various techniques in 1965 (Gr 65).

Probably none of the other methods are as good as klystron bunching (An 64, Da 64). This is done at low energies and is particularly adaptable to tandem accelerators where the ion source is outside. The idea is that the ion source beam, at energies of about 100 keV, is chopped with R. F. deflection. The beam pulses are then sent through a gap to an insulated region connected to an R. F. oscillator. The oscillator is phased in such a way that the leading edge of the beam pulse is slowed down and the trailing edge is accelerated. That is to say, it modulates the energy of the beam pulse with the result that the front end has a lower velocity than the trailing

Fig. 1. A schematic diagram of the fast-neutron time-of-flight area associated with the vertical Van de Graaff.

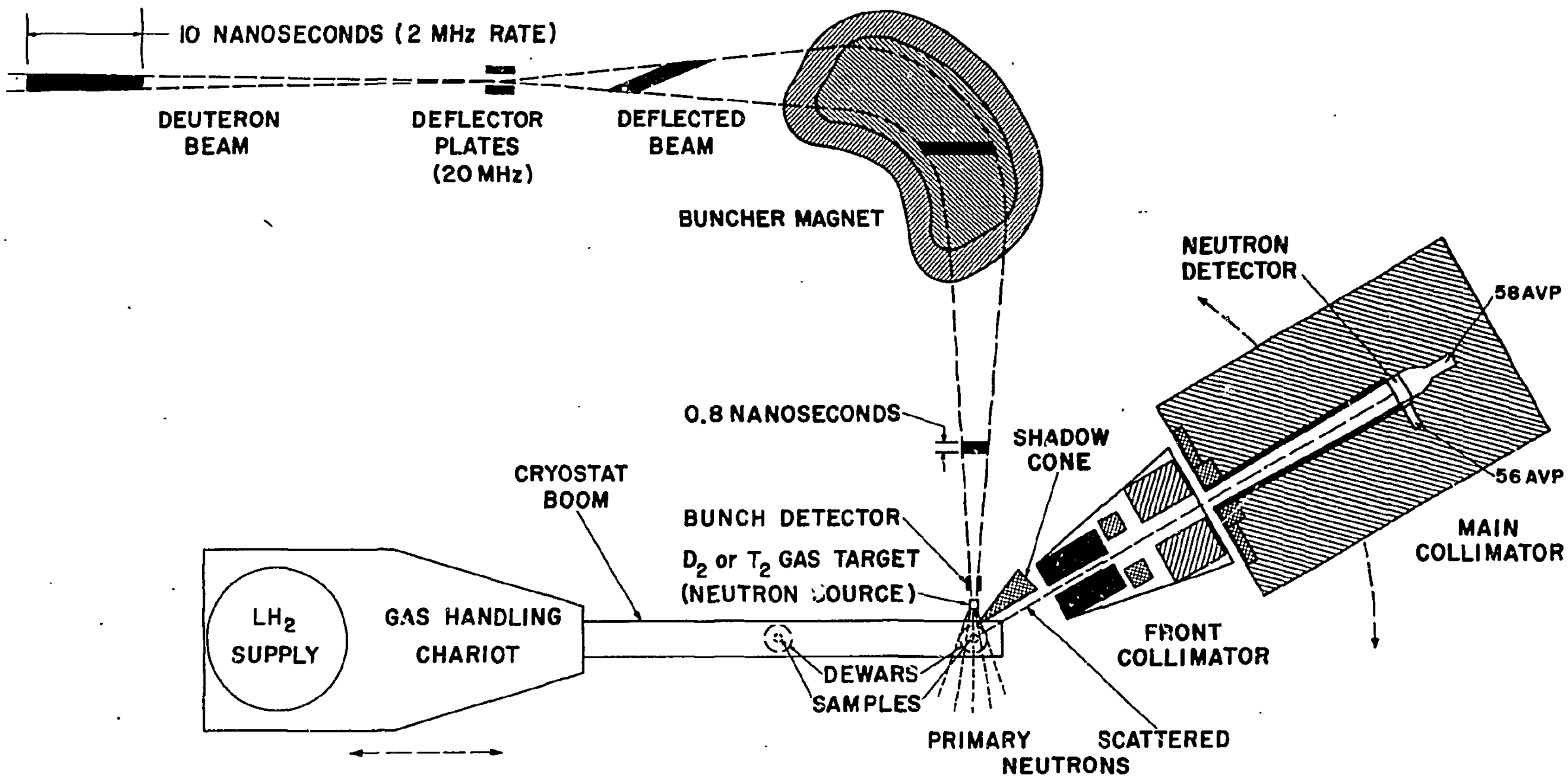

TIME-OF-FLIGHT APPARATUS
LIQUID TRITIUM EXPERIMENT

Fig. 1.

edge. The R. F. amplitude is appropriately chosen such that all parts of the pulse arrive at the target almost simultaneously. Most of the bunching actually takes place at low energy. The pulse travels several meters between the R. F. gap and the entrance to the machine.

Such a system is installed on the LASL tandem accelerator and yields a beam of 1-2 μA on target, $\Delta t < 1$ nsec, with a repetition rate of 5 MHz. The energy modulation is only a few keV.

The advantage of a klystron buncher is that a pulsed beam can be sent down any beam tube. The disadvantage is that the beam is modulated in energy.

The advantage of Mobley bunching is that there is very little energy modulation of the beam. The disadvantage is that the sweeping action builds in a large convergence (5° at LASL) in the beam and this leads to a kinematic energy spread in the reaction products.

We now have a pulsed beam of protons or deuterons impinging upon a target. The purpose of the target, of course, is to make short bursts of neutrons. The standard treatise on the subject was written by Brolley and Fowler in 1960 (Br 60). Their article is highly recommended, along with several others (Co 67a, Co 60) for a complete picture. Only the reactions that are used at LASL now will be discussed; i.e., $T(p,n)^3He$, the $D(d,n)^3He$, and the $T(d,n)^4He$.

Figure 2 shows the cross sections for the various reactions of interest. The $T(p,n)^3He$ reaction, with a Q of -0.764 MeV, is used exclusively on the tandem. That reaction yields a clean beam of neutrons with the forward energies approximately 1 MeV below that of the incident proton. Clean, in the sense used here, means that there is little contamination of the beam with neutrons of different (usually lower) energies. This is because protons do not make as much background radiation when they graze slits or strike beam stops as do deuterons. Neutrons from the breakup reactions of protons on tritium do not appear to be a problem for neutron energies up to 12 MeV.

Exothermic reactions such as $D(d,n)^3He$ with a Q of +3.266 MeV and the $T(d,n)^4He$ reaction with a Q of +17.586 MeV are required to obtain high-energy neutrons with low-energy machines. The last reaction yields copious quantities of 14-MeV neutrons when bombarded by ~100-keV deuterons. This, of course, accounts for all of the experiments at 14 MeV.

The $D(d,n)^3He$ reaction is used as a neutron source on the Van de Graaff accelerator for neutrons with energies between 5 and 7 or 8 MeV. Above that energy the D(d,np)D breakup reaction contributes too much beam contamination.

With 4-5 MeV incident deuterons, 21-22 MeV neutrons can be produced using the $T(d,n)^4He$ reaction. In this case, the neutrons emanating from the breakup reaction may not be as bothersome because of their low energy relative to the primary beam. This must be considered separately for each application.

Deuchars, Perkin, and Batchelor (De 63) have pointed out the advantages of the $^1H(t,n)^3He$ reaction. This, of course, is only available at those installations that accelerate tritium. The two most important advantages are the fact that all neutrons are emitted in the forward direction and that the zero degree neutron flux is greater than that obtained using the $T(p,n)^3He$ reaction, with the same incident beam current.

These targets are usually in the gaseous phase, separated from the machine by a thin foil of molybdenum, or some such suitable material. Here problems arise regarding the energy resolution. It is desirable to have the maximum amount of gas to obtain the maximum neutron flux. On the other hand, this must be paid for in increased neutron energy spread for two reasons: (1) More gas means more energy loss in the target itself, and (2) more gas pressure requires thicker foils and consequently more energy straggling in the foils. It is very difficult to get below a few tens of keV energy spread in the

Fig. 2. The cross sections for neutron production at zero degrees for various reactions of interest.

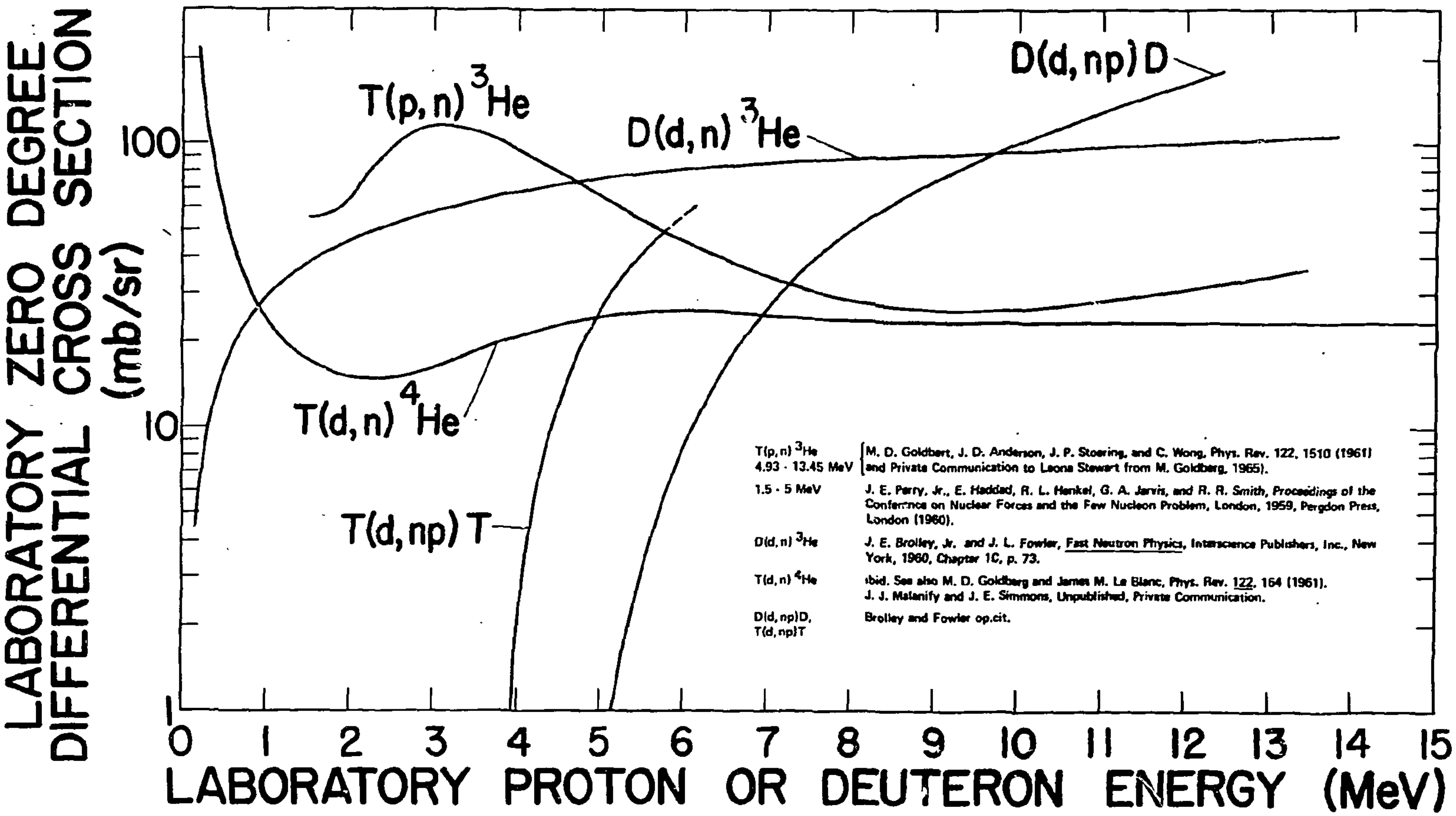

LABORATORY ZERO DEGREE DIFFERENTIAL CROSS SECTION (mb/sr)
100
10
1
0 1 2 3 4 5 6 7 8 9 10 11 12 13 14 15
LABORATORY PROTON OR DEUTERON ENERGY (MeV)
T(p,n) 3He
D(d,n) 3He
D(d,np)D
T(d,n) 4He
T(d,np)T
T(p,n) 3He 4.93 - 13.45 MeV
M. D. Goldbert, J. D. Anderson, J. P. Stoering, and C. Wong, Phys. Rev. 122, 1510 (1961) and Private Communication to Leona Stewart from M. Goldberg, 1965).
1.5 - 5 MeV
J. E. Perry, Jr., E. Haddad, R. L. Henkel, G. A. Jarvis, and R. R. Smith, Proceedings of the Conference on Nuclear Forces and the Few Nucleon Problem, London, 1959, Pergdon Press, London (1960).
D(d,n) 3He
J. E. Brolley, Jr. and J. L. Fowler, Fast Neutron Physics, Interscience Publishers, Inc., New York, 1960, Chapter 1C, p. 73.
T(d,n) 4He
ibid. See also M. D. Goldberg and James M. Le Blanc, Phys. Rev. 122, 164 (1961).
J. J. Malanify and J. E. Simmons, Unpublished, Private Communication.
D(d,np)D, T(d,np)T
Brolley and Fowler op.cit.

Fig. 2

neutron beam and still maintain a usable flux.

One very desirable feature of these reactions is that polarized neutrons can be obtained by just looking at angles other than zero degrees to the incident beam direction. One example is shown in Fig. 3, adapted from a similar plot presented by Barschall (Ba 65), for the polarization of the neutrons produced in the $T(d,n)^4He$ reaction.

All three reactions yield polarizations of varying degrees. They are not, however, as well known as the $T(d,n)^4He$ polarizations. Walter et al. have studied the polarizations produced in the $T(p,n)^3He$ reaction (Wa 62) at forward angles. Many groups have looked into the polarizations produced in the $D(d,n)^3He$ reaction (Hu 53, Le 57a, Pa 58, Tr 68, Dr 69c).

The next few pages will be devoted to a discussion of what is known about the neutron beam. Specifically how are the energy and the flux determined? The energy will be discussed first.

The technique that is usually employed to measure the energy is to analyze the charged-particle beam with a bending magnet containing a NMR unit somewhere in the "average" magnetic field. The NMR signal is calibrated using some convenient threshold reactions (Ma 66b). For a threshold of energy E observed at NMR frequency, f, the calibration factor is given by (Da 68b)

$$k(f) = \frac{M_o E}{f^2 q^2} \left(1 + E/(2M_o C^2)\right) ,$$

where M_o and q are the rest mass and charge of the bombarding particle, respectively. Most magnets are calibrated in such a way that the actual beam energy is know only to an accuracy of 20 to 40 keV. Usually this is not of much consequence to fast-neutron physics, where the neutron beam energy spread is 5 times this uncertainty. Also, if there is not much structure in the observed reaction, then an accurate knowledge of the energy is not important.

On the other hand, in many cases there is structure and a good energy determination is important. To get the best determinations, several methods should be used. Davis and Noda at Wisconsin (Da 68) have successfully used the threshold technique and the locations of resonance peaks to determine their energies with an accuracy of 0.1%.

A technique for precisely measuring the energy of a charged-particle beam to 1 part in 10^4 (i.e., 0.01%) was developed at LASL (Se 64a). This, however, is more precision than can be used for neutron work.

Now the flux measurements will be discussed.

For some measurements, for example neutron elastic and inelastic scattering, a knowledge of the actual flux is not necessary. This is because cross sections are measured relative to some well-known cross section such as the ^{12}C elastic scattering cross section or the n-p cross section. On the other hand, the runs do require a normalization. This could be accomplished with a well-designed Faraday cup. In practice this is not usually done since it is desirable to keep the mass to a minimum in the region of the target and it is difficult to minimize mass and volume and come up with a completely satisfactory beam monitor.

At LASL one or more plastic scintillators that view the neutron source directly are used to normalize runs. These are operated in the standard time-of-flight mode.

Some experiments, such as the gamma-ray production determinations, require a flux measurement. For these situations, proton recoil telescopes are usually used (Ba 57, Ba 60a, Ho 67c, Li 69a). There are, however, many other ways to measure neutron fluxes, and this whole subject was recently reviewed by Batchelor (Ba 68c). Since that review, Liskien and Paulsen have made

Fig. 3. Contour plot of the percent polarization (solid lines) and the energy (dashed lines) of neutrons from the $T(d,n)^4He$ reaction. Adapted from a similar plot by Barschall (Ba 65).

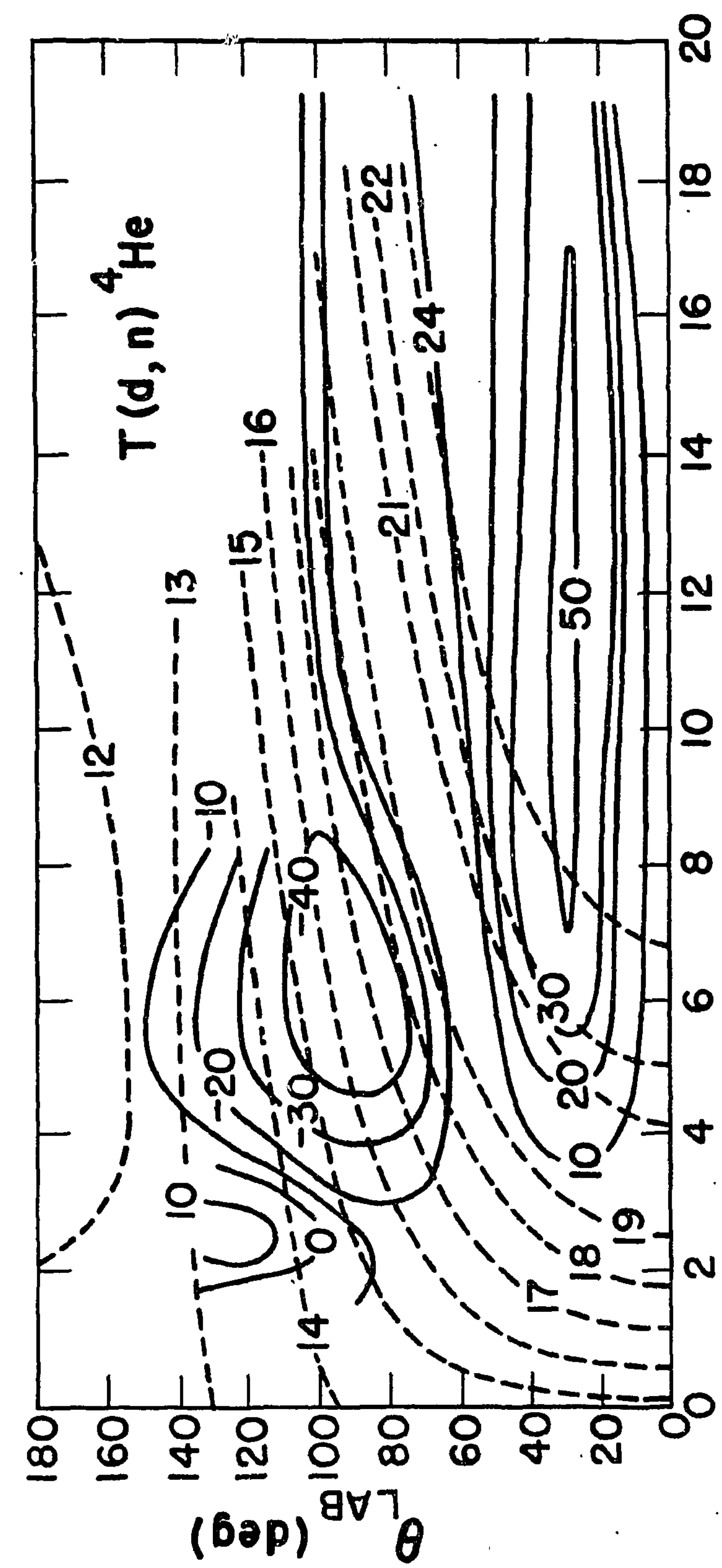

Fig. 3

some contributions to the associated particle technique (Li 69b).

The scattering samples will now be described. At this point, some terms will be defined.

The <u>target</u> will be defined as that piece of apparatus or material bombarded by the charged-particle beam. It is the source of neutrons.

The object bombarded by the neutrons is the <u>scattering sample</u>. This is the material under study.

With a monoenergetic neutron source, and the scattering sample near the source, the energies of the neutrons after scattering are measured. With the so-called white source (e.g., a bomb source), the sample is placed near the counters and energy separation of the incident beam is achieved by time-of-flight techniques.

In the situation described here, the sample is placed as close to the source as possible. There are two limitations to this distance. The first is that detectors must be shielded from the direct source neutrons. The second is that angular resolution is sacrificed as the target sample distance is decreased.

The LASL scattering samples are usually right circular cylinders with an o.d. of $\sim$1.5 cm and a length of $\sim$2 cm. They are placed 8-10 cm from the target, at 0° to the incident-beam direction if the experiment does not involve a polarization measurement.

Multiple scattering and attenuation corrections provide a limitation on the size of a scattering sample. An attempt is made to keep the neutron attenuation corrections below 15%. For gamma-ray production measurement, with high Z materials, such as plutonium or tungsten, the gamma-ray attenuation is very severe. In these cases, thin walled cylinders are used and measurements are made with various thicknesses to check on the accuracy of the corrections. These corrections will be examined in more detail when the data handling procedures are discussed.

It was mentioned that the detector must be shielded from the direct target neutrons. The guide lines are really quite simple and are demonstrated in Fig. 4. The detectors are placed at a convenient distance to obtain the optimum compromise between counting rate and energy resolution. Then all space between the target and detector is filled with suitable shielding materials. Tungsten and copper are the best above about 4 MeV (Ho 67b), the shielding effect being primarily due to the nonelastic cross sections.

With the exception of an axial hole, the detector is surrounded in order to shield it from room-scattered neutrons. The surrounding materials is mostly polyethylene, since the room-scattered neutrons have been degraded in energy. The material in a direct line between target and detector is copper and tungsten. Brass and iron are definitely inferior. The front section, called the shadow bar, must not intercept neutrons between the target and sample or between the sample and detector. Also, the front of the shadow bar, which could act as a scattering sample, must not be visible to the detector. Actually the optimum shadow bar position describes a rather complicated locus as a function of detector angle. This has been analyzed in some detail and techniques have been developed to automatically position the shadow bar in the optimum position (Ho 67e).

The detector shields, with shadow bars, weigh between 3000 and 4000 kilograms. These are used for elastic and inelastic scattering studies with incident neutron energies between 3 and 23 MeV.

The flight paths are normally about 2-3 m. This distance could not be decreased because of the shielding requirements. Beam intensity limitations would not normally make greater distances worthwhile.

The detectors are liquid sintillators (NE 213 or NE 218, manufactured by Nuclear Enterprises, Inc.) coupled to 13-cm high-gain photomultiplier tubes. The scintillators are 13 cm in diameter with thicknesses determined by the time resolution desired. For experiments involving neutron energies above 8 MeV, neutron-gamma ray discrimination techniques are used (Da 61, Ro 64).

Fig. 4. Schematic plan view of the use of a shadow bar.

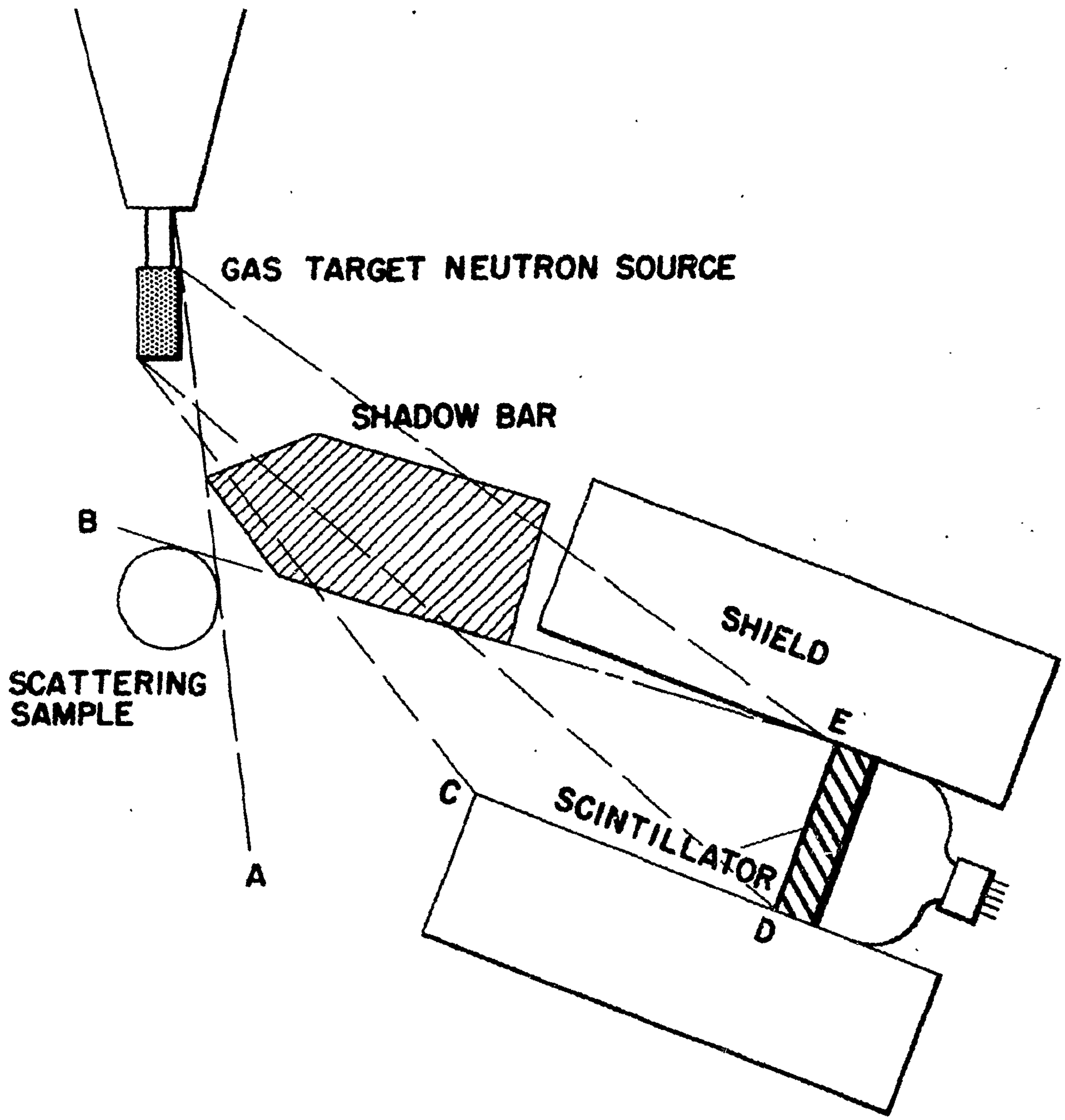
GAS TARGET NEUTRON SOURCE
SHADOW BAR
B
SCATTERING
SAMPLE
SHIELD
E
C
SCINTILLATOR
A
D

Fig. 4

From these detectors two fast signals are derived for timing purposes: a linear signal for recoil energy information, and an additional signal (positive for neutrons, negative for gamma rays) that identifies the detected particle. The contribution to the time resolution from the electronic time spread is very small compared to such things as beam burst length, neutron energy spread, and kinematic broadening at the sample.

The relative efficiency of the neutron detectors must be determined. This can be measured and calculated. The relative efficiency can be experimentally determined by measuring the relative angular distribution of neutrons scattered from protons and using the known differential cross section (Table I, Section III-1) to deduce the relative efficiency. It can also be determined by measuring the angular distribution of neutrons from a source reaction, such as $T(p,n)^3He$, and comparing the results with measurements of the reactions obtained using calibrated counters (Wi 61, Go 61). Figure 5 shows an example of a relative efficiency curve obtained using these techniques (Ho 68c).

There are a number of calculations of neutron detection efficiency with varying degrees of sophistication (Ba 61c, Dr 62, Wi 62, Cz 64, Ho 67d).

If the detector is thin and only neutron-proton collisions occur, then the efficiency for neutrons of energy E is given by

$$\varepsilon_1(E) = n_H \; \varepsilon_H \; (E) \; L(1 - \frac{B}{E}) \; .$$

L is the length of the scintillator, n_H is the number of hydrogen atoms per unit volume, $\sigma_H(E)$ is the n-p total cross section, and B is the proton energy corresponding to the bias pulse height. The general shape of relative efficiency vs E curve is

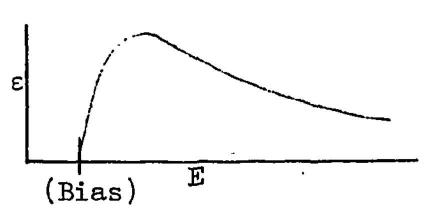

A number of refinements can be considered. These include (Dr 62):

1) attenuation of neutron flux,

2) production of recoil protons after a single scattering from a carbon nucleus,

3) production of a second recoil proton after a single scattering from hydrogen,

4) carbon nonelastic scattering,

5) angular distribution of the n-p cross sections.

The electronics will now be discussed briefly.

A block diagram giving only the barest of essentials looks like this.

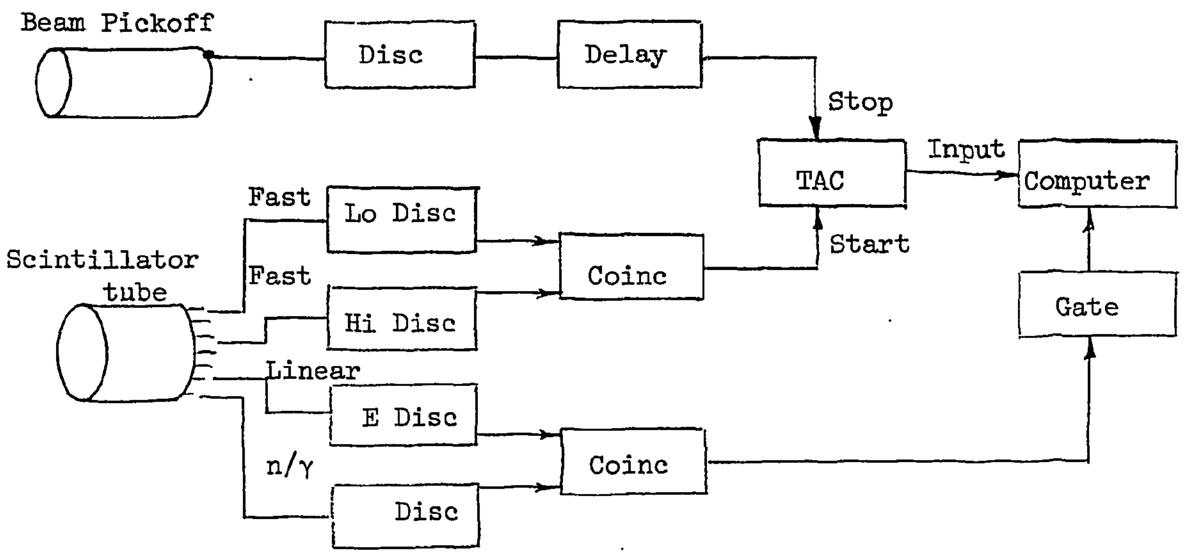

The pulsed beam passes through the insulated pickoff cylinder pictured schematically. The resultant signal is fed to a TAC (time-to-amplitude converter). The linear energy discriminator level corresponds to higher-energy particles than either of the two fast discriminators. The fast discriminator marked "Lo" is set to an extremely low level to obtain good timing. All timing is done on this signal. The fast discriminator marked "Hi" is only to reduce the counting rate.

Fig. 5. The relative efficiency or sensitivity of a neutron detector as a function of neutron energy.

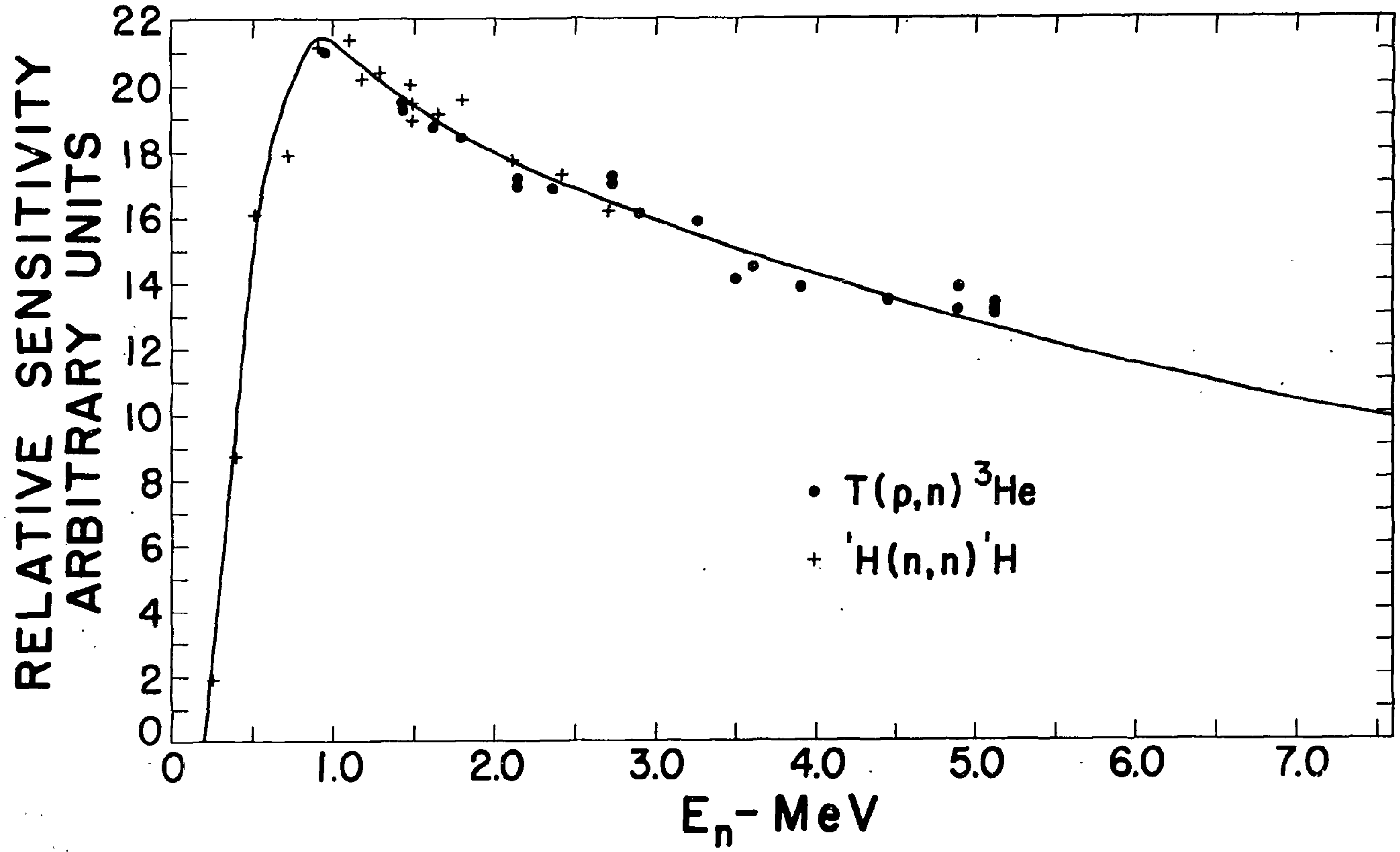
RELATIVE SENSITIVITY
ARBITRARY UNITS
22
20
18
16
14
12
10
8
6
4
2
0
0
1.0
2.0
3.0
4.0
5.0
6.0
7.0
E_n - MeV
• T(p,n) ^{3}He
+ ^{1}H(n,n)^{1}H

Fig. 5

The linear and n/γ coincidence is used to gate the computer on. These signals insure that the recorded signal corresponded to a neutron with the appropriate energy.

The computer is an on-line SDS 930 (Le 69, Ke 69) with a core memory of 24 K,* 24 bit words, and a disc storage with a 500-K word capacity.

The on-line computer is used as a pulse-height analyzer with the capability of doing a small amount of preliminary data reduction. Most of the data reduction, however, is done off-line with a CDC-6600 computer.

Consider now a differential scattering cross section measurement relative to the n-p standard. The cross section in the laboratory system is given as

$$\sigma_S(\theta) = \sigma_{np}(\theta) \left\{ \frac{n_H}{n_S} \quad \frac{f_S(E)\frac{N_S}{(E_S)}}{f_H(E)\frac{N_H}{(E_H)}} \right\} .$$

$\sigma_{np}(\theta)$ is the n-p differential standard cross section (see Table 1 of Section III-1).

n_H and n_S are the total number of hydrogen and sample nuclei, respectively.

$f_H(E)$ and $f_S(E)$ are attenuation and multiple scattering corrections for the hydrogen and sample, respectively.

N_H and N_S are counts (with background subtracted) for hydrogen and the sample, respectively.

$\varepsilon(E_H)$ and $\varepsilon(E_S)$ are the relative efficiencies for the detection of scattered neutron of energy E_H and E_S, respectively.

The n-p differential cross section will be examined in more detail in Section III. The multiple scattering and attenuation correction, f(E), will

*In this sense, 1 K is 1024 words.

now be discussed briefly.

If the attenuation corrections are less than about 15%, then the approximate procedure developed by Levin at LASL is suitable (Cr 59) for the evaluation of f(E). This is only an attenuation correction and does not account for multiple scattering, which tends to wash out the peaks and fill in the valleys.

The Aldermaston MAGGIE code is used for the multiple-scattering corrections (Pa 61, Pa 64b). This is a Monte Carlo program which also corrects for the effects of flux attenuation and for the angular spread of neutrons incident on a cylindrical sample. The advantage of using a code such as MAGGIE is that large (e.g., 1/3 mean free path thick) scattering samples may be used with some confidence that the appropriate corrections can be obtained.

There are a variety of other correctional codes, both analytic and Monte Carlo in use throughout the world (Co 67b, La 62, Sm 67, Ho 67a, Pe 68).

The techniques employed in the polarization measurements at LASL will now be described.

Figure 6 shows an elevation view of J. E. Simmons' apparatus for measuring the neutron source polarization (Si 69). Whatever polarization exists will be in the plane of the figure, normal to the direction of motion. The purpose of the solenoid is to precess the spin of the neutron 90° so that it is perpendicular to the plane of the figure (Ha 63a).

The neutrons then scatter from a liquid-^{4}He scintillator S-1 and are detected by plastic scintillators S-2 and S-3. Assume that $\theta_2 = \theta_3$. The polarization of the indicent beam at angle θ is

$$P(\theta_1) = \frac{1}{P_{He}(\theta_2)} \frac{N_{S-3} - N_{S-2}}{N_{S-3} + N_{S-2}} \quad .$$

Fig. 6. Schematic elevation view of apparatus for measuring the neutron source polarization (Si 69). See text for details.

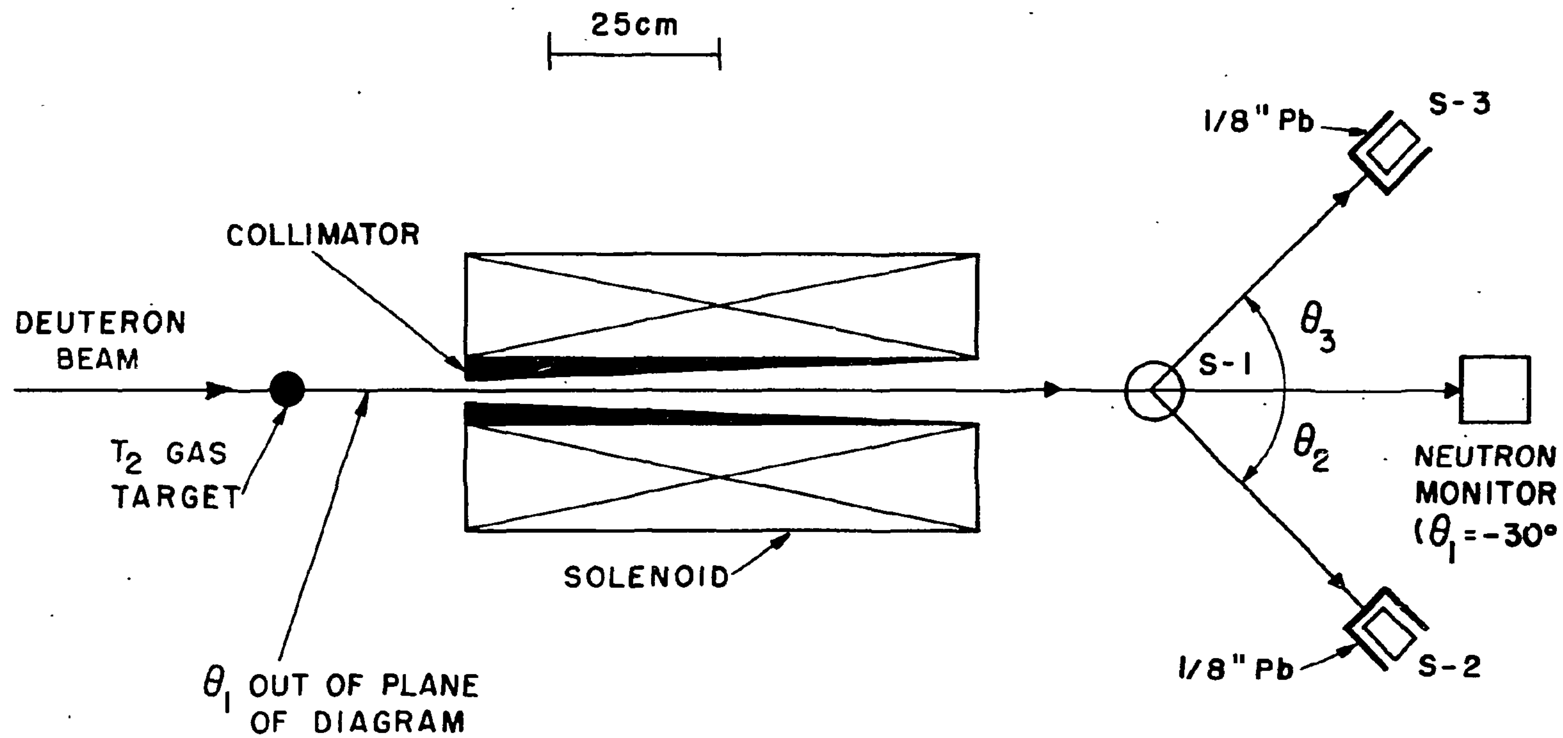
25cm
COLLIMATOR
DEUTERON
BEAM
T_2 GAS
TARGET
SOLENOID
θ_1 OUT OF PLANE
OF DIAGRAM
1/8" Pb
S-3
S-1
θ_3
θ_2
NEUTRON
MONITOR
(θ_1=-30°)
1/8" Pb
S-2

Fig. 6

Fig. 7. A simplified diagram of the LASL arrangement for measuring the analyzing power of deuterium and tritium.

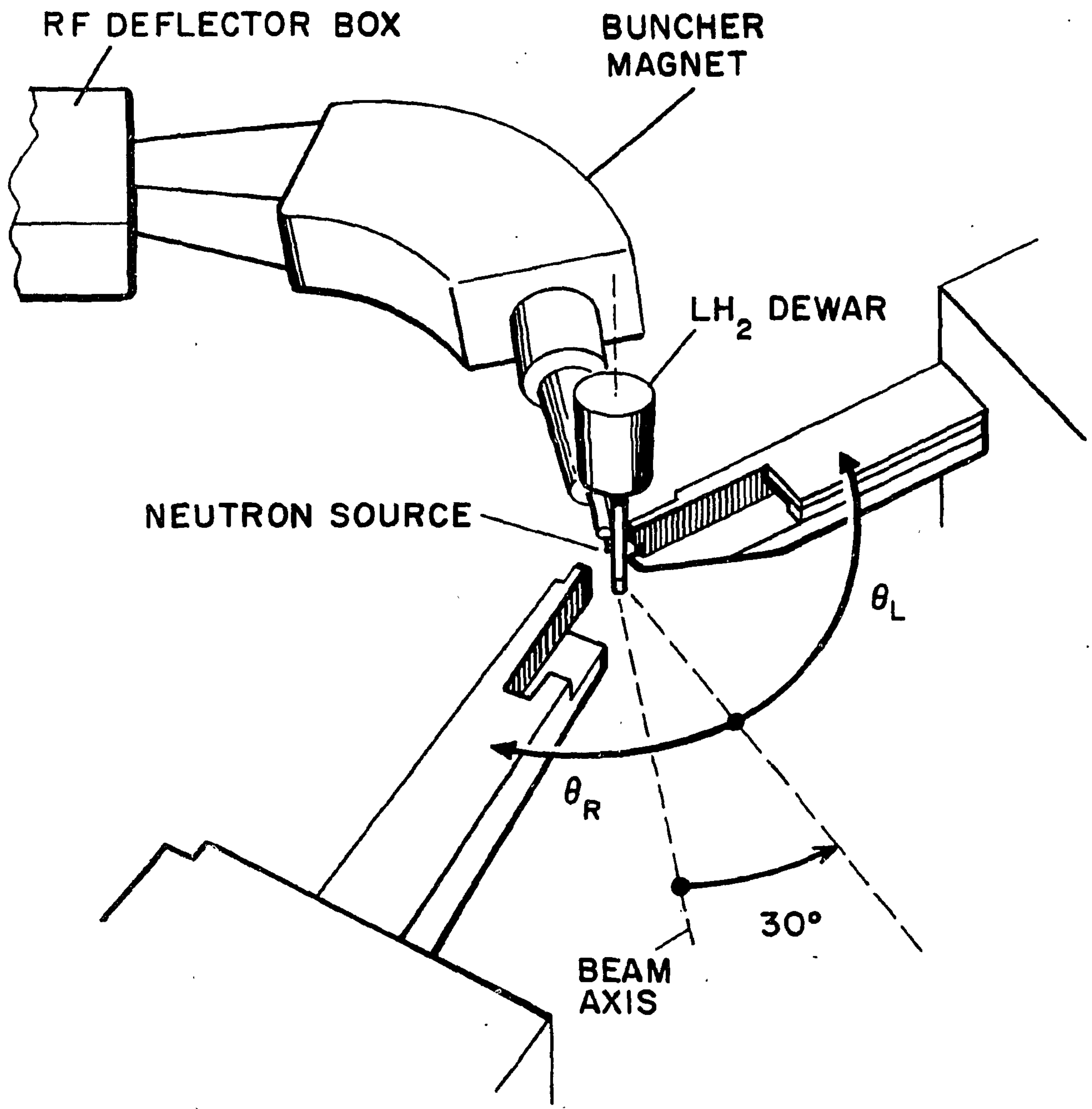
RF DEFLECTOR BOX
BUNCHER MAGNET
LH_2 DEWAR
NEUTRON SOURCE
θ_L
θ_R
30°
BEAM AXIS

Fig. 7

Fig. 8. Polarization apparatus at the LASL Mobley Buncher time-of-flight facility.

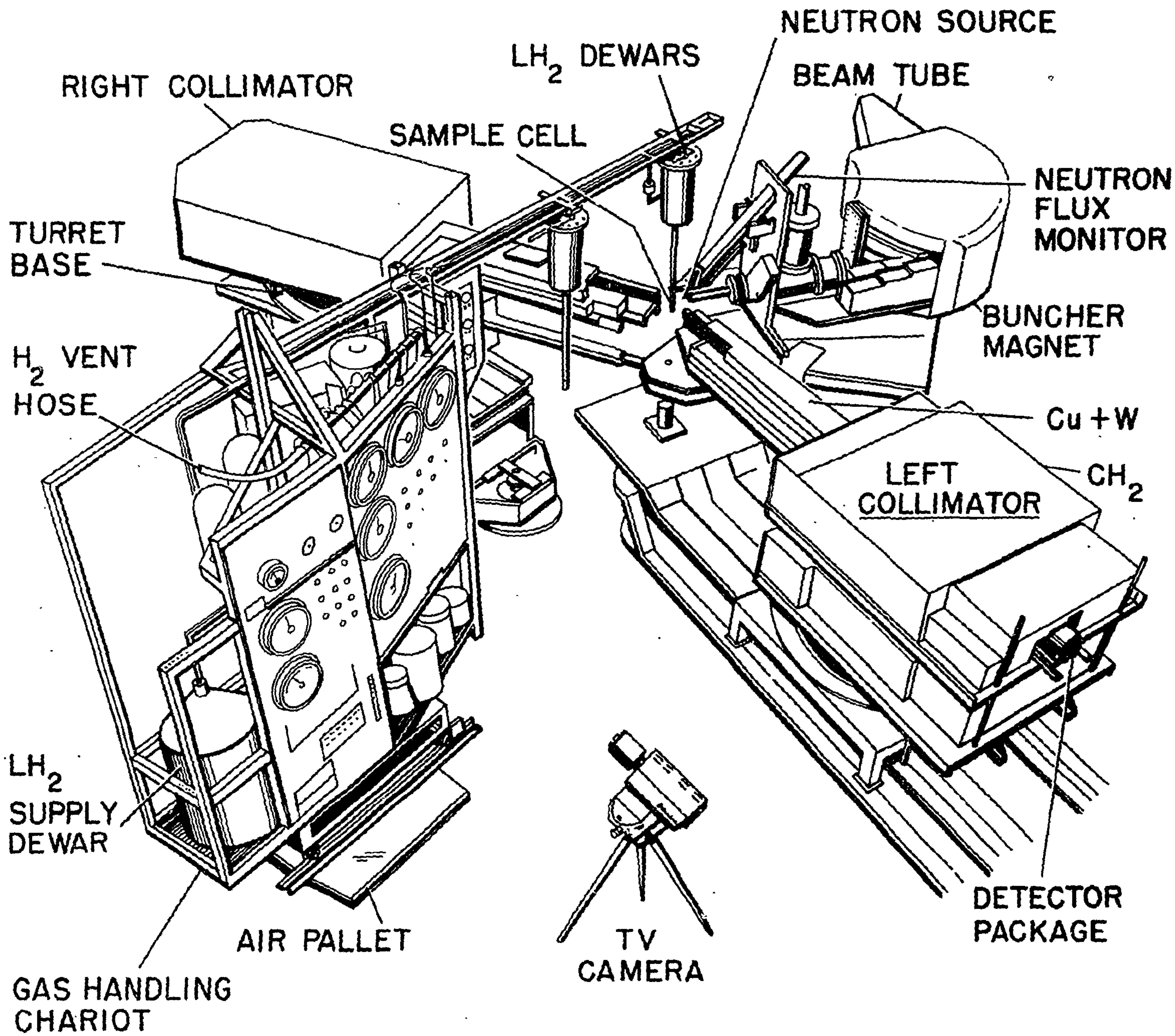
NEUTRON SOURCE
LH$_2$ DEWARS
BEAM TUBE
RIGHT COLLIMATOR
SAMPLE CELL
NEUTRON
FLUX
MONITOR
TURRET
BASE
BUNCHER
MAGNET
H$_2$ VENT
HOSE
Cu + W
LEFT
COLLIMATOR
CH$_2$
LH$_2$
SUPPLY
DEWAR
DETECTOR
PACKAGE
AIR PALLET
TV
CAMERA
GAS HANDLING
CHARIOT

Fig. 8

$P_{He}(\theta_2)$ is the analyzing power of ^{4}He at θ_2. N_{S-2} and N_{S-3} are the S-2 and S-3 counting rates, respectively, appropriately corrected for background, dead time, etc.

Notice that only one counter would be necessary if two runs were made, first with the polarization precessed 90° in one direction and second with the polarization precessed 90° in the opposite direction. This is frequently the way this apparatus is used.

Figure 7 shows the setup used by the time-of-flight group* for measuring the analyzing power of deuterium and tritium in the neutron energy region of 22 MeV. In this case the left-right asymmetry is measured in the reaction plane. The scattering sample is close (~10 cm) to the neutron source and off-axis at an appropriate angle to obtain the maximum neutron polarization. A value of the source polarization (Pe 61, Si 69) is assumed and the analyzing power is deduced using the same relationship that was just discussed. A more detailed diagram of the experimental arrangement is shown in Fig. 8.

The techniques and the values of the source polarization have been checked by remeasuring the analyzing power of ^{4}He (Ar 66, Bü 66, Le 57b, Ma 63, Pe 64, Sa 68). The preliminary agreement is quite good and results should be ready for release soon.

This concludes the discussion of the LASL fast-neutron time-of-flight facility. It has been assumed that this is typical of installations devoted to research with neutrons in the energy range of several MeV up to 10 MeV.

There are, of course, many differences in techniques and in methods between

---

*R. K. Walter, R. H. Sherman, J. D. Seagrave, A. Niiler, J. T. Martin, E. C. Kerr, and J. C. Hopkins.

the various laboratories. An attempt has been made to refer to these in the appropriate places. There are, however, excellent descriptions of two installation that were not covered. There are two additional papers covering the United Kingdom's AWRE (Aldermaston) Laboratory (Ba 58, To 62) and two papers covering the Research Institute of National Defence Laboratory in Stockholm (Be 64, Be 67b).

II-2. Fast-Neutron Experimental Facilities

Five facilities that are representative will now be discussed. This section is intended to provide a background for future discussions of the experiments and to provide suitable references for further study. Consequently, it will be brief.

The selection of the five facilities was necessarily somewhat arbitrary. This does not exhaust the supply of excellent laboratories. Indeed, there is no contention that these five are the best, only that they are not similar to the LASL facility and are representative of some phase of fast-neutron experimentation.

A. Argonne National Laboratory Reactor Division Van de Graaff Accelerator Facility

The Argonne National Laboratory has one of the most prolific and productive groups in the world under the direction of A. B. Smith.

The have specialized in cross-section measurements in the neutron energy range below 1.5 MeV. A schematic diagram of their system is shown in Fig. 1 of (Sm 67). The salient features include: a 3.2-MV Van de Graaff, Mobley (Mo 52) beam-bunching apparat , and an array of up to 10 detectors.

It is the machine, detector, and data-handling system that makes the Argonne facility particularly noteworthy.

Fig. 9. Schematic diagram of the Hanford fast-neutron time-of-flight facility.

FAST-NEUTRON TIME-OF-FLIGHT FACILITY

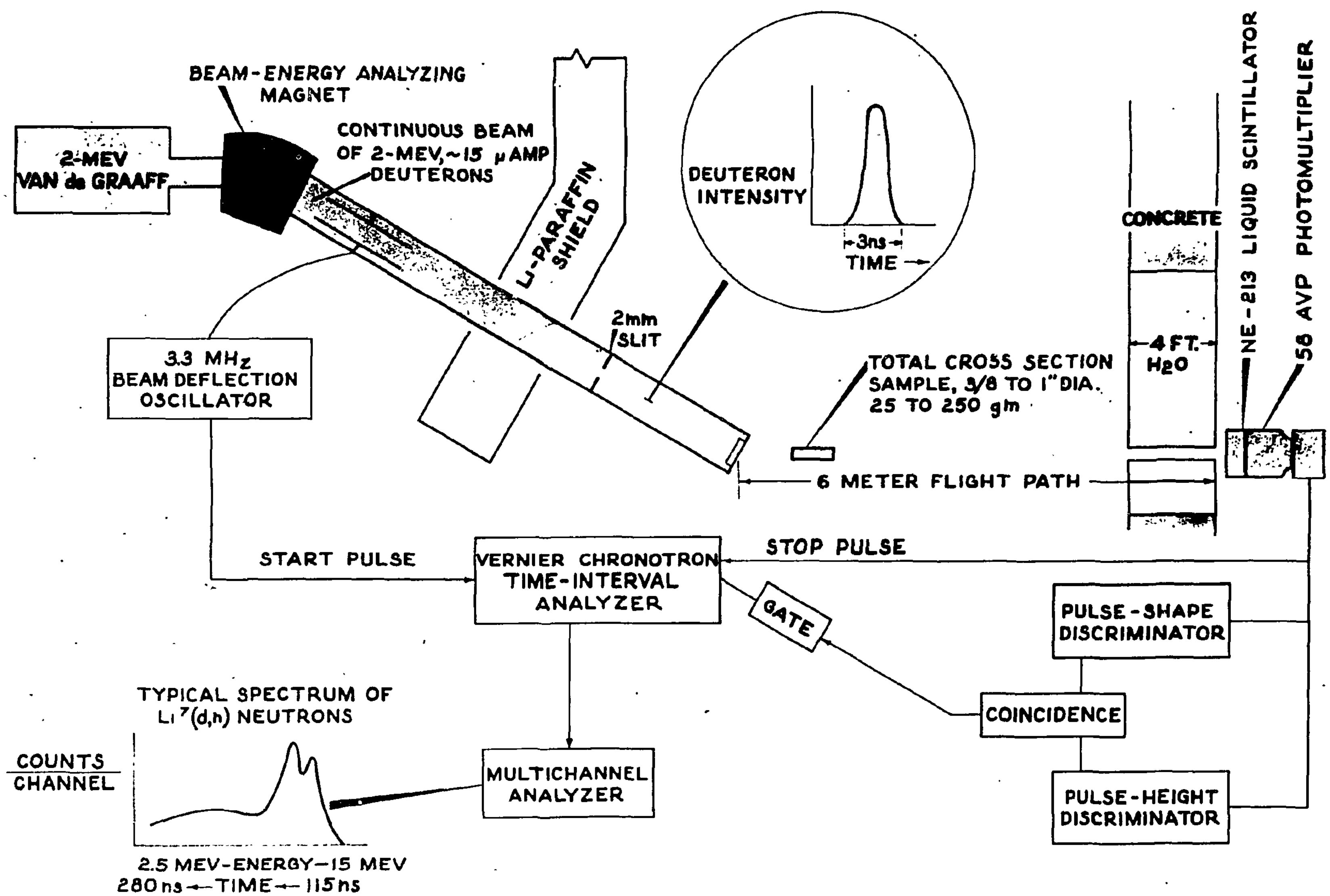

Fig. 9

They can operate 10 detectors simultaneously at scattering angles of 20° to 150° and at flight paths of 1.5 to 3.5 m. The various components of the pulsing, accelerating, and bunching system are controlled by feedback systems such that the beam handling and pulsing systems will automatically "track" the beam to the target following energy changes prescribed by the controlling computer (Wh 66).

Note the completely automated detector signal acquisition, selection, and routing. A computer corrects for the efficiencies, multiple scattering, and attenuation. It then makes a least-squares fit of the Legendre-polynomial series

$$\sigma(\theta) = \frac{\sigma}{4\pi}\left\{1 + \sum_{i=1}^{n} W_i \; P_i \theta\right\} \qquad \text{(for } n = 2 \text{ to } 6)$$

to the data.

Finally the computer puts out cross sections and Legendre coefficients with appropriate standard deviations.

B. Hanford 2-MeV Van de Graaff Facility

D. G. Foster, Jr. and D. W. Glasgow at the Hanford Laboratories have made a very substantial contribution to the total cross-section field by practically covering the periodic table for neutron energies between 2.5 and 15 MeV (Fo 65).

They have made transmission measurements using the pulsed-beam time-of-flight technique with a continuous spectrum of neutron energies.

Their experimental arrangement is shown in Fig. 9. Neutrons are produced by bombarding a thick (0.5 mm) natural lithium target with 2-MeV deuterons. Neutrons are detected with an NE-213 liquid scintillator coupled to a 58-AVP photomultiplier tube. The vernier chronotron was later replaced by a commercial TAC-ADC combination feeding a PDP-8 computer.

The energy resolution, over the 6.14-m flight path, varies from 2.5% at the lowest energies to 4.5% at the highest energies.

The distance from the source to the sample is chosen so that the diameter of the sample is 1.25 times the minimum diameter which barely shadows the detector completely from the source at that distance. In practice the source-to-sample distances were between 26 and 105 cm.

Figure 3 of (Fo 65) shows the time-of-flight spectrum of the neutron source. The sharp structure in the source spectrum above 11 MeV caused some difficulties in determining the total cross sections. The final precision varied throughout the energy range from 1 to 3%.

The Hanford group is no longer making total cross-section measurements.

C. Karlsruhe Cyclotron Group

The Karlsruhe 90-inch isochronous cyclotron is used as an intense neutron source for total cross-section measurements (Ci 68) in the energy range 0.5 to 30 MeV.

A particularly interesting feature of the Karlsruhe machine is the so-called deflection-bunching system (Ci 66a). An internal deflector is used to perform two tasks: It eliminates 2 out of 3 microstructure pulses and it forms ion bunches of 4.5-μsec duration (50 microstructure pulses) with a repetition rate of 20 kHz. An outer deflector is then used to extract the whole set of microstructure pulses to a target positioned above the median plane of the cyclotron. At the time of deflection the bunch is distributed over a distance of 4 inches in radius. The net result is that the repetition rate is reduced from 33 MHz to 20 kHz, while the average neutron intensity

Fig. 10. Schematic diagram of the Gulf General Atomic neutron time-of-flight facility for the study of $(n,x\gamma)$ reactions.

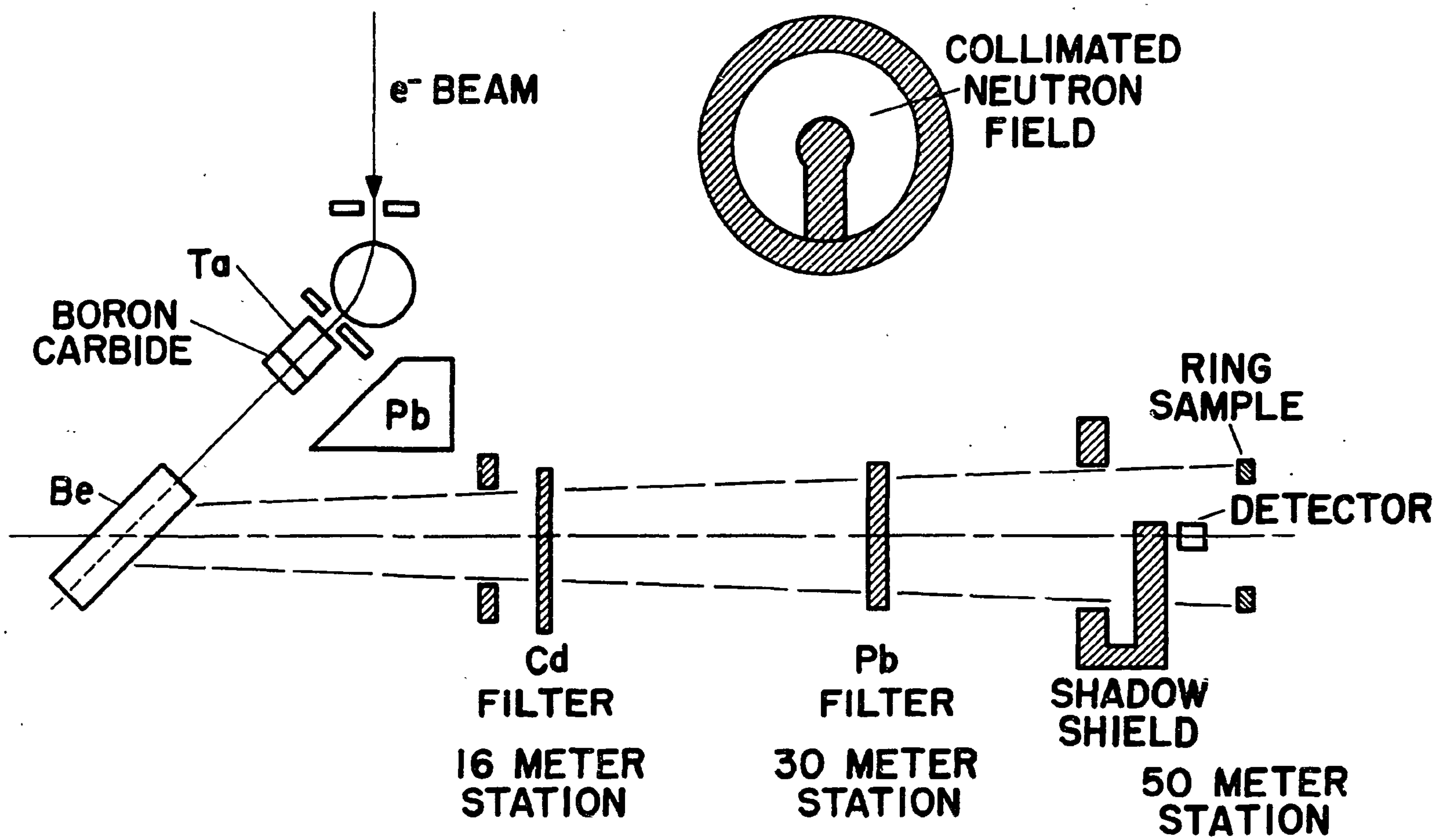
e⁻ BEAM
COLLIMATED
NEUTRON
FIELD
Ta
BORON
CARBIDE
Pb
Be
RING
SAMPLE
DETECTOR
Cd
FILTER
16 METER
STATION
Pb
FILTER
30 METER
STATION
SHADOW
SHIELD
50 METER
STATION

Fig. 10

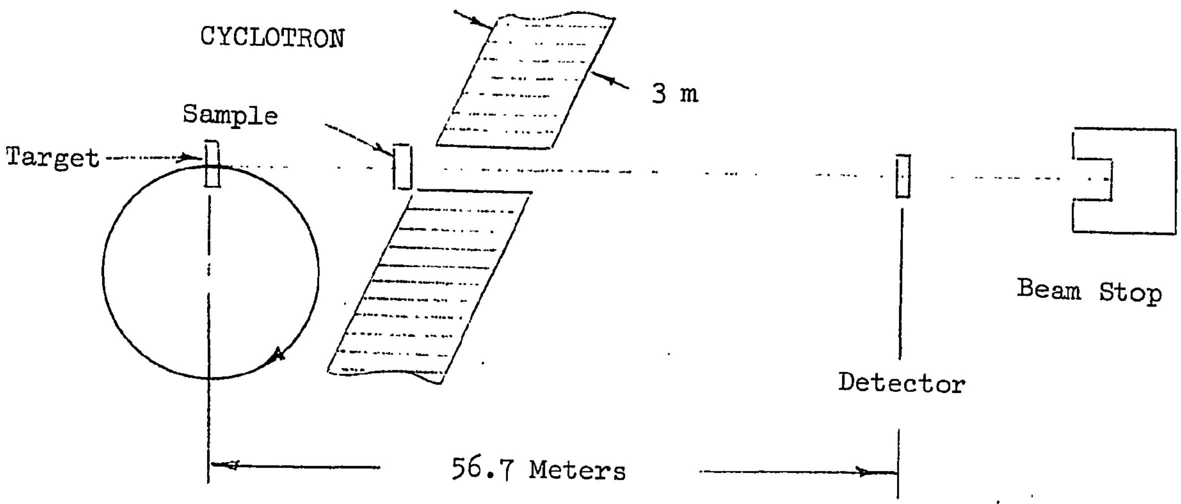

is reduced by only a factor of 30.

A thick natural uranium target is used for neutron production. The characteristic features are given as (Ci 66):

Flight path	56–57 m
Deflection radius	0.930 m (40.5-MeV deuterons) to
	1.030 m (50-MeV deuterons)
Time resolution	1 ± 0.3 nsec FWHM
Energy resolution	200 eV at 0.5 MeV
Resolution of spectrometer	0.02 nsec/m
Integrated neutron flux	$(5 \pm 2) \times 10^4$ neutrons cm^{-2} sec^{-1}
at 3-μA target current	above 250 keV at 56 m .

The Karlsruhe group obtain 1% statistical accuracy in 10 to 12 hours of running time (Ci 68).

D. United States National Bureau of Standards LINAC

A group has been formed at the relatively new NBS electron linac to measure total neutron cross sections (Sc 68).

For the energy range of interest, 0.7–4 MeV, almost any heavy element

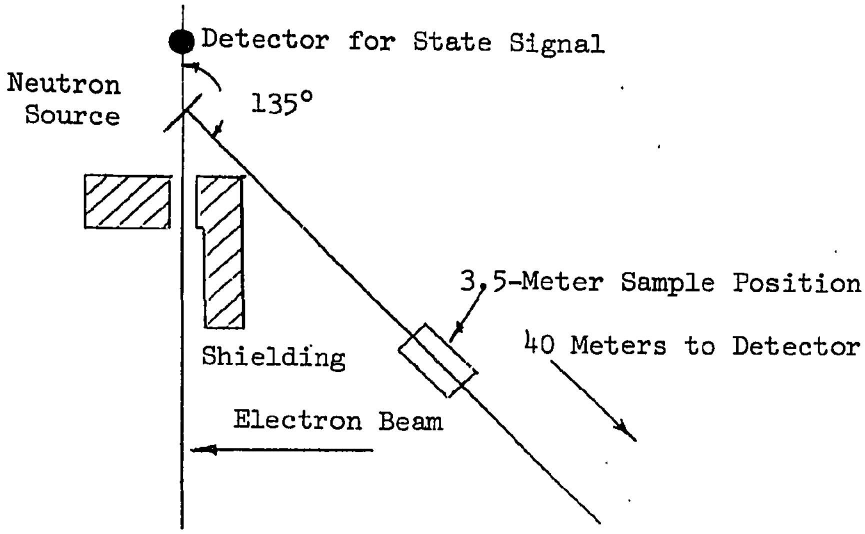

will do as a neutron source. They use ~2 cm of Cd.

The neutron detector is a liquid scintillator 33 cm in diameter and 12.7 cm thick, viewed by three 58-AVP photomultiplier tubes.

The overall time resolution is 6.5 nsec or 0.16 nsec/m (e.g., 25 keV at 3 MeV).

E. Gulf General Atomic Gamma-Ray Studies

A new program has been initiated at Gulf General Atomic to measure gamma-ray production cross sections using a pulsed-LINAC neutron source (Or 68, Or 69, Be 69).

Figure 10 shows schematically the experimental arrangement. A bending magnet deflects the electron beam through 45°. The beam then strikes a 0.3-cm tantalum electron-to-bremsstrahlung converter and a 5-cm-thick boron carbide electron beam stop.

Neutrons are produced, mainly by the (γ,n) reaction, in beryllium. The sample and detector are placed at 135° to the incident electron beam to reduce the gamma-flash effects. The pulse width is adjustable from 5 nsec to 4.5

Fig. 11. Neutron spectra, at 50 meters, from the Gulf General Atomic neutron facility. The operating conditions are described in the text.

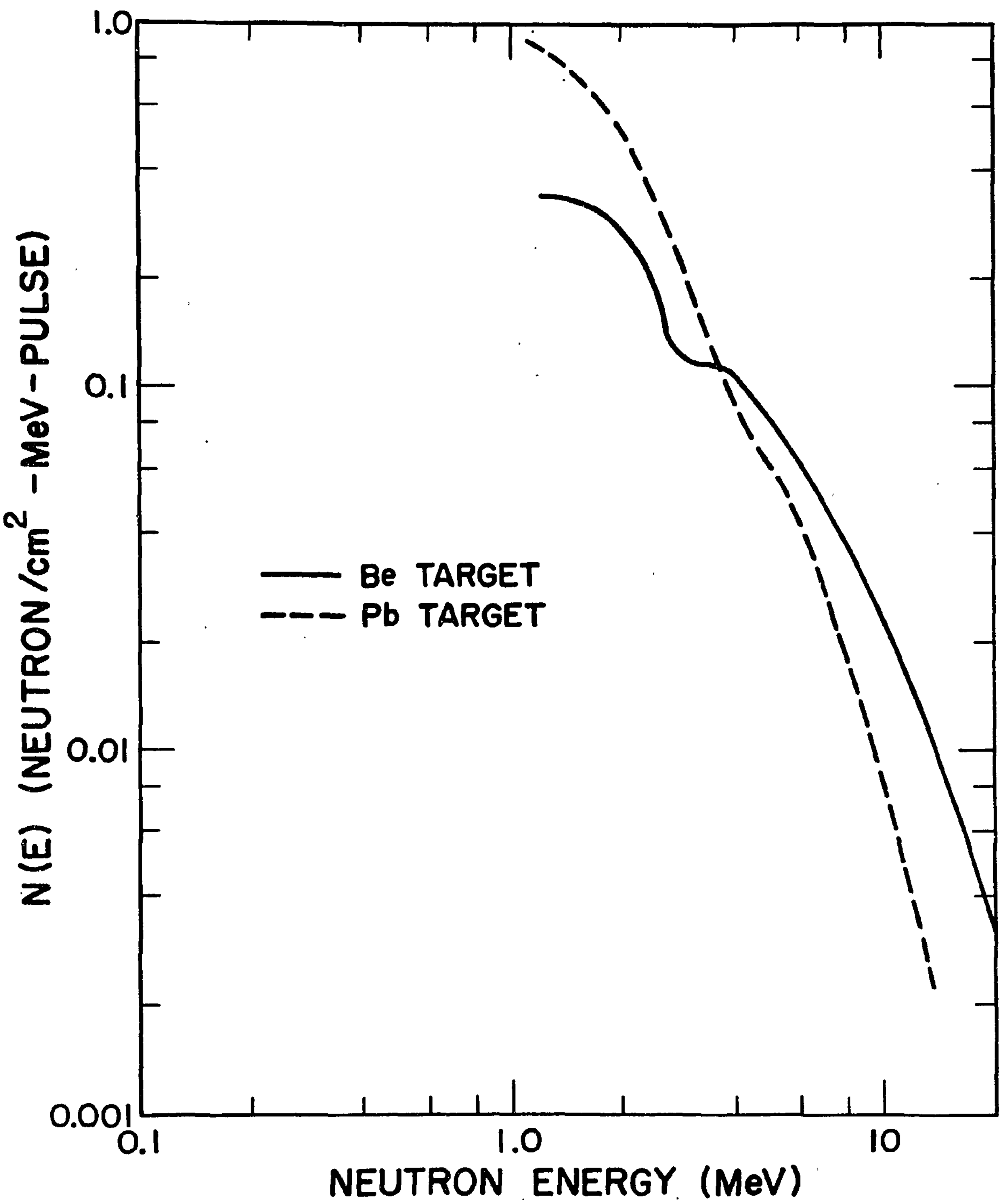
1.0
0.1
0.01
0.001
N(E) (NEUTRON/cm^2 -MeV-PULSE)
Be TARGET
Pb TARGET
0.1
1.0
10
NEUTRON ENERGY (MeV)

Fig. 11

μsec, with a repetition rate of 720 pulses per sec. The flight path from the target to the sample is 50 m.

With the following operating conditions the GGA group obtained the neutron spectra shown in Fig. 11.

Pulse width	50 nsec
Electron energy	55 MeV
Electron current	3 amps
Repetition rate	500 pps
Time resolution	1 nsec/m
Flight path	50 m

Note that the high-Z lead target yields more low-energy neutrons and fewer high-energy neutrons than the low-Z Be target. They have improved the spectrum by tailoring beam filters and optimizing their locations. The net gain was about a factor of two in neutron flux at 14 MeV in addition to a reduction in the energy of the gamma flash.

There are still many problems associated with these techniques. They have, however, a potentially power ful method.

III.

III-1. Nucleon-Nucleon Interactions

The interaction of one nucleon with another is of major importance to nuclear physics for two reasons, the most significant being that this is a basic interaction out of which more complicated interactions may eventually be described. For example, we must understand this reaction if we are to understand nuclear matter. The second and more pragmatic reason is that the neutron-proton cross section is used as a nuclear standard (Ho 67c,d). The neutron-nucleon interaction will be discussed from both viewpoints.

First, the use of the n-p cross section as a nuclear standard will be briefly described. Then the experimental situation will be reviewed with regard to our understanding of the nucleon-nucleon interaction.

A. $^{1}H(n,n)^{1}H$ Cross Section as a Nuclear Standard

The use of the $^{1}H(n,n)^{1}H$ cross section as a nuclear standard was described in great detail at the 1967 Brela Conference (Ho 67d). Consequently, only the salient features will be mentioned.

By cross-section standard, we mean a reasonably well-known nuclear cross section that can be employed as a value for comparison or as a basis for measurement. The standard material must have well-behaved and well-understood chemical and physical characteristics. Hydrogen, either alone or in some chemical form such as polyethylene, has served this purpose admirably.

Neutron cross sections, measured with time-of-flight techniques, have usually been made relative to the $^{1}H(n,n)$ cross section for incident energies above 2 MeV. In these cases the accuracy of the measured cross section can be no better than the uncertainty in the differential $^{1}H(n,n)^{1}H$ cross section.

In the case of proton recoil telescopes, which are used for making accurate neutron flux measurements, the main problem at neutron energies above about

10 MeV is the uncertainty in the anisotropy of the cross section. Professor Gregory Breit and the author have tried to reduce this uncertainty by calculating the n-p differential cross section between 100 keV and 30 MeV and presenting the resultant cross sections in terms of coefficients of the expansion (c.m. system)

$$\sigma(\theta) = C_o + C_1 \cos\theta + C_2 \cos^2\theta \qquad \text{(Ho 69d)} .$$

These coefficients are shown in Table I, along with the values of the calculated total cross sections. These values of the total cross section were obtained directly from the phase-shift calculation and not from an integration of the $\cos\theta$ expansion of the differential cross section.

The energies are given in the laboratory system whereas the angles are given in the center-of-mass system. This is the usual practice.

Between 100 keV and 3.200 MeV, only S- and P-wave phase shifts were used. At 3.205 MeV and above, phase shifts through $^3H_4$ were employed. This accounts for the aberration in the coefficient C_2 around 3.205 MeV. If one wishes to plot the value of C and interpolate, we suggest that this be done above and below 3.205 MeV separately. The horizontal line in the table indicates the dividing point.

Above 3.205 MeV a version of the Yale (Y-IV) phase shifts were used (Br 67a). More detailed calculations of the various observables such as the polarization, C_{nn}, C_{KP}, D, A, and R are now being prepared (Ho 69d).

The values calculated with the aid of this table represent the results of a complete phase-shift calculation as well or better than the data justify. The 3 coefficient expansion should not be used above 30 MeV; however, at lower energies it is quite satisfactory.

TABLE I

n-p Differential and Total Cross Sections

100 keV-30 MeV

$$\sigma(\theta) = C_o + C_1 \cos\theta + C_2 \cos^2\theta$$

$\sigma(\theta)$ in mb/sr, θ cm scattering angle

E_{LAB}	C_o	C_1	C_2	σ_T (mb)
0.100	1016.87	-0.581	0.0003	12778.3
0.200	769.79	-0.843	0.0010	9673.5
0.400	549.02	-1.104	0.0040	6899.2
0.600	444.48	-1.263	0.0088	5585.5
1.000	339.04	-1.487	0.0232	4260.6
2.000	231.97	-1.818	0.0829	2915.4
3.000	182.42	-1.977	0.1599	2293.0
3.200	175.212	-2.016	0.1764	2202.5
3.205	175.128	-2.004	-0.0766	2200.4
4.749	134.93	-2.114	-0.0633	1695.3
7.170	99.068	-2.160	0.1187	1245.4
8.77	83.865	-2.129	0.3112	1055.2
10.42	72.209	-2.111	0.5505	909.7
11.13	68.014	-2.110	0.6532	857.4
13.70	55.941	-2.031	1.060	707.4
16.40	46.686	-1.886	1.504	592.9
20.5	36.661	-1.608	2.168	469.6
23.7	30.985	-1.394	2.684	400.4
27.2	26.128	-1.164	3.315	342.0
30.0	22.995	-0.9822	3.800	304.6

The total cross sections given in Table I have an absolute standard deviation of less than 1%. The differences $|\sigma(90°) - \sigma(180°)|$ have standard deviations of approximately ±30% for incident neutron energies between 100 keV and 10 MeV, ±20% for incident neutron energies between 10 MeV and 15 MeV, and ±15% for energies between 15 MeV and 30 MeV. The standard deviations in the differences $|\sigma(0°) - \sigma(90°)|$ are the same as the standard deviations in the differences $|\sigma(90°) - \sigma(180°)|$. For example, around 20 MeV the standard deviation in $|\sigma(0°) - \sigma(90°)|$ is approximately $\pm 0.15\ [\sigma(90°) - \sigma(180°)]$.

The experimentalists who use n-p scattering as a standard, for relative measurements or in conjunction with some form of proton recoil device, should use the cross sections from Table I and not any of the ancient formulas developed before the advent of modern phase-shift analyses (Ga 60). In particular, it should be emphasized that the C_1 term is not negligible as was assumed in the past. In fact it is larger than C_2 for all energies below 20 MeV!

B. The Neutron-Nucleon Interaction: A Summary of the Experimental Situation

The neutron-nucleon interaction cannot be divorced from the general nucleon-nucleon interaction for various reasons, including the fact that most of the neutron-proton isospin 1 phase shifts are determined from proton-proton data. This is true at least for partial waves with ℓ values greater than 0. Consequently, while most of the emphasis will be placed upon the interactions involving neutrons, e.g., n-p and n-n, occasional mention will be made of the p-p data.

In this section the survey will be limited to the energy region below the point where pion production becomes a substantial part of the cross section, i.e., to an energy less than about 450 MeV.

B.1 Description of Experiments

a) Types of Experiments

In this section just a few of the possible measurements will be discussed. The Wolfenstein notation (Wo 56) will be used throughout, with the sign of the polarization corresponding to the Basel convention (Ba 61a).

Two measurements, of total cross section and of differential cross section, need no introduction. A polarization measurement is shown in Fig. 12. This is a polarization analyzer where P_A is the analyzing power of the scatterer and "L" and "R" are left and right counting rates, respectively. An analyzer of this type is used in the experiments that will be described. Figure 13 shows a depolarization measurement. A polarization analyzer is used to measure P, where P_S is the analyzing power of the scatterer. Figure 14 shows a spin-correlation experiment C_{nn}. An unpolarized beam is scattered from an unpolarized target. The two outgoing particles are detected in coincidence by the polarization analyzers shown. The subscript nn refer to the analysis of two spins normal to the scattering plane.

There is another way to measure C_{nn}. If time reversal holds, a differential cross-section measurement of the scattering of a polarized beam from a polarized target yields the quantity A_{YY} which is the same as C_{nn}.

These are 3 examples of the 256 possible experiments enumerated in Fig. 15 (Table II). This table, from Wilson's book (Wi 63), shows how many types of each measurement are possible. For example, with an unpolarized target, and a polarized beam, there are 3 different cross-section measurements corresponding to the 3 possible directions of polarization of the beam.

Fortunately, 256 measurements are not required to completely specify the scattering matrix. If parity conservation, charge symmetry, and time reversal (equality about the diagonal of this table) hold, then the measurement

Fig. 12. A diagram of a polarization, P, analyzer.

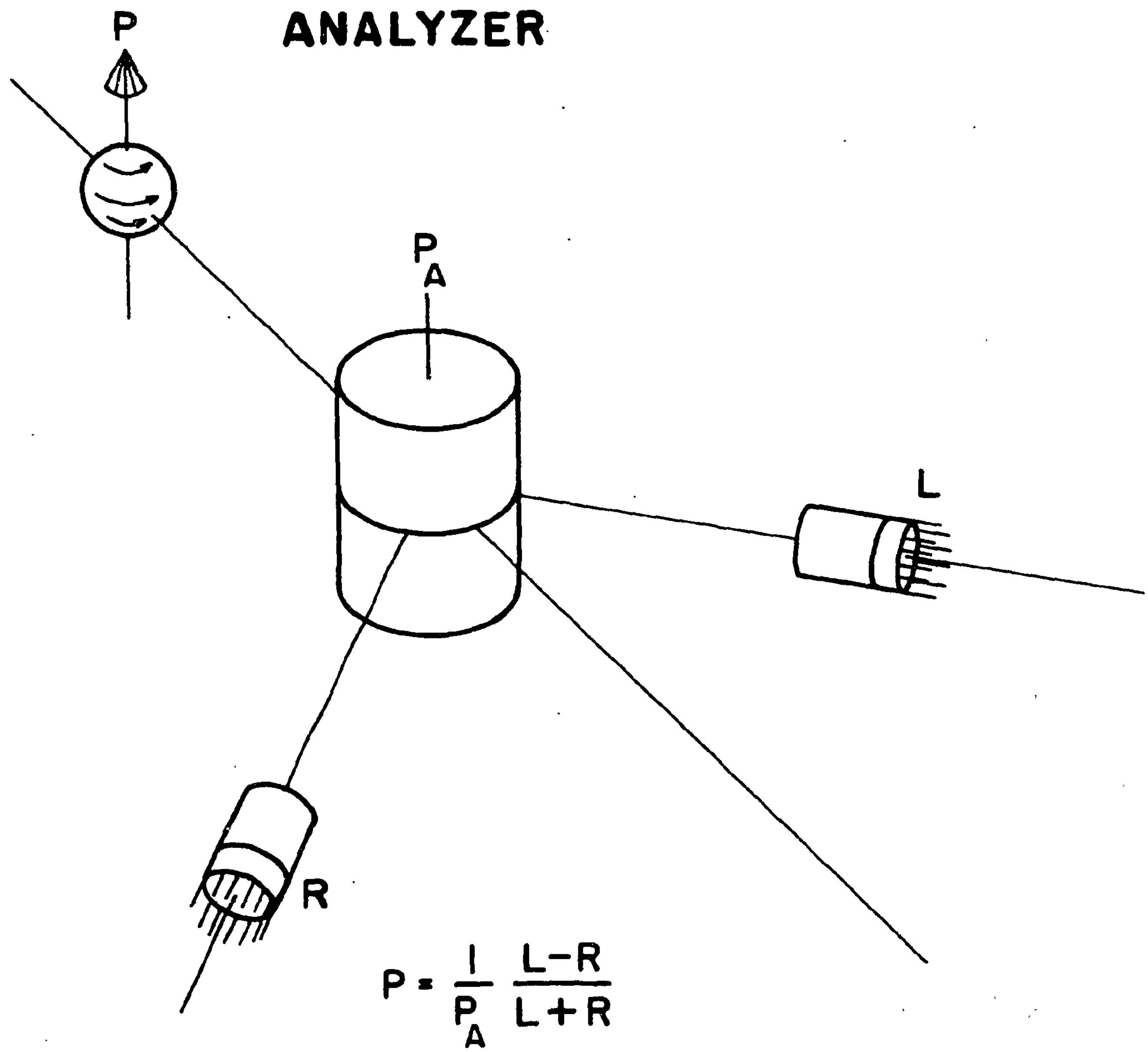

$$P = \frac{1}{P_A} \frac{L-R}{L+R}$$

Fig. 12

Fig. 13. A depolarization, D, experiment.

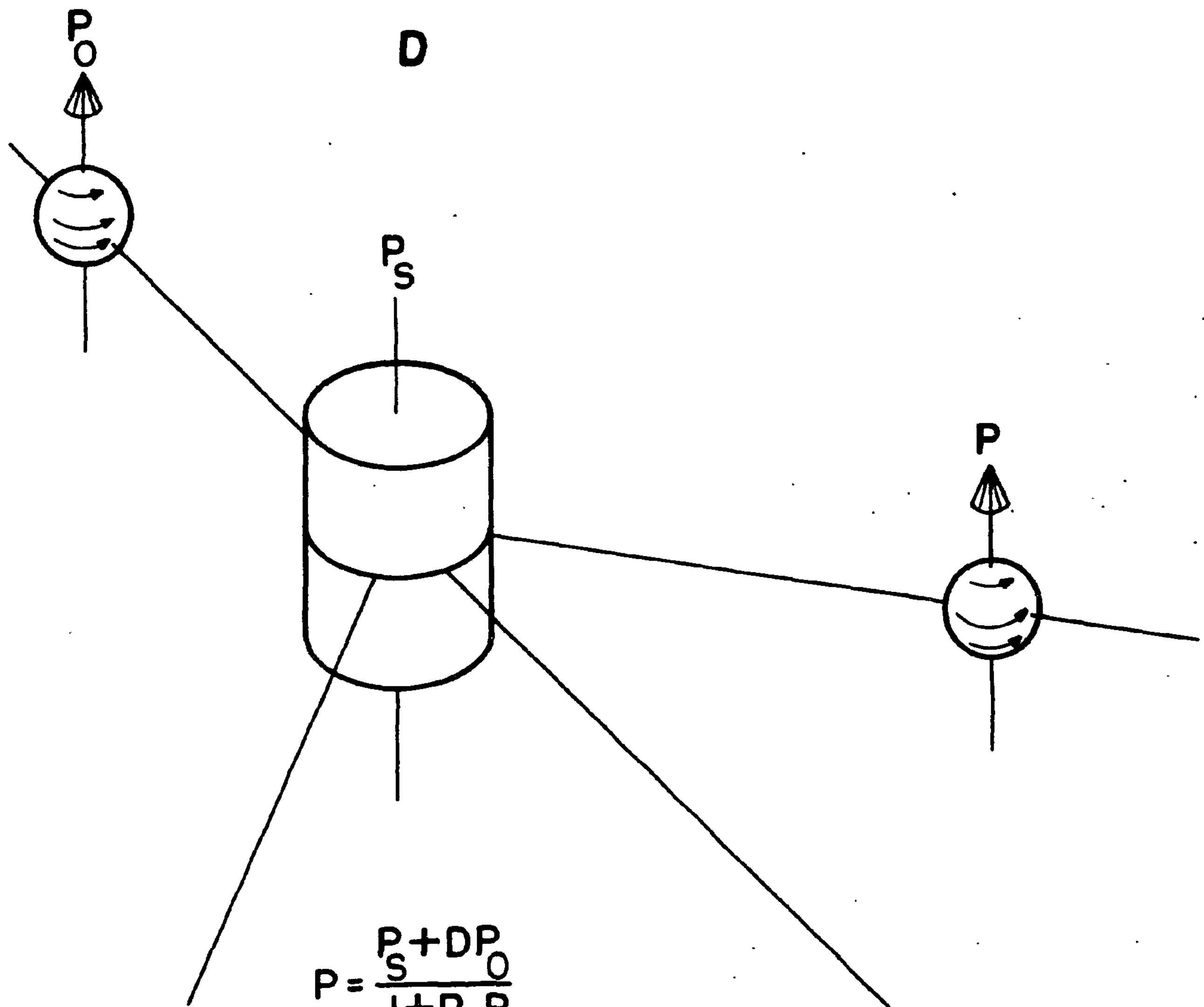

$$P = \frac{P_S + DP_O}{1 + P_O P_S}$$

Fig. 13

Fig. 14. A spin-correlation experiment, C_{nn}.

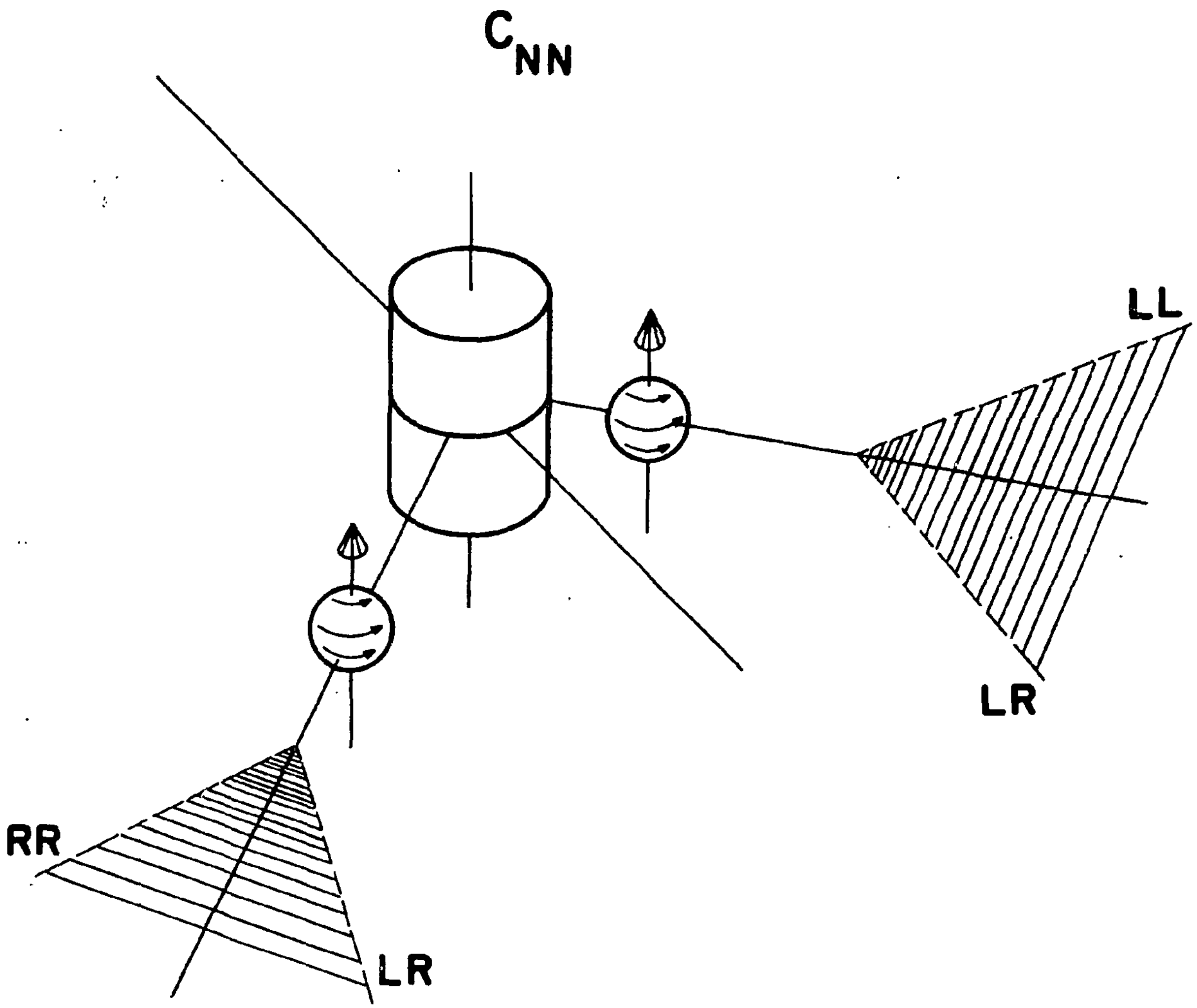

$$C_{NN} = \frac{1}{P_A^2}\,\frac{(LL)(RL)+(LR)(RR)-(LL)(RR)-(LR)(RL)}{(LL)(RL)+(LR)(RR)+(LL)(RR)+(LR)(RL)}$$

Fig. 14

Fig. 15. Table II. This table shows how many types of each nucleon-nucleon measurement are possible.

TARGET BEAM	UNPOLAR		POLAR		TOTAL
	UNPOL	POL	UNPOL	POL	
CROSS SECTION	(1) σ	(3) e	(3)	(9) A_{YY}	(16)
POLARIZATION	(3)	(9) D,A,A' R,R'	(9)	(27)	(48)
POLARIZATION (RECOIL)	(3)	(9) D_T	(9)	(27)	(48)
CORRELATIONS	(9) C_{NN},C_{KP}	(27)	(27)	(81)	(144)
TOTAL	(16)	(48)	(48)	(144)	(256)

Fig. 15

of 9 observables for p-p scattering, or 11 for n-p scattering, are required at one angle and energy to construct a scattering matrix, though not uniquely, at that energy.

If measurements are made at all angles, then unitarity imposes 5 conditions relating the imaginary parts of the scattering-matrix coefficients at one angle to integrals of their products over all angles. This leaves 5 p-p measurements or 6 n-p measurements. For n-p scattering, all angles means 0° to 180°. For p-p scattering, I_o, P, C_{nn}, and C_{KP} are symmetric, or anti-symmetric, about 90° center of mass. In these cases, all angles means 0° to 90°. However, D, A, A', R, and R' are not symmetric and require determination in the two quadrants.

Some care must be exercised in the selection of the 5, or 6, experiments to insure that all observables are independent. For example, A, A', R, and R' are related to the laboratory scattering angle α through the relationship (Mo 63)

$$\frac{A + R'}{A' - R} = \tan \frac{\alpha}{2} \, .$$

b) Polarized Targets

A very important experimental breakthrough, namely the successful development of polarized targets, will now be discussed. Because of the 3 possible directions of polarization, there are 3 times as many experiments with polarized targets as with unpolarized targets.

Complicated triple-scattering spin-correlation experiments such as C_{nn} are reduced to simple scattering cross-section measurements with a polarized beam and a polarized target. This is the A_{YY} measurement discussed previously.

Polarized proton targets with polarizations between 45% and 65% have been developed by Jeffries at Berkeley (Je 63) and Abragam and Borghini at Saclay and CERN (Ab 64) using dynamic nuclear-polarization techniques. The targets are large single crystals of lanthanum-magnesium double nitrate [$La_2Mg_2(NO_3)_{12}24H_2O$ or LMN for short] in which 1% of the lanthanum is replaced by neodymium.

The single crystal weighing as much as 25 gms is placed in an 18 Kg magnetic field which polarizes the free electrons supplied by the neodymium. A very high frequency, roughly 60 gigaHz, is applied which flips proton and electron spins. At the 1.2°K operating temperature, the protons have a long relaxation time, whereas the electrons have a short relaxation time. The result is that each free electron polarizes a proton, then flips back ready to polarize another proton.

Other materials, such as toluene and alcohol, are being examined as replacements for LMN; however, none of these have yet achieved the polarizations attainable with LMN (Ca 66, Ha 66).

B.2 Data

a) n-p Data

The p-p data, which would logically come at this time, will not be discussed. It is sufficient to say that they are much more numerous, and far easier to obtain then n-p data which in turn are far easier to obtain than n-n data.

Figure 16 shows where, on an energy scale, the n-p scattering experiments have been performed. This table does not include the recent Wisconsin differential cross-section measurements by Rothenberg (Ro 69b). The important feature, however, is that only 2 experiments, differential cross section and polarization, have a reasonable coverage. The total does not count as one of the 6 necessary experiments to determine the scattering matrix. There is not a complete complement of six experiments anywhere except in the 140-MeV region.

Fig. 16. This figure shows where, on an energy scale, the n-p scattering measurements have been performed.

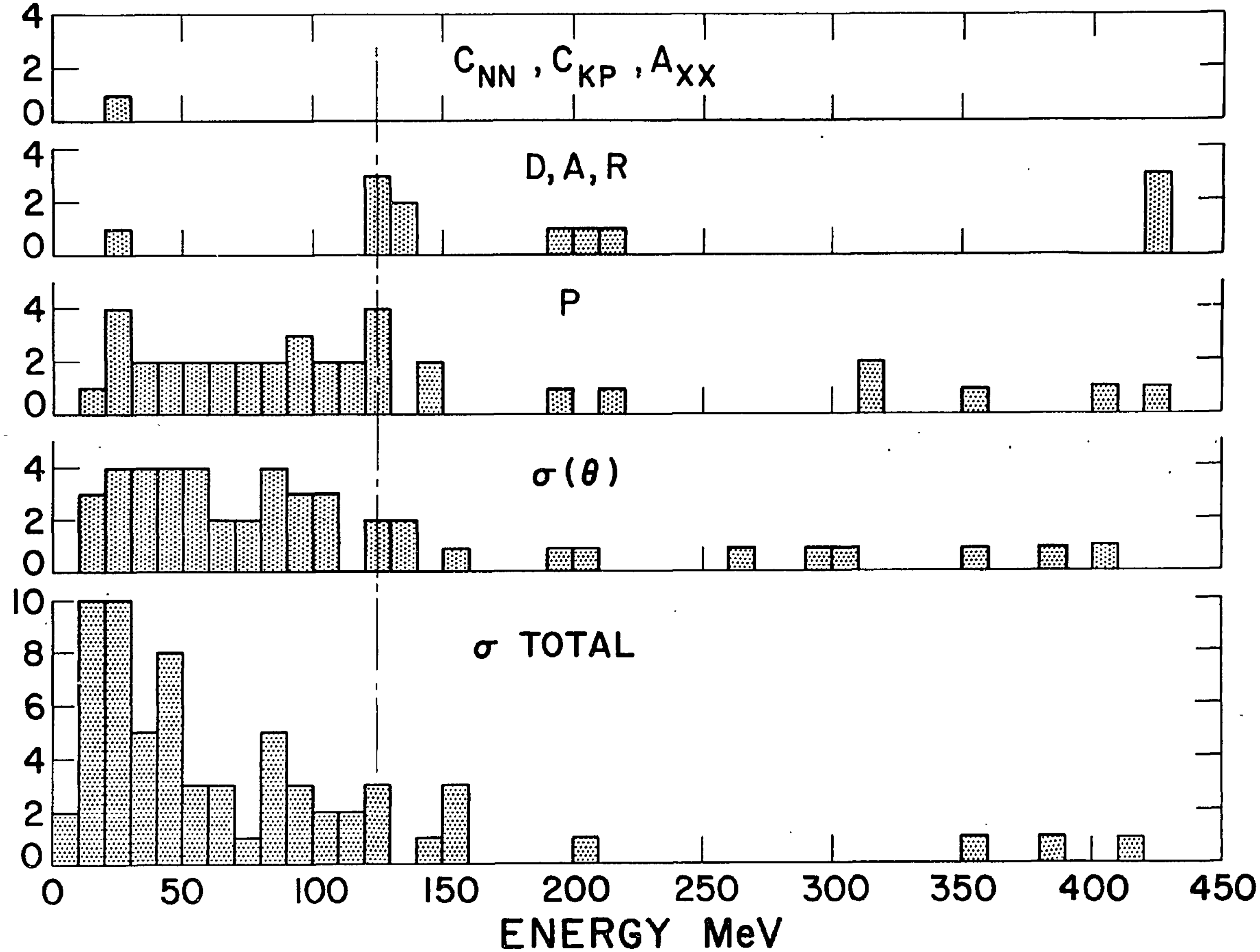

C_{NN}, C_{KP}, A_{XX}
D, A, R
P
$\sigma(\theta)$
σ TOTAL
0
2
4
6
8
10
0
50
100
150
200
250
300
350
400
450
ENERGY MeV

Fig. 16

Note the paucity of spin-correlation data. The one lone measurement of C_{nn} was made at Los Alamos by Malanify, Bendt, Roberts, and Simmons (Ma 66a), using a polarized 23-MeV neutron beam and polarized proton target.

Note also the recent P, D, R, and A measurements from the Chicago-Wisconsin group (Wr 68). These measurements contribute substantially to the determination of the high-energy behavior of the phase shifts.

Figure 17 shows the n-p total cross section as a function of energy between 3 MeV and 400 MeV. The rule-of-thumb has been to assume that this cross section is linear on a log-log scale. Obviously that is roughly correct only between 10 and 100 MeV. The percentages above the graphs are intended to give some idea of the quoted experimental uncertainty in the cross-section measurements in those regions.

Figure 18 shows $\frac{\sigma(180)}{\sigma(90)} - 1$ versus E on a log-log scale with most of the available data below 100 MeV. This ratio, of course, is of practical importance since it is a measure of the anisotropy. Measurements were ignored only if they were subsequently superseded by more accurate data at or near the same energy. The points attributed to Scanlon et al. (Sc 63) were computed by the author. He assumed smooth curves through their data. No errors were assigned to these ratios. The dashed line is a calculation based upon the values in Table I. The solid line was obtained using Gammel's formula

$$\sigma(\theta,E_n) = \frac{\sigma_T}{4\pi}(1 + b\cos^2\theta)(1 + \tfrac{1}{3}b)^{-1} ,$$

where $b = 2(E/90)^2$, with E in MeV (Ga 60).

b) Impulse Approximation

A problem specifically associated with some of the n-p data will now be briefly discussed. This problem concerns the use of deuterium as a neutron target. This scattering is called quasi-elastic scattering and the corrections are derived from the impulse approximation (Ch 52), the spectator model (Ku 61), the final-state interaction model (Cr 63b), or from the Glauber theory (Fr 66). Bascially there are several considerations; the neutron is bound, the neutron in the deuteron spends some fraction of its time in the shadow of the bound proton, and there are final-state interactions between the 3 interacting particles.

Experimental and theoretical comparisons between bound and free total cross sections (Ri 65, Me 66b), differential cross sections (Th 68), polarizations (Wi 63, Th 68, Ch 67a), bremsstrahlung measurements (Ed 66, Ko 67, Ko 68), and various triple-scattering parameters (Th 67) have been made.

The theories and experiments have been refined to such a degree that the details of the 3-body interaction play a decisive role (Th 67, Br 68). From now on more will probably be learned about the 3-nucleon system than the nucleon-nucleon interaction by studying the corrections for the nucleon-deuteron interaction.

c) Neutron-Neutron Scattering and Charge Independence

Turn now to the neutron-neutron scattering data. Since there are no direct neutron-neutron scattering experiments, the discussion will be confined to circumstantial evidence.

First look at the singlet-scattering lengths and effective ranges.

	p-p	n-p	n-n
	L. Heller(He 67)	H.P. Noyes(No 63,No 68a)	R.P. Haddock et al.(Ha 65)
a_S	-7.819±0.009fm	-23.678±0.028fm	-16.5±1.9fm*
r_{oS}	2.820±0.044fm	2.73 ±0.03fm	No direct evidence

*A new, unpublished analysis of the data yields the value -18.4±1.5fm(Cz 68).

Fig. 17. The n-p total corss section as a function of energy between 3 and 400 MeV.

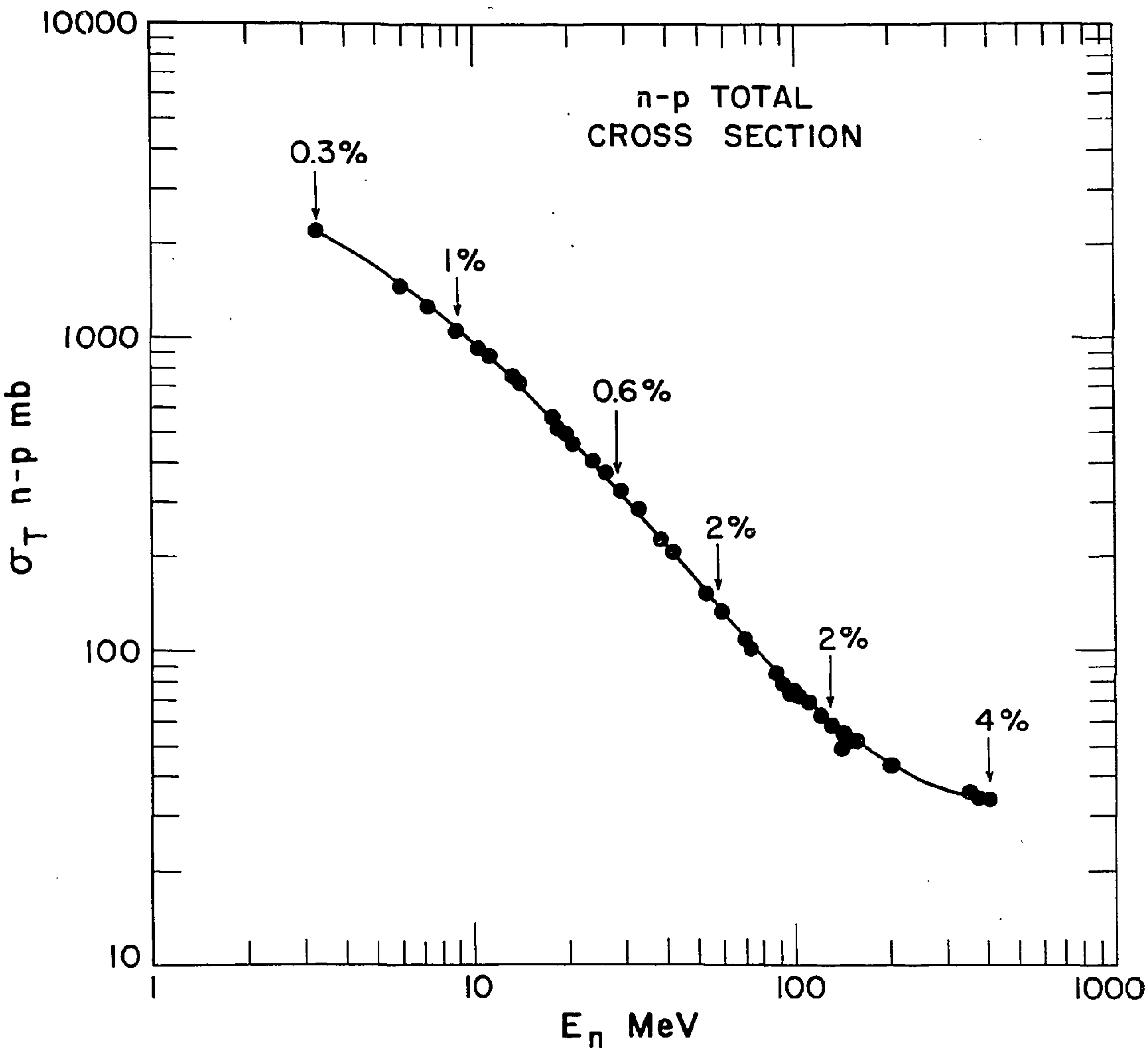
n-p TOTAL
CROSS SECTION
0.3%
1%
0.6%
2%
2%
4%
10000
1000
100
10
1
10
100
1000
σ_T n-p mb
E_n MeV

Fig. 17

Fig. 18. The ratio $\frac{\sigma(180^\circ)}{\sigma(90^\circ)} - 1$ vs E for n-p scattering. The dashed line is the result of a phase-shift calculation.

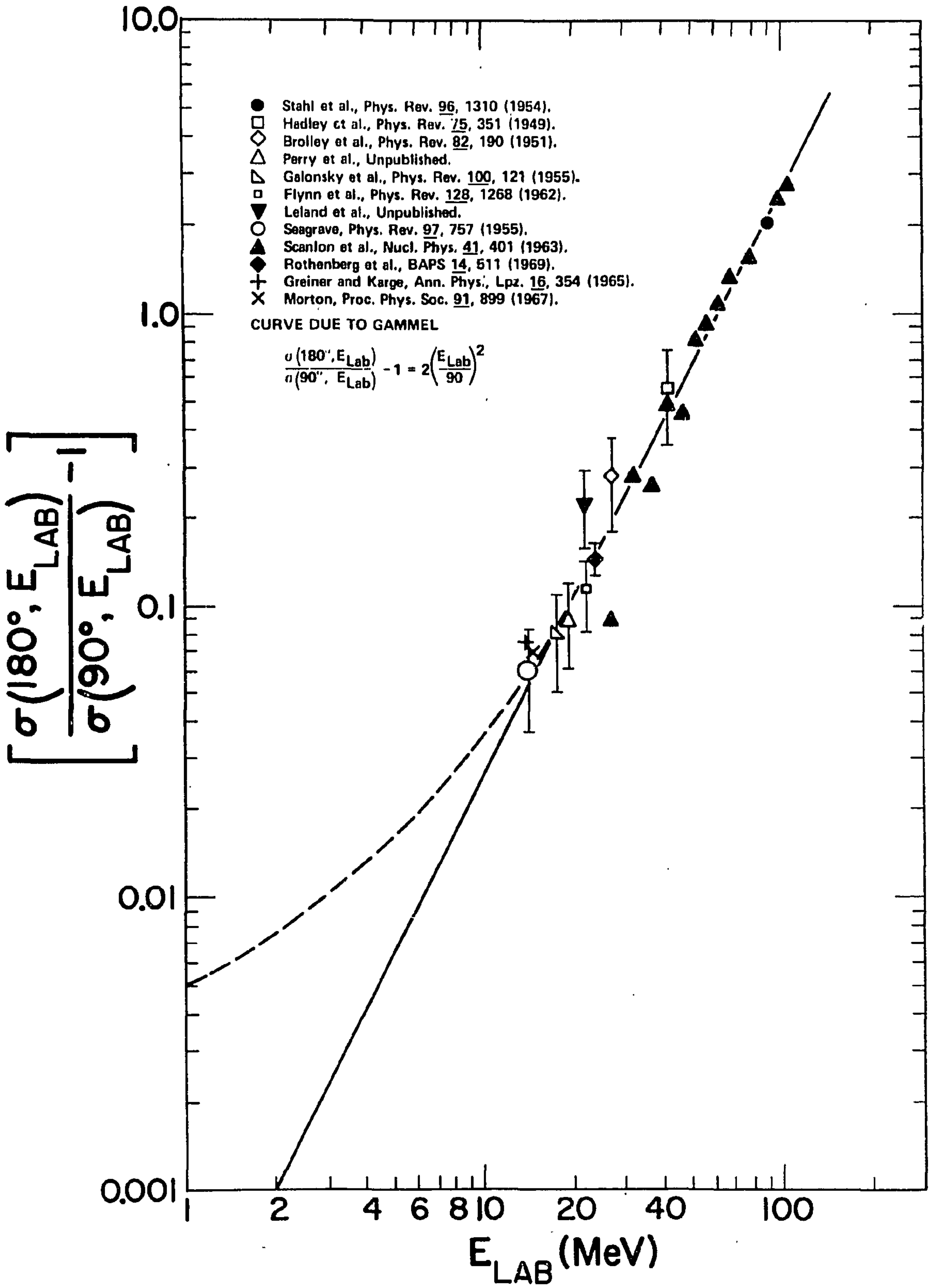
Stahl et al., Phys. Rev. 96, 1310 (1954).
Hadley et al., Phys. Rev. 75, 351 (1949).
Brolley et al., Phys. Rev. 82, 190 (1951).
Perry et al., Unpublished.
Galonsky et al., Phys. Rev. 100, 121 (1955).
Flynn et al., Phys. Rev. 128, 1268 (1962).
Leland et al., Unpublished.
Seagrave, Phys. Rev. 97, 757 (1955).
Scanlon et al., Nucl. Phys. 41, 401 (1963).
Rothenberg et al., BAPS 14, 511 (1969).
Greiner and Karge, Ann. Phys., Lpz. 16, 354 (1965).
Morton, Proc. Phys. Soc. 91, 899 (1967).
CURVE DUE TO GAMMEL
$\frac{\sigma(180°, E_{Lab})}{\sigma(90°, E_{Lab})} - 1 = 2\left(\frac{E_{Lab}}{90}\right)^2$
$\left[\frac{\sigma(180°, E_{LAB})}{\sigma(90°, E_{LAB})} - 1\right]$
E_{LAB} (MeV)
10.0
1.0
0.1
0.01
0.001
1
2
4
6
8
10
20
40
100

Fig. 18

There are dissenting opinions on these various values. For example, Slobodrian (Sl 68) has a new proton-proton scattering length* (-7.7856±0.0078fm), and Butler et al. (Bu 68) from Liverpool have a new neutron-neutron scattering length ($-13.1^{-3.4}_{+2.4}$fm).

Examine now charge symmetry, which is a phrase meaning equality of proton-proton or neutron-neutron processes. For this to be valid, the proton-proton and neutron-neutron scattering lengths would have to be equal after turning off the Coulomb potential and correcting for effects of finite-charge distributions, magnetic-moment distributions, and vacuum polarization.

Blatt and Weisskopf (Bl 52a) supply an approximate relation between the p-p and n-n scattering lengths:

$$\frac{1}{a_{nn}} = \frac{1}{a_{pp}} + \frac{1}{R}\left(\ln \frac{R}{r_{oS}} - 0.33\right)$$

(where R is the proton Bohr radius $\frac{\hbar^2}{Me^2}$ = 28.8 fm and r_{oS} is the effective range -2.82 fm); this gives -17 fm for a_{nn}.

This expression corrects for the Coulomb part which, of course, is most important. Heller, Signell, and Yoder have examined various potentials and concluded that on the basis of charge symmetry a_{nn} probably falls in the range -16.6 fm to -16.9 fm (He 64).

Šlaus (Šl 67a) has reported that with the existing experimental and theoretical uncertainties the value of a_{nn} is consistent with the assumption of charge symmetry within 1.5%.

Now look at charge independence. Henley and Morrison (He 66b) claim that the mass differences between neutral and charged mesons are able to

*Slobodrian's value of the scattering length is questionable. It relies, in part, upon incorrect data (Ma 68a, No 68b).

account for a large fraction, or possibly all, of the difference between the measured n-n and n-p scattering lengths. They also point out that a better theoretical framework for low-energy scattering will be necessary to make firmer theoretical statements concerning the origin of the discrepancy, if any, in the scattering lengths.

If charge independence holds, the effective ranges for p-p and n-p scattering should differ by about 0.1 fm. The p-p effective range is about 2.8 fm. In 1963, Engelke, Benenson, Melkonian, and Lebowitz (En 63) made exceedingly precise total n-p cross-section measurements at nominal energies of 0.4926 MeV and 3.200 MeV. They deduced from these measurements, and the accepted values of the deuteron binding energy, the coherent scattering length, and the free neutron-proton cross section, a singlet n-p effective range of 2.44 ±0.11 fm. Noyes pointed out that this was not compatible with the p-p effective range if charge independence held (No 65).

In the spring of 1968, Houk and Wilson, who have made the most precise measurement of the free neutron-proton cross section, discovered an error in their data reduction computer code (Ho 68d). The correct result now yields an effective n-p range of 2.704±0.095 fm which equals the p-p effective range, allowing for the $\pi^+ - \pi^0$ mass splitting.

Meanwhile Davis and Barschall (Da 68a) had redetermined the neutron resonance energies at which the various other groups have measured the n-p total cross section below 5 MeV. In some cases they obtained rather substantial changes. For example, the old value of 3.200±0.006 MeV changed to 3.184±0.003 MeV. Using the new energies, Davis and Barschall recalculated the singlet effective ranges for various experiments and provided a tabulation of their results. I have made a weighted average of the values given in their table and obtain 2.78±0.06 fm with a χ^2 per point of 1.0. The value for the singlet effective range is settling down a bit, but there are still rather large discrepancies between the various measurements. This subject is not closed yet.

There have been attempts to examine neutron-neutron scattering at high energies by bombarding deuterium with neutrons, subtracting the n-p contribution, and extracting the n-n total (Ri 65, Me 66) or differential cross section (Wi 63). Within the accuracies of the correction, and of the data, neutron-neutron scattering deduced from neutron-deuteron scattering resembles proton-proton scattering with the Coulomb potential turned off.

Certainly the most accessible approach to the study of the neutron-neutron interaction is by examining the final-state interactions in multiparticle reaction. There are two avenues:

1. The analysis of neutron-induced breakup, such as the D(n,p)2n and the ^{3}H(n,nd)2n reactions. These analyses suffer from a lack of theoretical understanding of details of the three-body problem.
2. The comparison procedures (Va 67c). The idea behind this is that processes leading to two final-state protons, a final-state neutron and proton, and to two final-state neutrons would be measured. A suitable model, which should be applicable to all processes and that yields the correct p-p and p-n scattering lengths, should also yield the correct n-n scattering length.

   This technique has been summarized by Šlaus (Šl 67) who explains in some detail the limitations and restrictions, and concludes with the admonition that this approach should be used with great caution.

Moravcsik has argued for direct neutron-neutron scattering measurements (Mo 64c). He has specifically investigated the information contained in a neutron-neutron scattering experiment at low energies which could be performed by colliding beams coming from an underground nuclear explosion. He shows that 10% cross-section measurements suitably distributed between 20 keV and 2 MeV can determine the sign of the scattering length with a high degree of confidence, the magnitude of the effective range to 50-70%, and the magnitude of the scattering length to about 3%. He concludes also that 10% measurements at 30 energies between 20 keV and 2 MeV would be able to get information on the potential parameters sufficiently accurately so that charge-dependent or charge-symmetry violating effects could be detected.

Dickinson and Bowman at LRL have concluded that such a measurement is feasible (Di 67). From his own experience in this business, the author agrees. As far as he can tell, however, it is not being done.

A proposal to make a neutron-neutron scattering measurement with a reactor instead of a bomb as a neutron source has been discussed by a number of individuals (Mu 63). Perhaps the most active group consists of Muehlhause of the NBS, Whittemore of Georgia, Sailor of BNL, and Dickinson and Bowman from LRL. Their proposal looks feasible, perhaps even better than the bomb proposal.

B.3 Neutron-Proton Scattering Anomaly

An n-p total cross-section measurement and an n-p differential cross-section measurement by a group from Budapest will now be discussed. These experiments will be treated separately because the results are at variance with some of the fundamental tenets of n-p phenomenology.

The first experiment is the n-p total cross-section measurement and theoretical analysis by Hrehuss and Czibok (Hr 69). They calculate that the n-p total cross section, from about 1.5-100 MeV, should have an oscillatory behavior with maximum deviations, from a smooth energy dependence, of about 5%. They claim that this behavior is demonstrated by the existing data. I do not believe that this is so. It certainly is not reflected in the phase-shift analyses of either the LRL (Ma 68b) or the Yale (Br 68) groups. With split s-wave phase shifts, these two groups both get excellent (i.e., < 1% deviation agreement with many of the most precise total cross sections. Hrehuss and Czibok have made some measurements of the n-p total cross section which, they claim, support their hypothesis.

This effect was then examined in some detail by the United States National Bureau of Standards group composed of R. B. Schwartz, R. A. Schrack, and H. T. Heaton (Sc 69). They measured the n-p total cross section from 1.5 to 15 MeV using the NBS Linac and white neutron source described previously (Sc 68). To make any fluctuations in the data more apparent they subtracted the experimental points from a smooth theoretical curve based upon the shape-independent effective range relationship:

$$\sigma = 3\pi \left\{k^2 + [1/a_t - (k^2/2)\ r_{ot}]^2\right\}^{-1} + \pi \left\{k^2 + [1/a_S - (k^2/2)\ r_{oS}]^2\right\}^{-1} .$$

The four parameters are:

a_t: triplet scattering length, 5.426 fm

a_S: singlet scattering length, -23.715 fm

r_t: triplet effective range, 1.763 fm

r_S: singlet effective range, 2.66 fm.

The result should not be sensitive to small changes in these parameters. In any case the effective range curve will be smooth and will not show an oscillatory behavior.

The NBS group then fit the difference, or deviation from a smooth effective range curve, with an expression suggested by Hrehuss and Czibok and determined that the coefficient of this expression is probably no more than 20% of the magnitude reported by the Budapest group and is indeed consistent with zero.

Schwartz and his colleagues also looked in some detail at the data quoted by the Budapest group and find that they disagree with the contention that the valid data exhibit significant fluctuations. Seagrave (Se 69a) has also reached the same conclusion for both the n-p and n-D data. The supposed oscillations are also absent from the Hanford data (Fo 69).

The n-p total cross section has also been measured recently by Clements and Langsford (Cl 69) and by Cierjacks et al. (Ci 69). No evidence was found for the supposed oscillation in either experiment.

In an effort to examine this situation in more detail, Czibok, Hrehuss, Kovacs, Nagy, and Vinnay (Cz 69) made some measurements of the differential cross sections at 2.5, 2.7, and 2.8 MeV. They claimed that they measured the ratio $\sigma(0°)/\sigma(30°)$ to be in the neighborhood of 1.048 ± 0.010. They observed recoil protons at laboratory angles of $0°$ and $15°$ and consequently really measured the $\sigma(180°)/\sigma(150°)$ ratio. Notice that a phase-shift calculation of this ratio gives ~ 1.0015 from Table I. This value should have a standard deviation of $\lesssim 0.0005$.

The implications of the Hungarian results are shattering. The phase shifts and coupling parameters are expected to have a smooth behavior and are reasonably well determined between 10 MeV and 350 MeV (Ma 68b, Br 68). The extrapolation to zero energy approaches $E^{\ell+\frac{1}{2}}$ at sufficiently low energies and should not deviate very much from this up to several MeV. The Hungarian results imply a substantial deviation from this extrapolation. In fact, they imply a large negative spike in the $^1P_1$ phase shift and consequently a large positive spike in the S-D wave coupling parameter $\bar{\varepsilon}_1$. This, if true, would be extraordinary and would be very hard for the theoreticians to explain (He 69).

Paulsen and Liskien (Pa 69), who have recently made a detailed investigation of this phenomena, are unable to uncover any evidence for the supposed fluctuations in the n-p differential cross section.

C. Conclusions

This section will be concluded with just a few general remarks about the neutron-nucleon situation. The first is that by and large it is in fairly good shape, at least with regard to elastic scattering below 450 MeV. This assumes that the results reported by the Budapest group are wrong. If they should turn out to be correct then the field is wide open. It is true that neutron-neutron scattering has not been studied directly. However, no surprises are expected there. Above about 450 MeV the situation is far worse. This area needs attention and will be discussed separately in Section III-11 entitled High Energy.

The second general remark is aimed at the experimentalists who need or will need to use n-p scattering as a nuclear standard.

The point that should be made is that the phase-shift analyses are now refined to such a degree that they can produce the best estimates of the differential cross section. Specifically, the use of the cross sections obtained from Table I should be used in preference to any other formula.

III-2. Total Cross Sections

A. Introduction

There are several reasons for measuring fast-neutron total cross sections, and a number of them will be discussed now. One motive, however, is sufficiently large that it will be given a section of its own. That motive, or reason, is the study of fluctuation phenomena that will be discussed in the following section. First, however, some of the aspects of widths that will be needed here and in the discussion of fluctuations will be reviewed. Next, the nuclear structure information that can be learned from measurements of the total cross section will be discussed. Finally, a brief view of the problems that are being pursued by several of the groups measuring total cross sections will be presented.

B. Widths

The total cross section for light nuclei bombarded by fast neutrons in the few tenths to few MeV region shows a fairly smooth behavior with superimposed sharp peaks. The sharp peaks are compound nuclear resonances and the smooth continuum is the so-called potential scattering.

The width at half maximum of the resonance is related to the mean lifetime of the state of the compound nucleus by the uncertainty relationship

$$\tau = \hbar/\Gamma \ ,$$

where τ is the mean lifetime and Γ is the width $\Gamma = \Gamma_n + \Gamma_\gamma$, assuming that we can only have neutron or gamma-ray emission.

It is possible to get a feeling for τ from a rather simple quantum mechanical picture described by Newson and Gibbons (Ne 60b).

In the keV region, $\Gamma_n >> \Gamma_\gamma$ so that $\Gamma \simeq \Gamma_n$. Then the problem is to calculate the escape probability of a neutron, which has sufficient energy, to escape from a square potential well. On each collision with the surface the escape probability is

$$P = 4\nu_\ell \; k \; K/(K + k)^2$$

$$\simeq 4\nu_\ell \frac{k}{K} \quad \text{where } K >> k \ .$$

K and k are the neutron momenta, divided by $\hbar$, inside and outside the potential well, respectively. ν_ℓ is the probability of passing a centrifugal barrier. For neutrons

$$\nu_0 = 1$$
$$\nu_1 = k^2R^2/(1 + k^2R^2)$$
$$\nu_2 = k^4R^4/(9 + 3k^2R^2 + k^4R^4) \; .$$

R is the well radius, approximately given by

$$k^2R^2 \simeq E_{cm} \text{ (MeV) } A^{2/3}/8 \; .$$

Let f be the fraction of time that the compound nucleus spends in the configuration where a neutron may escape as a free nucleon.

Then the mean lifetime is

$$\tau = \frac{t}{fP} = \frac{\hbar}{\Gamma_n} \; , \qquad \text{where } t = \frac{2mR}{K\hbar}$$

is the mean time between collisions with the nuclear surface for a neutron traveling on the diameter.

Then

$$\Gamma_n = \frac{\hbar fP}{t} = 4f \frac{\hbar k \nu_\ell}{K} \quad \frac{K\hbar}{2mR}$$

or

$$\Gamma_n = (\frac{2\hbar^2}{mR}) \; k\nu_\ell f \quad ,$$

which is an approximation to the Wigner limit

$$\Gamma_W = \frac{3}{4} (\frac{2\hbar^2}{mR}) \; k\nu_\ell \; .$$

This is the greatest width, which corresponds to the shortest lifetime, that a resonance may have.

In actual compound nuclei, the widths are usually much narrower than the Wigner limit.

The quantity of interest is usually not the width but the reduced width defined as

$$\Gamma_n^{\ell} = \Gamma_n \, \nu_{\ell}^{-1} \, (E_1/E_o)^{1/2} \; ,$$

where E_1 is the resonance energy, in eV, and $E_o = 1$ eV. The purpose of the reduced width is to remove the specific dependence of the width on the neutron wave length and the barrier penetration probability.

For S-wave neutrons the reduced width is

$$\Gamma_n^{o} = \Gamma_n \, (E_1/E_o)^{1/2} \; .$$

There are other definitions for the reduced width which are discussed by Seth (Se 66). The definition given here is, however, the most common.

Using this definition the Wigner limit of the $\ell = 0$ reduced width takes on a particularly simple value:

$$\frac{\Gamma_n^{\ell}}{f} = \Gamma_W^{\ell} = \Gamma_W \, (E_1/E_o)^{1/2} \, \nu_{\ell}^{-1} = 20A^{-1/3} \text{ keV}$$

when $R = 1.35 \; A^{1/3}$ fm.

Another quantity of interest is the strength function

$$S(\ell,J) = \langle\Gamma_n^{\ell} \, (J)\rangle / \langle D(\ell,J)\rangle \; ,$$

the average reduced width divided by the average level spacing, for neutron angular momentum ℓ, and compound nucleus spin J.

The distribution function for the reduced neutron widths is of considerable importance. For S-wave resonances in the eV range, the distribution falls off approximately exponentially as the reduced width increases. The theoretical distribution, the so-called Porter-Thomas distribution is (Po 56)

$$N(\Gamma_n^o) = (\overline{\Gamma}_n^o/\Gamma_n^o)^{1/2} \exp - (\Gamma_n^o/2\overline{\Gamma}_n^o) \ ,$$

where $N(\Gamma_n^o)$ is the number of resonances with reduced width Γ_n^o, and $\overline{\Gamma}_n^o$ is the average reduced width.

C. Structure Information from Resonance Study

Barschall (Ba 60b) has provided a good general review of this subject as it existed in 1960. This review is still useful, though the emphasis has changed and new fields have emerged during the last decade.

In a study of individual compound nucleus resonances, there are four properties of the compound nucleus state that could be determined: the energy, the angular momentum, the parity, and the width. Total cross section measurements, measured as a function of incident neutron energy, can provide information on all such properties.

The determination of these quantities can become rather subtle and even subjective. As the energy or mass number increases, the widths increase, levels overlap, and we enter the realm of Ericson fluctuation, intermediate structure, and perhaps, even more complicated phenomena. At present the assumption will be made that there are individual compound nucleus resonances superimposed upon a continuous background of potential scattering. There may even be constructive or destructive interference between the resonance and potential scattering.

The cross section can be fitted with a 1-level, 2-level, or multilevel formalism and the resulting resonance energies and widths extracted.

Some limits on the minimum and maximum angular momentum values of the compound state can be deduced from measurements of the difference in the magnitudes of the potential and resonance scattering, and the resonance width, respectively. The difference between the cross section at the resonance peak and the potential scattering cross section or, if there is interference, between the peak and the minimum, must be equal to or less than

$$\Delta = (2\pi/k^2)(2J' + 1)/(2J + 1) \ ,$$

where k is the wave number of the neutron in the center-of-mass system, J' the angular momentum of the compound state, and J the spin of the bombarded nucleus. Both J and k are known. Consequently, it is possible to deduce a minimum value of J'.

The maximum value of J can be deduced from the maximum value of ℓ compatible with the Wigner limit.

Statements about the parity can sometimes be made from total cross-section measurements. This is usually true only at the lowest neutron energies where interference between resonance scattering and potential scattering establishes the fact that the resonance is excited by S-wave neutrons. For example, if the spin of the target nucleus is zero a strong interference between potential and resonance scattering would imply the excitation by S-wave neutrons, and consequently an angular momentum of 1/2 with the same parity as the ground state of the target.

D. Giant Resonances - Past and Present

At higher energies, i.e., 1-30 MeV, and at large A values, i.e., above 10, there exist broad resonances a few MeV wide once described as "giant" resonances associated with the single-particle states predicted by the optical model. This picture is not true. It has been thoroughly demolished by McVoy (Mc 67) and by Peterson (Pe 62b) who demonstrated in detail that the observed broad maxima in the total cross sections are in almost all cases nonresonant optical-interference phenomena.

The "giant" resonances do indeed exist, but the maxima that they produce are so small compared to the optical interference effects that they show up in the total cross sections merely as minor irregularities. Consequently, if one wishes to study giant resonances, a measurement of the energy dependence of the total cross section is not the way to do it. McVoy (Mc 67) suggests that systematic measurements of the energy dependence of a particular reaction cross section over a range of A values might provide considerably more reliable evidence for the existence of giant resonances.

E. Total Cross Section Measurement Programs

Now some of the salient features of a few of the total cross section programs throughout the world will be discussed. The intention is not to supply a catalog including every group that ever measured a total cross section. The ones that will be mentioned are, however, significant and represent the field, or part of the field, reasonably well.

E.1 Foster and Glasgow (Fo 65)

This group from the Battelle Institute at the Pacific Northwest Laboratory (i.e., Hanford), Richland, Washington, has recently finished a large-scale program of measurements of fast-neutron total cross sections for 78 naturally occurring elements and 14 separated isotopes comprising almost all of the elements from H to Pu. These data are available through the brookhaven Sigma Center. They are not, however, published yet.

Using this large body of data, Glasgow and Foster recently studied the effect of nuclear deformation on fast-neutron total cross sections (Gl 69). They assumed that the phenomenological, spherical, nonlocal optical potential of Perey and Buck (Pe 62a) provides the correct energy variation of the neutron total cross sections for all spherical nuclei, and that any gross deviations of the theory from the data may be correlated with nuclear deformation.

They calculated total cross sections at 14 energies between 3 and 15 MeV using the Perey-Buck parameters (Pe 62b) for all of the measured elements and separated isotopes above ^{44}Ca.

The authors summarize their results as follows. The experimental and theoretical results agree to within 0.5-4.0% for (1) 39 spherical nuclei within $45 \leq A \leq 144$ and (2) 9 spherical nuclei within $190 \leq A \leq 209$. However, the experimental results deviate from the theoretical results by as much as 17% for (1) 15 deformed nuclei within $152 \leq A \leq 186$ and (2) 5 deformed nuclei within $228 \leq A \leq 240$.

Foster and Glasgow have been considering a calculational procedure to artificially eliminate the effects of nuclear deformation upon the phenomenological nonlocal optical potential by explicitly treating the strong coupling between the ground and excited states in a coupled-channel analysis. This calculation would be similar to that done by Marshak et al. on ^{165}Ho (Ma 68d).

E.2 United States National Bureau of Standards Group

This is one of the newest groups measuring total cross sections. Their machine and work on the n-p total cross section has already been discussed. Therefore, only a few brief comments about their general program will be included.

They are making high resolution total cross-section measurements in the energy region from 0.7-4.0 MeV (Sc 68). They have several immediate aims over and above obtaining reactor data. These include establishing a very accurate energy scale, which they feel will help resolve some discrepancies, and to look in some detail into fluctuations in the Pb total cross section.

E.3 Karlsruhe Group

Their experimental setup has already been described. Now their research program will be outlined.

This group has measured the total cross section of various elements ranging from C to Bi in the energy range of 0.5–30 MeV (Ci 68). They have studied a large number of nuclei and analyzed the individual resonances where possible and attempted to make sense of the Ericson fluctuations and intermediate structure at higher energies. They point out that the broad structure in the cross section curves at higher energies is important to the atomic energy program. Consequently, they are attempting to obtain a better understanding of intermediate structure phenomena both for the basic physics interest and to contribute to the solution of applied problems.

E.4 Lockheed Group

A relatively recent example of a nuclear structure interpretation of a total cross section measurement (Fo 66) should be included here. This group measured the total cross section for ^{15}N for neutron energies between 3.4 and 6.5 MeV corresponding to ^{16}N excitation energies from 5.5–8.5 MeV.

The authors analyzed the data using the ideas outlined in Section III-2-C. The amplitudes of the resonance structure observed in the cross section have been used to deduce limits on the J values for levels in ^{16}N.

F. Fluctuations

Many total cross-section measurements analyzed in terms of fluctuation theory have been reported recently. These will be discussed in the next section.

III-3. Fluctuation Phenomena

During the last decade there has developed a new field involved with the study of fluctuations in the energy dependence of cross sections, both total and partial, in the higher-energy regions where individual compound nucleus resonances are overlapping. There are various causes of such fluctuations: (a) Ericson fluctuations, (b) intermediate structure, and (c) fluctuations in spacings and widths of the compound-nucleus levels. Each of these will be discussed in turn. The objective here is to convey some idea of the analytical techniques and not to supply recipes for the analysis. Also when the analysis gets very involved (e.g., El 69), the reader will be directed to the literature.

Finally, some general comments will be made regarding the quality and quantity of data, concluding in an attempt at a summary.

A. Ericson Fluctuations

Ericson has shown, in a succession of paper (Er 60a, Er 60b, Er 63), that if the total cross section is measured with an energy spread that is small compared to the width of compound nucleus levels, then fluctuations would appear in the energy dependence of the cross section, even if a large number of levels overlap, as a result of interference of levels of the same spin and parity. The widths of such fluctuations should be similar to the widths of the compound nucleus levels.

Ericson neglects the fluctuations in Γ and takes it to be a constant that he calls the "coherence energy." Similarly, he neglects fluctuations in the level spacing.

With these assumptions Ericson defines the total cross section correlation function (Eq. 51 of Er 63)

$$F(\varepsilon) = \langle(\sigma^{TOT}(E+\varepsilon) - \langle\sigma^{TOT}(E)\rangle)(\sigma^{TOT}(E) - \langle\sigma^{TOT}(E)\rangle)\rangle$$

$$F(\varepsilon) = \frac{\Gamma^2}{\varepsilon^2+\Gamma^2} \kappa \frac{D_o}{\pi\Gamma} \cdot \frac{(\pi\lambda^2)^2}{(2i+1)(2I+1)} \sum_{\ell} (2\ell+1) T_\ell^2 \quad ,$$

where κ is a measure of the distribution of the partial width around its mean value and is model dependent. The value may be approximately 1 to 2. The T_ℓ are the optical-model transmission coefficients. The i and I are the spins of the incident particle and target, respectively.

Following the procedure of Brink and Stephen we find that the relationship, when applied to partial cross sections, can be simplified substantially if we take the ratio (Br 63)

$$C(\delta) = \frac{\langle\sigma(E+\ \ )\sigma(E)\rangle}{\langle\sigma(E+\delta)\rangle\langle\sigma(E)\rangle} - 1$$

$$= \frac{1}{N}(1 - Y^2) \frac{\Gamma^2}{\Gamma^2+\delta^2} \quad ,$$

where N = number of contributing independent channels and Y = the proportion of direct reactions.

If ε and δ are zero we obtain

$$C(0) = \frac{1}{N}(1 - Y^2)$$

$$F(0) = k \frac{D_o}{\pi\Gamma} \frac{(\pi\lambda^2)^2}{(2i+1)(2I+1)} \sum_{\ell} (2\ell+1) T_\ell^2 \quad .$$

These expressions are then used to obtain N (Gi 67) and Γ from the measured cross sections (Sm 69).

B. Fluctuations in Spacings and Widths of Compound-Nucleus Levels

An investigation of the effects of fluctuations in widths and spacings of compound nucleus levels has been carried out by Agodi and Pappalardo (Ag 63). These authors examine the case where the experimental energy resolution is greater than the level spacing, i.e., $\Delta > D$. Analyses of this type have been applied by Carlson and Barschall (Ca 67), and by Smith, Whalen, and Takeuchi (Sm 69).

The formation cross section for the compound nucleus averaged over an energy interval Δ_n which is much larger than the spacing and widths of the compound nucleus levels is given

$$\sigma_n = \frac{\pi\lambda^2}{\Delta_n} \sum_{J\pi} g(J) \sum_{\ell S} \sum_{i=1}^{N^n_{J\pi}} 2\pi\ \Gamma_i\ (\ell S|J\pi) \quad ,$$

where

$$g(J) = \frac{2J+1}{2(2I+1)} \quad .$$

The λ is the reduced wavelength, I = target spin, $N^n_{J\pi}$ is the number of compound nucleus levels of spin J and parity π in Δ_n. $\Gamma_i(\ell s|J\pi)$ is the partial width for neutron emission into the entrance channel with relative orbital angular momenta ℓ and channel spin S. The subscript i refers to the i^{th} level having spin J and parity π in Δ_n.

The average cross section σ_n will fluctuate for different Δ_n because of fluctuations in the number of levels or widths in that region.

A measure of that fluctuation is the variance F defined as

$$F = \langle(\sigma_n - \overline{\sigma})^2\rangle \quad ,$$

where σ_n = average cross section in Δ_n and $\bar{\sigma}$ = average compound nucleus formation cross section. Carlson and Barschall (Ca 67) have shown that, with certain assumptions, F can be expressed as

$$F = (\pi\lambda^2)^2 \sum_{J\pi} g^2(J) \frac{1}{\langle N^n_{J\pi}\rangle} [k_W \sum_{\ell S} (T^J_{\ell S})^2 + k_N(\sum_{\ell S} T^J_{\ell S})^2]$$

where

$$k_W = \frac{\mathrm{Var}[\Gamma_i(\ell s|J\pi)]}{\langle\Gamma_i(\ell s|J\pi)\rangle^2}$$

and

$$k_N = \frac{\mathrm{Var}\ N^n_{J\pi}}{\langle N^n_{J\pi}\rangle} \quad .$$

The assumptions are: (1) the shape of the distributions over which the variance is taken is the same for the various quantum numbers, (2) for a given level partial widths for different quantum numbers are not correlated, and (3) the spacings of levels with the same quantum numbers are not correlated.

In these equations, F is determined from the experiments. The transmission coefficients are calculated using the optical model. If the neutron width and level spacing distribution are known, the quantities k_W and k_N may be calculated.

The quantity $\langle N^n_{J\pi}\rangle$, which is essentially the level density, is treated as an unknown. Carlson and Barschall break this up into an energy dependent factor $\omega(E)$ and a spin-dependent factor $H(J\pi)$ using a level density expression given by Gilbert and Cameron (Ca 67).

Finally one ends up with an expression for the variance of

$$F\Delta_n = (\pi\lambda^2)^2 \frac{1}{\omega(E)} \sum_{J\pi} \frac{g^2(J)(T^J)^2}{H(J\pi)} \ [k_W + k_N] \ .$$

This expression can be calculated for various subdivisions of the interval Δ_L and for various intervals, δ, of the compound-nucleus-formation cross section.

Using this procedure the level densities can be deduced and compared with those given by Gilbert and Cameron (Gi 65c).

Intermediate structure will be discussed, however, before any general comments about the success of these efforts.

C. Intermediate Structure

In this discussion the term "intermediate structure" will apply only to the phenomenon interpreted in terms of the so-called doorway states. Historically the distinction between the phenomenon and the interpretation has been ambiguous. In the early days (i.e., before 1964) of intermediate state phenomenology, it was common practice to attribute any structure intermediate in width between compound nucleus resonance width and broad high-energy widths to the doorway states. This is dangerous, and there is no longer much justification for such a cavalier approach. Singh, Hoffman-Pinther, and Lang (Si 66) have shown that width alone is not a good criterion in making an identification of the origin of the observed structure. They developed a computer program to generate cross sections with parameters chosen in a random fashion from preset distributions. They found that they could generate spurious intermediate "structures." In fact, in a sample whose width is 25 Γ_{cn} there is a 30% chance of finding a resonance 6 Γ_{cn} wide with a $\sigma_{peak} = 1.4$ $\sigma_{average}$.

A quantitative approach to the analysis of intermediate structure has been suggested by Pappalardo (Pa 64a). He defines an average cross section $\sigma_\Delta(E)$ where Δ is the interval of average. He then defines an auto-correlation function

$$C(\varepsilon,\Delta) = \left(\frac{\sigma(E)}{\sigma_\Delta(E)} - 1\right)\left(\frac{\sigma(E+\varepsilon)}{\sigma_\Delta(E+\varepsilon)} - 1\right) .$$

$C(0,\Delta)$ can be plotted versus the averaging interval Δ. It has the general form

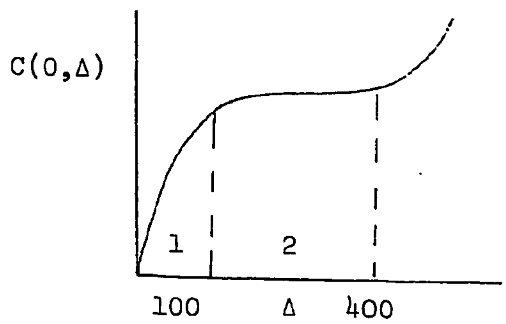

This curve can be understood as follows.

1) When Δ < width of the statistical fluctuations, the average curve follows these fluctuations. Then $C(0,\Delta)$ is small and tends to increase with increasing Δ.

2) When Δ > width of statistical fluctuations then $C(0,\Delta)$ is approximately independent of Δ and $C(0,\Delta)$ is roughly constant with increasing Δ.

3) If there is further, much broader structure, then $C(0,\Delta)$ will again increase as Δ becomes comparable to the width of such structure.

The technique then is to look for the second rise, which is indicative of further structure which may be the intermediate structure.

Unfortunately, there can be a very serious limitation produced by an uncertainty arising from the limited statistical sampling of a finite energy range of data. This effect has been examined by Hall (Ha 64), by Gibbs (Gi 65a , Gi 65b), and by Halbert et al. (Ha 67) and is called FRD.

If FRD is not a serious problem in a particular set of data, then the analysis can proceed by computing values for the auto-correlation function $C(\varepsilon,\Delta)$ for various values of ε and examining the results for evidence of intermediate structure.

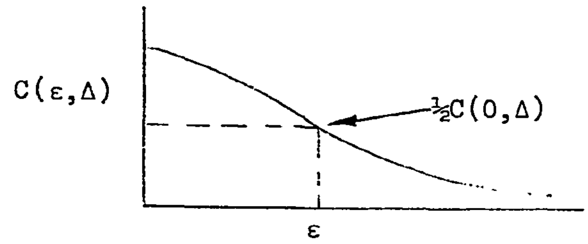

The uncorrected value of Γ is the value of ε for which $C(\varepsilon,\Delta)$ has half the value of $C(0,\Delta)$. The various corrections to Γ include effects of energy spread and counting statistics.

The corrected Γ's can then be compared to theory (Fe 67a) to see whether there is evidence for intermediate structure.

D. General Comments

Carlson and Barschall (Ca 67) have noted that the expressions for the cross-section variance for the case of fluctuations in the level spacings and widths is similar to the variance as calculated for Ericson fluctuations. This means that Ericson fluctuations produce effects in the total cross section similar to the effects produced by fluctuations in the compound nucleus level widths and spacings. In fact, Ericson's assumption of equally spaced levels, used in Section A, is equivalent to setting $k_N = 0$ in the expression for the variance used in Section B. It should be pointed out, however, that the effects on the partial cross sections are not the same. More will be said about this later.

There appears to be some confusion in some circles about whether intermediate structure exists. Feshbach, Kerman, and Lemmer (Fe 67) have made a detailed study of intermediate structure and report most of the evidence as of 1967. Certainly intermediate structure exists. Analog states are perhaps the most conspicuous examples; however, there are others. With the exception of analog states, and probably the elegant experiment and analysis of Fe by

Elwyn and Monahan (El 69, Mo 68a), no really clear-cut examples of intermediate structure have appeared from neutron experiments. This, of course, does not deny the existence of intermediate structure. This just means that such states do exist in certain nuclei under very specific circumstances. Feshbach and his colleagues (Fe 67) hasten to point out that there is no *a priori* reason for expecting intermediate structure to be a universal phenomenon.

A search for doorway states would be expected to be most fruitful at low energies where only a few processes are energetically possible. Also studies with closed shell nuclei and light nuclei should have a better chance of success. In addition, under these circumstances the doorway state density is low, with the consequence that they would be more obvious.

On the other hand, the intermediate structure in heavier nuclei would be more interesting because in these cases it will depend more critically upon the details of nuclear structure and nuclear interactions.

Actually it would be desirable to learn as much as possible about intermediate resonances apart from knowing that they exist in a particular nuclear reaction. For example, spin and parity assignments, differential cross sections, and particularly correlations between the structure in different reaction channels leading to the same compound nucleus. One characteristic that should be exhibited by doorway states is that the resulting structure should appear in all reaction channels that connect to the compound nucleus through the same doorway.

Several cross section measurements were analyzed for doorway state evidence. In some cases the evidence was either not completely clear or not convincing (Ma 65, Se 65, Fa 66). In others there appeared to be no evidence, or requirement, for intermediate structure (Ca 67, Gr 69). A few showed tantalizing examples of what probably is intermediate structure (Mo 67, Ba 68a, El 68, Mo 68).

One conclusion, immediately apparent from a survey of the various measurements, is that it is absolutely necessary to study the various partial cross sections to make convincing statements about the existence of intermediate structure. Without evidence for correlations in fluctuations for different reaction channels, it is relatively easy to attribute the observed structure to other phenomena.

The most likely candidate as a source of structure is in Ericson fluctuations. Many experiments have been interpreted, more or less successfully, in the context of this theory (Co 62, Fa 62, Er 63, Ts 64, Gr 69).

On the other hand, the fluctuations may be due to fluctuations in the nuclear level densities. Calvi (Ca 63) among others pointed out that while in the Ericson theory fluctuations for reactions with the same entrance channel but different exit channels are uncorrelated, this is not the case for structure due to fluctuations in the level densities of the compound nucleus. In this case the fluctuations of the cross sections for various reactions for which the same states of the intermediate system are excited are strongly correlated, regardless of which extrance and exit channel is considered.

E. Summary

It is extremely difficult to make a concise and useful summary of the situation in fluctuation analysis with neutrons. The whole field is clouded and confusing. It is time to re-examine the theories in light of the recent experiments, try to make a unified picture, and give some guidance with regard to the most sensible experimental programs.

III-4. (n,n) and (n,n')

The study of elastic and inelastic scattering occupies a substantial amount of time and effort. It also encompasses some very diverse interests.

A brief survey of 50 reprints was taken to see what the purposes were for the various investigations. The survey netted these results:

- 8% Studies of very light nuclei
- 50% Cross section studies for nuclear energy programs
- 15% Optical-model studies
- 15% Statistical model studies
- 12% Nuclear spectroscopy and miscellaneous studies

I will use this breakdown and will discuss the various topics in order.

A. Studies of Very Light Nuclei

This field has been reviewed in detail recently: at the 1967 Brela meeting on Few-Body Problems, Light Nuclei, and Nuclear Interactions, and at the 1969 Birmingham Conference on the 3-Body Problem. The proceedings of the Brela Conference have been published (by Gordon and Breach) and the proceedings of the Birmingham Conference will be published (by North Holland). Consequently, in the light of the proliferation of published proceedings of meetings on this subject, only a very cursory survey will be presented.

A rather detailed view of the two-nucleon system has already been presented. Therefore, the discussion will start with the 3-nucleon system.

Perhaps the experimental situation can be summarized by saying that we need really good n-D and p-D elastic scattering data so that accurate and unique phase shifts can be extracted and compared with theory based upon the Faddeev approach. We also need more so-called kinematically complete 3-nucleon breakup experiments and better theories to explain them (Ph 67).

A major need, felt by purveyors of reviews of this business, is a closer coordination between the experimentalists and theoreticians with regard to sensible interpretation and guidance of investigations (Se 69b).

The situation with regard to light nuclei, involving 4-, 5-, 6-, and 7-nucleon systems is improving rapidly. There is a large effort underway now at LASL to study the 4- and 5-body systems with some interest also on 6- and 7-body systems. Most of this is with charged-particle work and takes us somewhat afield of the main theme. The fast-neutron effort, however, has been summarized by Seagrave at the Brela Conference (Se 67).

B. Cross Section Studies for Nuclear Energy Programs

These are immediately useful experiments that provide important design information to scientists and engineers engaged in the atomic energy industry. In a very real sense, it is just these experiments that provide the justification for support of more esoteric endeavors of neutron physicists.

Actually a great deal of interesting physics is contained in these experiments. For example, it was the systematic study of total neutron cross sections which lead to the adaption of the optical model to the low MeV region (Ba 52).

Below 1.5 MeV the field is dominated by the Argonne group under the direction of A. B. Smith. Their experimental facility has already been described, and Cox has recently summarized their cross-section program (Co 68c).

Above 1.5 MeV there is activity at Duke (Wi 65), Rice (Bo 69a), Case-Western Reserve (Sh 69), LRL (Ba 67), LASL (Dr 69b), ORNL (Pe 69a), Texas Nuclear Corporation (Tu 69), Ohio University (Be 67a), University of Kentucky (Re 67a), and Wisconsin (Ro 69b) in the U. S. In addition, there are active groups at JAERI (Ts 69) in Japan, AWRE (Ow 68) and AERE (Ma 68e) in the U. K., Geel (Kn 67) in Belgium, Studsvik (Ho 68a) in Sweden, Grenoble (Pe 69b) and Cadarache (Le 67) in France.

This is not a complete list, and the references are only general guides to the literature to get one started if they are interested in pursuing a survey of the programs of the various laboratories.

The general experimental procedure is to measure the cross sections, usually by time of flight, including appropriate corrections for attenuation and multiple scattering. The results are then compared with optical-model codes, such as ABACUS (Au 67), usually including a Hauser-Feshbach (Ha 52) calculation of the shape elastic and compound nuclear inelastic contribution. It is frequently found that better agreement with the measured inelastic cross sections is obtained by including corrections for the Moldauer width fluctuations (Mo 64a). In some cases the inelastic scattering cross sections are compared with a DWBA calculation (Ta 68). If a boil-off inelastic spectrum is present, then a comparison with the statistical model is indicated. More will be said about this later.

It is usually difficult to measure the differential cross section at very forward angles. There is, however, a lower limit that can be set for the zero degree elastic cross section. This is called Wick's limit and is easily deduced from the optical theorem. The form developed by Leona Stewart will be presented (St 65):

Since

$$\sigma(0°) = |f_R(0°)|^2 + |f_I(0°)|^2 ,$$

it follows that

$$\sigma(0°) \geq |f_I(0°)|^2 ,$$

where $f_R(0°)$ and $f_I(0°)$ are the real and imaginary parts, respectively, of the complex scattering amplitude at zero degrees.

The optical theorem states that

$$f_I(0°) = \frac{k\,\sigma_{TOT}}{4\pi} \quad ,$$

then

$$\sigma(0°) \geq \sigma_W = \frac{k^2(\sigma_{TOT})^2}{(4\pi)^2} \quad ,$$

where σ_W is the minimum 0° elastic scattering cross section.

$$k^2 = (2.187)^2 \frac{m_1 m_2^2}{(m_1+m_2)^2} E_o \; ; \quad [\text{units barn}^{-1} \text{ or } \frac{10^{24}}{cm^2}]$$

for mass m_1 incident on target mass m_2, and E_o the incident neutron energy in the laboratory system in MeV. Then

$$\sigma_W = (3.0276 \times 10^{-2}\, E_o) \frac{m_1}{(1 + \frac{m_1}{m_2})^2} (\sigma_{TOT})^2$$

in [barns/sr] with σ_{TOT} in barns.

Another point that is worth mentioning is the limit on the reaction cross section. This is a valuable tool in the evaluation of cross sections. The notation of Wu and Ohmura (Wu 62) will be used.

The scattering cross section can be written as

$$\sigma_{SC\ell} = \sum_{\ell} \frac{(2\ell+1)\pi}{k^2} |1-n_\ell|^2 \quad ,$$

and the reaction cross section can be written as

$$\sigma_r = \sum_\ell \frac{(2\ell+1)\pi}{k^2} (1-|\eta_\ell|^2) .$$

$\eta_\ell = \exp(2i\delta_\ell)$ is the "amplitude factor" or the coefficient of the outgoing wave with angular momentum ℓ. δ_ℓ is the usual phase shift.

$$0 \leq |\eta_\ell|^2 \leq 1$$

if

$$|\eta_\ell|^2 = 0 \qquad \text{then} \qquad \delta_\ell = 0 ,$$

and

$$\sigma_{SC} = \sigma_r = \frac{1}{2}\,\sigma_{TOTAL} .$$

On the other hand, if $|\eta_\ell|^2 = 1$ then $\sigma_r = 0$.

Look now at Fig. 19, a plot of $\frac{\sigma_{SC\ell}k^2}{(2\ell+1)\pi}$ vs $\frac{\sigma_{r\ell}k^2}{(2\ell+1)\pi}$ where the subscript ℓ refers to the ℓ^{th} term in the sum. The format of this plot was taken from Blatt and Weisskopf (Bl 52b). Values inside the shaded region are possible. Inside the double-hatched region $\sigma_{r\ell} > \sigma_{SC\ell}$. The chance, for each partial wave, that $\sigma_{r\ell} > \sigma_{SC\ell}$ is fairly small. The chance that $\sum_\ell \sigma_{r\ell} > \sum_\ell \sigma_{SC\ell}$ is even smaller.

Consequently, there is a rule-of-thumb that the maximum value of σ_r is 1/2 σ_T. It is not guaranteed, but it is a good guess.

C. Optical Model Studies

The object of these studies is to determine optical model parameters. The leading practitioners include Hodgson (Ho 63), Perey and Buck (Pe 62a), Auerbach (Au 67), and Rosen (Ro 65b). Many more have made less exhaustive studies of optical model parameters. This subject will not be discussed

Fig. 19. The scattering versus the reaction cross section. The values inside the shaded region are possible. Inside the double-hatched region $\sigma_{r\ell} > \sigma_{SC\ell}$.

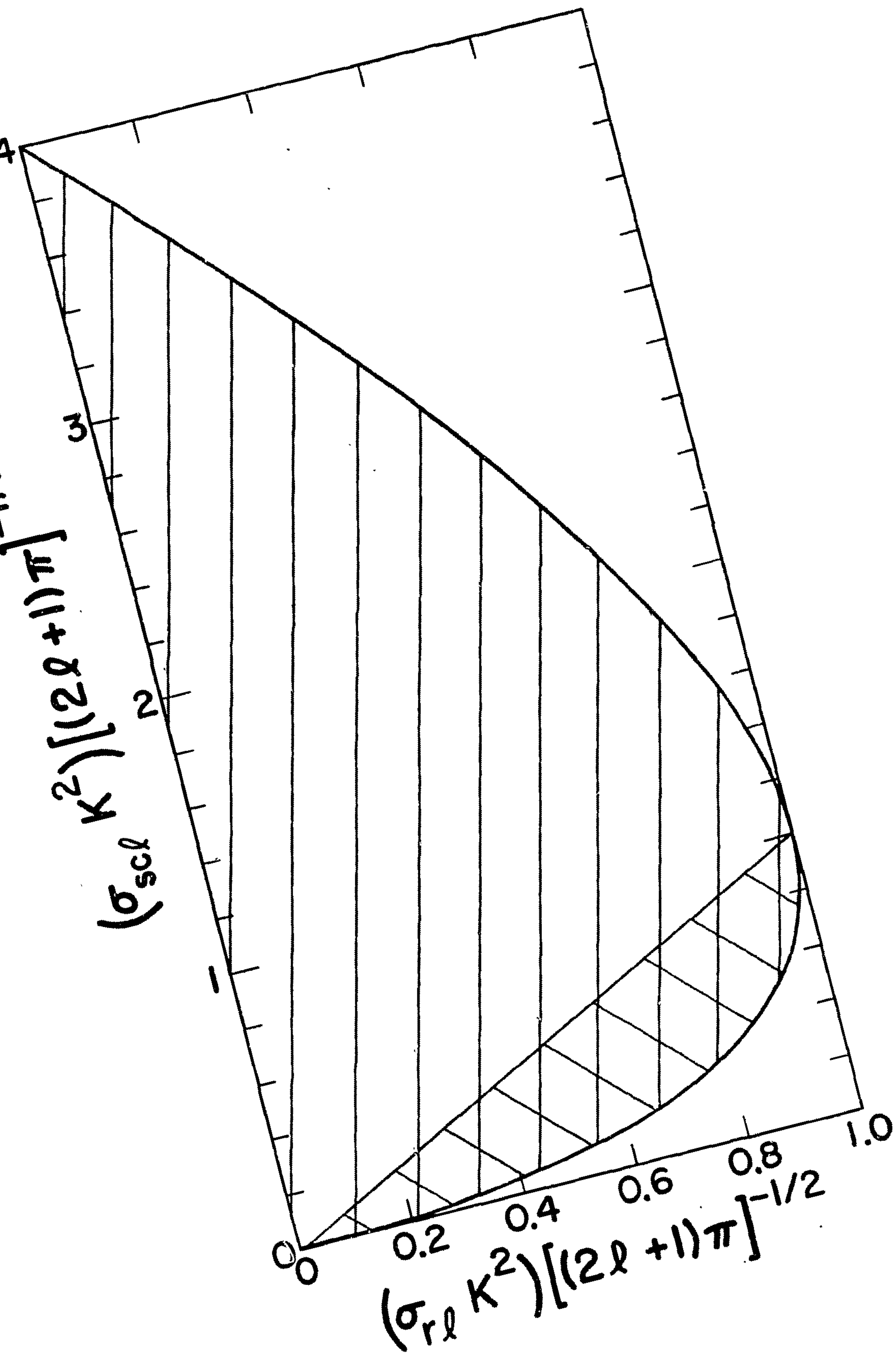

4
3
2
1
0
0
0.2
0.4
0.6
0.8
1.0
$(\sigma_{sc\ell} K^2)[(2\ell+1)\pi]^{-1/2}$
$(\sigma_{r\ell} K^2)[(2\ell+1)\pi]^{-1/2}$

Fig. 19

here. It will, however, be examined in a subsequent section dealing with polarization phenomena.

D. Statistical Model Studies

The spectrum of emitted neutrons, from the statistical model is given by

$$N(E_n) = \text{const } E_n \, \sigma_C \, (E_n, E) \, \rho(E) \ .$$

$\sigma_C(E_n,E)$ is the compound nucleus cross section for the process where the nucleus, with excitation energy E, absorbs a neutron with energy E_n. Frequently this is considered a constant. $\rho(E)$ is the level density of the residual nucleus with energy E.

Most of the statistical model studies are involved with questions of which methematical representation of the level density is appropriate to which nuclei and under what circumstances. Less frequently studied is the question of the actual form of $\sigma_C(E_n,E)$.

The usual expressions for the level density are:

1) $\rho(E) \propto \exp\,[E/T]$, and

2) $\rho(E) \propto E^{-n} \exp\,[2\sqrt{aE}]$.

T, in expression 1, is the nuclear temperature obtained from the Blatt and Weisskopf (Bl 52) thermodynamic treatment of the nucleus. This is the constant-temperature density model.

The second expression for the level density is based on the Fermi gas model. The n is sometimes taken as an adjustable parameters. Usually it is 2. The a is the level density parameter (Th 64a).

This has been examined experimentally by Thomson (Th 63) who made measurements on 20 nuclides at an incident neutron energy of 7 MeV. He compared his results with the two-level density expression and tabulated values for T and a. The data were not sufficiently sensitive to allow a determination of n. Thomson commented that the data could be fitted with $n = 0$ or $n = 2$.

Seth, Wilenzick, and Griffy (Se 64b) studied the spectra for 18 elements at 6 MeV. They found that the constant termperature model fit their data slightly better than the various other forms considered. They also observed an angular dependence of the nuclear temperature which they interpreted as a 5 to 10% contribution from direct interactions.

Buccino, Hollandsworth, Lewis, and Bevington measured the inelastic neutron spectra from 23 medium and heavy elements for incident neutron energies of 4, 5, 6, and 6.5 MeV (Bu 64). They found that the Fermi gas model, with constant level density coefficients, describes the data reasonably well for nuclei between closed shells but that the constant temperature model seems somewhat better for nuclei near the shell closures at $N = 82$, $Z = 82$, and $N = 126$. This conclusion has also been reached by Owens and Towle (Ow 68) and Maruyama (Ma 69a).

Tsukada et al. (Ts 66) looked at the level density parameters as a function of incident neutron energy and found that for some nuclei there are definite breaks in the observed parameters. For example, below the breaks the observed points fit the curves calculated by the constant temperature model while above the breaks either the constant temperature model or the Fermi gas model could produce satisfactory results.

Thomas (Th 64a, Th 64b) has examined the angular momentum dependence of the level density parameters to see whether it could account for the variation of these parameters with changes in the energy of the bombarding particle. He concluded that it could not.

Other features of the statistical theory, which will not be discussed, have been reviewed by Lang and LeCouter (La 54), Ericson (Er 60c), Bodansky (Bo 62), Cindro (Ci 66b), and by Vogt (Vo 68).

E. Nuclear Spectroscopy and Miscellaneous Studies

It is more difficult to do nuclear spectroscopy with neutrons than it is with charged particles, and when it is done with neutrons the results are likely to be inferior. Consequently, there are not many neutron spectroscopy experiments.

It is also true that when compound nuclear processes dominate the reaction mechanism, the angular distributions of inelastically scattered neutrons are usually almost isotropic. This means, of course, that it is difficult to make spin identifications from the shapes of the differential cross sections. This is not true, however, for zerp spin states in nuclei with zero-spin ground state (Cr 63a, Cr 67), where large forward-backward peaking is observed. For example, the Hauser-Feshbach calculation for the excitation of the ground state of ^{206}Pb at 2.5 MeV gives a value of 7 for the ratio $\sigma(90°)/\sigma(0°)$, symmetric about 90°.

Other attempts have been made to determine spins and parities of excited states from neutron inelastic scattering. See, for example, Smith et al. (Sm 68) and Gilboy and Towle (Gi 65d). A major problem is that to make predictions with the Hauser-Feshbach model the spins and parities of all of the levels must be known. If there are only a few levels then it is possible to try various combinations and assume that the best fit was calculated with the true set of spins and parities. Above 4 or 5 MeV in medium and heavy nuclei there are tens or hundreds of levels and it is impossible to make a proper assignment.

With the advent of Li-drifted Ge gamma-ray counters, it became easier to determine spins and parities from the resulting gamma-ray spectra. This will be discussed in more detail in Section III-7.

Johnson and Fowler at Oak Ridge (Jo 67) have measured the differential cross sections for elastic scattering from ^{16}O for incident neutrons with energies between 2.2 and 4.2 MeV. From a phase-shift analysis they assign resonance parameters for states in ^{17}O between 7.3 and 8.2 MeV excitation energy.

In another example of a structure study, Lane, Koshel, and Monahan (La 69b) have measured the polarization and differential cross section for the scattering of neutrons with energies between 0.1 and 2.0 MeV from ^{12}C. The results are simultaneously described reasonably well over this energy range in terms of a 2-level R-function formalism.

III-5. (n,2n) Cross Sections

The (n,2n) reaction has been considered an excellent example of the evaporative process (Ch 69, Ci 66b, Bl 52c). Even a relatively simple theoretical approach yields respectable agreement with most nuclei in the medium to heavy mass region. On the other hand, the attempts at a systematic understanding of the (n,2n) cross section behavior for a wide range of nuclei at 14 MeV have, until recently, been only partly successful (Hi 68).

Before the data are discussed, however, it would be appropriate to describe three experimental techniques. The activation technique is the simplest and most common method used to obtain (n,2n) cross sections. After an appropriate sample is irradiated in a beam of neutrons, the radioactive decay that is characteristic of the nucleus that resulted from an (n,2n) process is counted. Usually relative measurements are made against some standard cross section, such as $^{63}Cu(n,2n)$, so that it is not necessary to know the actual neutron flux.

Another technique, which is a great deal more involved, is actually to count the 2 neutrons emitted in the (n,2n) process (As 63, Ho 69c). This usually means surrounding the sample with a 100% efficient neutron detector. The closest thing to such a detector is a large liquid scintillator.

A neutron, upon entering the detector, is thermalized in a few microseconds and diffuses in the scintillator until it is finally captured by a Gd nucleus producing a large pulse due to the capture gamma radiation.

In the technique developed by Holmberg and Hansén (Ho 69), the time between two successive liquid scintillator pulses was measured in the range up to 40 μsec. For an (n,2n) event there is a time correlation between the capture pulses of the two neutrons which is absent for the random background.

The incident neutron flux was measured by means of a plastic scintillator, located at the sample position and surrounded by the large liquid scintillator tank.

The rather complicated electronic arrangements and data handling techniques that are required to extract (n,2n) cross sections from the observed quantities are discussed in detail in the published report of this experiment.

The two neutrons can also be detected in coincidence by two or more small scintillators (Vo 69). The advantage of such a system is that the angular correlations in the two outgoing neutrons can be studied. The obvious disadvantage is that the counting rates are very small.

A third technique used to measure (n,2n) cross sections is the time-of-flight method (An 65, Ma 69b). The usual time-of-flight technique is used to obtain the neutron emission distribution as a function of energy. Some model then has to be adopted to reduce the emission spectrum to one-neutron and 2-neutron emission cross sections. This is a controversial procedure.

Lang and LeCouteur (La 54) have derived the following expressions, used by Mathur et al. (Ma 69).

The energy distribution for the emission of the first neutron can be expressed as

$$N_1(E) = C_1 E^{5/11} \exp(-12E/11\theta_1) .$$

θ_1 is the temperature associated with the emission of the first neutron. C_1 is a constant. $N_1(E)$ is the higher energy part of the observed neutron distribution. θ_1 is derived by fitting this expression to the data.

The cross section is

$$\sigma(E) = C_1' E \exp(-E/\theta) .$$

C_1' is a new constant, evaluated in such a way that the emission cross section in the appropriate region is twice the (n,2n) cross section. The assumption is made that a neutron will always be emitted when energetically possible. Cohen has shown, surprisingly, that this is not true (Co 68a). However, in most cases the error in making this assumption would be negligible.

To obtain the statistical model parameters and cross section for the emission of the second neutron, the calculated distribution for the first neutron is subtracted from N(E), the entire observed spectrum. From this point on, the problem is similar to that for the statistical model emission of one neutron.

Each technique has its advantages and disadvantages. The activation method is simple, but is limited to those nuclei that will yield, after the (n,2n) reaction, radioactive products with suitable emissions and half lives. The large liquid scintillator can be employed with any element. It is, however, complex to set up and use correctly. The time-of-flight technique is relatively simple to use. The disadvantage is that the interpretation of the data is model dependent.

The discussion will now turn to the results of the various measurements and will concentrate on systematics.

There have been some studies of isomeric ratios in an effort to obtain information about the distribution of spins in the compound nucleus (Va 60, Vo 64). This subject has been reviewed by Cindro (Ci 66) and recently by Károlyi, Csikai, and Petö (Ká 68). The latter group also made a number of measurements. They present values for the spin cutoff parameter, σ, which enters into an expression for the relative density of levels, and the moment of inertia of the nucleus

$$I = (\sigma^2 h^2)/T.$$

I is the moment of inertia.

σ is the spin cutoff parameter.

T is the nuclear temperature.

There have been a number of observations of shell effects in (n,2n) reactions (St 62, Ch 63a, Ch 63b, Bo 65). There also have been studies of the dependence of the (n,2n) cross sections on the asymmetry parameter (N-Z)/A, first noticed by Barr et al. (Ba 61b). Hille (Hi 68) showed that the 14-MeV data demonstrated the asymmetry parameter dependence. He also showed that the 14-MeV data alone exhibited no shell structure.

The whole subject of (n,2n) systematics has been reviewed recently by Swapna Chatterjee and Aparesh Chatterjee (Ch 69). Fortunately, they may have cleared up at least some of the puzzles.

They have made a survey of data at excitation energies of 3, 6, and 7 MeV. Three general trends emerge: (1) the gross, structureless, trend of the cross sections plotted against neutron excess, (2) a trend demonstrating the general Csikai-Petö observation (Cs 66), and (3) a trend exhibiting shell effects.

The Csikai-Petö observation is that the logarithm of the (n,2n) cross sections, for a constant (bombarding-energy)-((n,2n) threshold) energy difference, fall on straight lines when plotted against the neutron excess; i.e.,

$$\ell n \, \sigma_{(n,2n)} = k(N-Z)$$

where k is a constant.

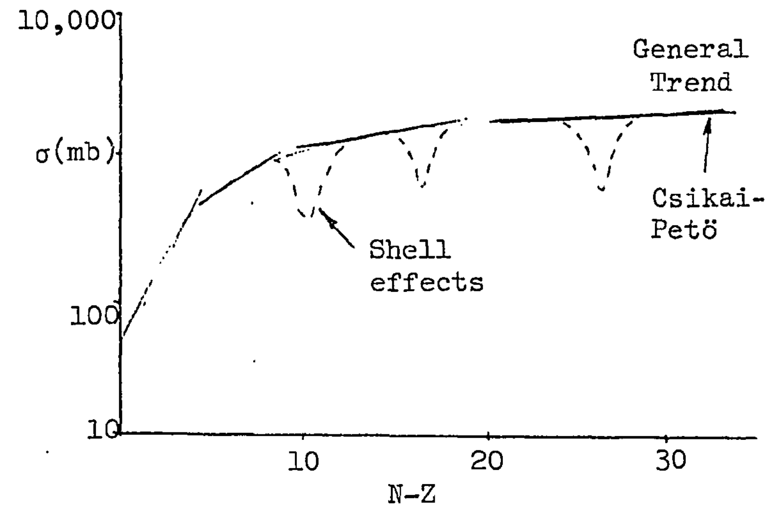

Chatterjee and Chatterjee have derived an expression for the gross trend of

$$\sigma_{(n,2n)} \simeq 45.2 \, (A^{1/3}+1)^2 \exp[-0.5 \, (\frac{N-Z}{A})] \text{ mb}$$

at 6.0-MeV excitation, above the (n,2n) threshold. At 3.0-MeV excitation the coefficient of (N-Z)/A is -2.60.

This is a phenomenological expression patterned after the general form used by Levkovskii to explain 14-MeV (n,p) cross sections (Ch 69).

The Csikai-Petö effect and the shell effect are both assumed to be due to an excitation energy shift from U to U' through a shift function f,

$$U = U' + f \; ,$$

where $f < U$. This is a technique used to account for shell effects in (n,p) and (n,α) reactions.

The f is a function of the neutron and proton level spacings, the extra core neutrons and protons, and the maximum occupation numbers of the neutrons and protons of the unfilled subshells.

The suitably shifted excitation energy has been used in a Fermi gas model to arrive at a description of the shell effects and the neutron excess, or isospin, effects.

Chatterjee and Chatterjee point out that it is necessary to normalize the excitation energies for comparison purposes and for detailed studies of the nuclear structure effects. This, of course, is the gist of the Csikai-Petö observation. They also assert that this explains why the structure was washed out in Hille's analysis of the 14-MeV data. On the other hand, Bormann (Bo 69b) contends that when the appropriate isomeric cross sections are included at the same reaction energy the evidence for shell effects disappear. Obviously the subject is not closed.

III-6. (n, charged particle)

In this section the (n,p), (n,d), (n,t), and (n,α) cross sections will be discussed. Most of the time will be devoted to the reactions involving 1 particle plus a nucleus in the final state. However, the more complicated reactions involving 2 particles plus a nucleus in the final state will be mentioned. Most of the studies that will be discussed have employed 14-MeV neutrons.

The (n,α) reaction has been studied extensively (Fa 64, Ga 64, Ch 64a) and will be discussed first. For very light nuclei, $A < 20$, the reaction, at first glance, appears predominantly direct. Between $A = 20$ and $A = 80$ the reaction is mainly compound nuclear, and above $A = 80$ the direct reaction mechanism again predominates. This is not difficult to understand qualitatively and the experiments will now be examined in some detail.

The direct reactions are fit with one or more of the reaction mechanisms for the knockout (KO) of ^4He, for the pickup (PU) of ^3He, or for heavy particle stripping (HPS). The first two are characterized by sharp forward peaking of the outgoing α particle while heavy particle stripping exhibits backward peaking.

The $^{12}C(n,\alpha)^{9}Be$ reaction, with 14-MeV incident neutrons, exhibits both forward peaking, which tends to favor the KO description, and backward peaking (Ci 66b). This would be expected from the α cluster model of ^{12}C. The $^{16}O(n,\alpha)^{13}C$ distribution is peaked in the backward direction and HPS provides an excellent fit (Ci 66). Paić, Rendić, and Tomaš have studied the $^{9}Be(n,\alpha)^{6}He$ reaction at 14-MeV neutron energy (Pa 67a). The backward peaked shape, with no forward peak, agrees reasonably well with heavy particle stripping calculations. This has been compared with the $^{9}Be(p,\alpha)^{6}Li$ reaction at E_p = 15.6 MeV. The shapes of the α distributions are similar, but the backward cross section for the (n,α) reaction is twice as high as for the (p,α) reaction. This is interpreted (Sl 67b) as being due to the fact that the ^{6}He neutron reduced width is larger than the ^{6}Li proton reduced width.

The picture presented, which was based upon the 14-MeV data alone, is an oversimplification. Recently observed excitation functions of the (n, charged particle) reactions yield structure inconsistent with the direct reaction mechanism (Bo 69b). These observations indicate the importance of having a variable energy neutron source. This point deserves some emphasis.

In the medium mass ($20 < A < 80$) region, the statistical theory, using the Fermi gas model for the level densities, can account fairly well for the energy spectra of the (n,α) reactions. There are exceptions, however, For example, Liskien and Paulsen (Li 65), who measured the excitation function for the reaction $^{63}Cu(n,\alpha)^{60}Co$ in the neutron energy range 12.5-16.5 MeV find that statistical model calculations are off by factors of 2-4. There is also a small direct reaction component, roughly constant throughout the periodic table, which may, however, be a surface effect. The cross section does show a slight increase, which would be expected from the increase of the nuclear surface, as Z increases from 70 to 90.

For heavy elements $A > \sim 80$, the compound nucleus contribution to α emission falls rapidly because of the Coulomb barrier. The only process left is the underlying direct reaction component with a relatively small cross section (300-500 μb/sr at 0° (Ku 64)). There is also some evidence that the knockout mechanism predominates (Ci 66).

Chatterjee (Ch 64a) has discussed, in some detail, shell effects in (n,α) reactions in a vein similar to that used for the description of the (n,2n) phenomena. He is reasonably successful in the description of both the general behavior of the (n,α) cross section, as a function of atomic number, and the shell structure superimposed upon the general trend. He also uses the Rosezweig shift function, to relocate the excitation energy and hence alter the level density.

Turn now to some of the other (n,charged particle) reactions.

The interpretation of the (n,p) reaction is similar to that for the (n,α) reaction. The results, however, are not as clear cut (Re 68a, Lu 68, An 67). Antolković et al. (An 67) have only limited success in explaining the $^3He(n,p)T$ reaction, with 14-MeV neutrons, in terms of a direct process where both forward and backward peaks are observed.

In the medium mass region Chatterjee (Ch 64b) again has some success in his description of the general cross section trends and shell effects; yet the results are less convincing than for the (n,α) reaction.

A substantial amount of work has gone into studies of the (n,d) reaction mechanism recently (Mi 68b, Re 68, An 67, Mi 68c, Va 67a). Šlaus and Paić have presented a compilation of the various (n,d) experiments as of 1967 (Šl 67).

As with most of the (n,charged particle) work, these experiments were studied almost exclusively with 14-MeV neutrons. The experiments were predominantly with low A nuclei.

The cross sections generally decrease with increasing A of the target, from about 10 mb/sr for A $\sim$ 10, decreasing to 0.5-2 mb/sr for A $\sim$ 50.

The analyses have usually employed the PWBA or DWBA, and the agreement between theory and experiment has been good. One problem, particularly with the very light nuclei, is in the selection of suitable optical model parameters.

Look now at the (n,t) reaction (Li 67, Fe 67, Va 67, Re 67b, Re 67c, Re 68).

There has not been a great deal of work in this field. The cross sections are fairly small ($\sigma(0^\circ-90^\circ) \sim$ 5-30 mb) and the Q values are large and negative (e.g., $\sim$-10 MeV). The most favorable conditions, as might be expected, are encountered in light nuclei.

The angular distributions of the outgoing tritons are analyzed in terms of the Newns (Ne 60a) plane wave theory, the Butler (Bu 57) plane wave theory, or the DWBA (see Fe 67). Fessenden and Maxson (Fe 67) were successful in also fitting the $^{14}N(n,t)^{12}C$ reaction with a diffraction mechanism.

The (n,t) situation can be summarized by saying that the data are sparse, but those that do exist can be fitted will with several formulations of direct reaction theory.

The last part of this section will contain a few brief comments regarding neutron induced reactions involving 3 particles in the exit channel (Ba 63, Ho 68b, Va 67). The main point that should be made is that the interpretation is rather dismal without incurring the experimental complexity of the so-called kinematically complete experiment.

It is possible to make some qualitative comments, such as for the processes $^7Li(n,t)\alpha n$, $^6Li(n,d)\alpha n$, and $^{10}B(n,t)2\alpha$ sequential decay is important. It is

Fig. 20. CN schematic diagram. This shows the general ideas involved in $(n,x\gamma)$ reactions.

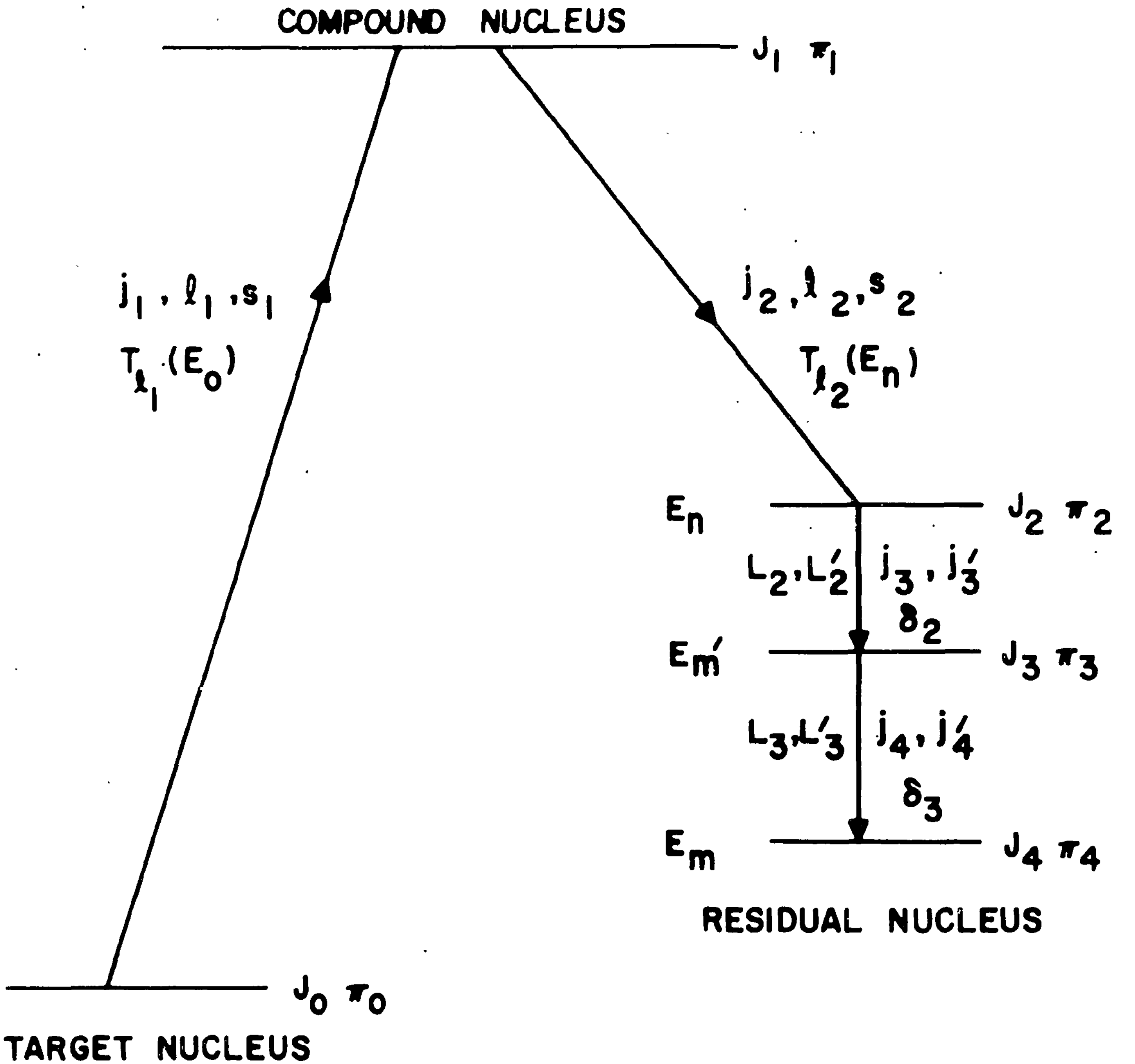
COMPOUND NUCLEUS
$J_1\ \pi_1$
j_1, ℓ_1, s_1
$T_{\ell_1}(E_0)$
j_2, ℓ_2, s_2
$T_{\ell_2}(E_n)$
E_n
$J_2\ \pi_2$
L_2, L_2'
j_3, j_3'
δ_2
E_m'
$J_3\ \pi_3$
L_3, L_3'
j_4, j_4'
δ_3
E_m
$J_4\ \pi_4$
RESIDUAL NUCLEUS
$J_0\ \pi_0$
TARGET NUCLEUS

Fig. 20

impossible to say what fraction of the decay is sequential and what fraction is 3-body breakup.

Needless to say, this area deserves more effort, theoretical and experimental.

III-7. $(n,x\gamma)$ Reactions

A. General Comments

Usually $(n,x\gamma)$ reactions are, in fact, $(n,n'\gamma)$ reactions. These processes are closely related to (n,n') inelastic scattering where the outgoing neutron is detected. When a reaction is written as $(n,x\gamma)$, it is understood that at least the gamma ray is detected. In a few rare cases, that will be described at the end of this session, both x and γ are observed in coincidence.

Studies of (n,n') reactions supply information regarding what, and how, states of the residual nucleus are formed. On the other hand, studies of the resulting gamma radiation provide information on how these same states decay. In addition, as will be seen in a particular example, studies of the gamma radiation as a function of incident neutron energy may provide information on the states of the compound nucleus. This is appropriate to light nuclei where the compound nucleus states are not overlapping at the excitation energies considered (i.e., at 7 or more MeV above the ground state of the compound nucleus).

Figure 20 shows the general ideas involved in $(n,x\gamma)$ reactions where only the γ ray is detected. The salient features are as follows:

1) There is a target nucleus with angular momentum J_o, parity π_o, bombarded by neutrons ($S_1 = 1/2$) with orbital angular momentum ℓ_1.

2) A compound nucleus state, $J_1\pi_1$, is excited and subsequently decays by particle emission to state $J_2\pi_2$ in the final nucleus. $T_{\ell_1}(E_o)$ and $T_{\ell_2}(E_n)$ are the optical model transmission coefficients.

3) State $J_2\pi_2$ decays by gamma-ray emission to the ground state or to some excited state of the residual nucleus.

4) If cascade transitions are present, then there are several gamma rays resulting from a sequential decay to successively lower levels leading ultimately to the ground state.

The angular distribution of the gamma radiation is determined by a product of angular momentum coupling coefficients, one for each step of the overall process, and Legendre polynomials ultimately summed over all possible states of the compound nucleus. The magnitude is determined from appropriate transmission coefficients and statistical spin factors (Sh 66).

The general expression for a differential cross section can be written as a summation over <u>even</u> Legendre polynomials.

$$\sigma(\theta) = \sum_{L_{even}} a_\nu P_\nu (\cos\theta) .$$

It should be emphasized here that all gamma-ray transitions between any two levels are symmetric about 90° (Sh 66, Bl 52d). This follows if (1) parity is conserved in the reaction, (2) if the system in which the measurement is made makes no distinctions between right- and left-hand coordinate systems, and (3) if the parity of the wave function describing the reaction is definite.

Condition (2) is tantamount to averaging over spins. This condition is not obeyed if aligned targets or polarization sensitive detectors are used.

Similar arguments show that while the angular distribution of the gamma radiation depends upon the mulitpolarity L, it does not depend upon the parity, and hence upon the multipole character (e.g., E or M). Consequently, the angular distribution cannot yield information about the parities of the nuclear states between which the γ transition takes place.

On additional point should be made regarding the γ-ray observations. That is that the center-of-mass and the laboratory system are the same for all intents and purposes. They can be treated as identical.

Before proceeding with a discussion of the experiments, it would be appropriate to dispose of one more fact.

It used to be known that with a reaction of the type (x,yn) (where x and y are any 2 particles and n is a neutron) if y was emitted with low enough energy for a neutron to be subsequently emitted, then the neutron would come off with essentially unit probability. This belief was based upon the reasonable assumption that gamma-ray emission could not compete with neutron emission in the MeV region.

Cohen and his co-workers at Pittsburgh (Co 68b) showed that this was not always the case. In particular, they showed for ^{119}Sn and ^{61}Ni that (p,p'γ) competes favorably with (p,p'n) even when neutron emission is energetically possible by 2 MeV. This effect is not as pronounced in most scattering samples as it is in the case of Sn and Ni (Co 69). So far, however, there is no explanation for this behavior.

It should be pointed out that interpretational errors can arise where the competition between neutron and gamma-ray emission is not negligible. This could be the case, for example, in a statistical model analysis of (n,2n) cross sections as measured with a neutron time-of-flight technique.

The various experiments will now be discussed. Five active groups within the U. S. will be selected and their techniques and programs compared. Four of these, LASL, Texas Nuclear, Oak Ridge, and the University of Kentucky, use similar arrangements. The fifth, Gulf General Atomic, has developed an entirely new technique with unique features.

There are, of course, many other groups in many laboratories working on similar gamma-ray production problems. The five groups that have been chosen, however, are typical of the field.

B. LASL

The LASL facility will be described first. Their experimental setup is typical of the sophistication achieved in this field (Co 66).

Figure 21 conveys the major features. This apparatus is installed at the neutron facility of the HVEC 15-MeV tandem accelerator. The accelerator is equipped with an ORTEC klystron buncher capable of supplying 1-2 μA average beam current at a repetition rate of 5 MHz, with pulse lengths of 1 nsec. The experimental interest is mainly in the 6-14 MeV region where the $T(p,n)^3He$ reaction can be used as a clean, relatively background-free, neutron source.

The salient features include the scattering sample, the copper shadow bar and tungsten collimator, the lithium-drifted germanium detector surrounded by the large NaI(Tl) annulus, and the neutron telescope. The telescope is used to make absolute neutron flux measurements. The scatterer must be kept thin to reduce corrections for attenuation of the outgoing gamma rays. This is not much of a problem for light nuclei such as carbon or silicon, but for a sample such as tungsten the self-absorption is substantial. This correction is calculated and checked experimentally by making measurements with samples of various thicknesses.

Perhaps the most important feature is the anti-coincidence annulus. This arrangement was invented by Trail and Raboy (Tr 59) and perfected by Morgan (As 66) at Texas Nuclear. The annulus, a large NaI(Tl) detector, suppresses not only the Compton background and the various escape peaks, but also discriminates against neutron capture in the vicinity of the Ge detector.

Fig. 21. Schematic diagram of the LASL apparatus for measuring $(n,x\gamma)$ cross sections.

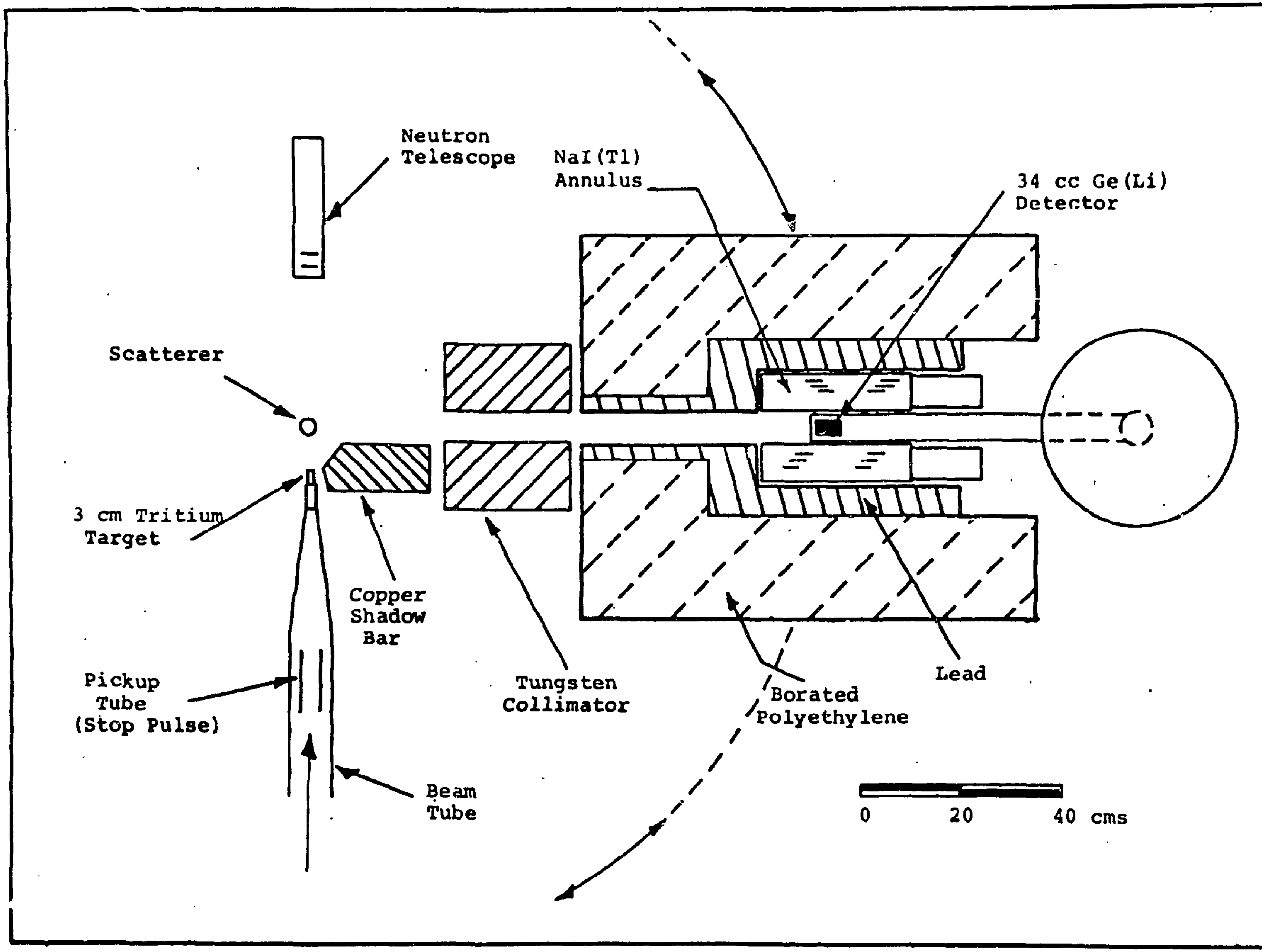
Neutron
Telescope
NaI(Tl)
Annulus
34 cc Ge(Li)
Detector
Scatterer
3 cm Tritium
Target
Copper
Shadow
Bar
Pickup
Tube
(Stop Pulse)
Beam
Tube
Tungsten
Collimator
Borated
Polyethylene
Lead
0
20
40 cms

Fig. 21

Fig. 22. A simplified LASL electronics block diagram.

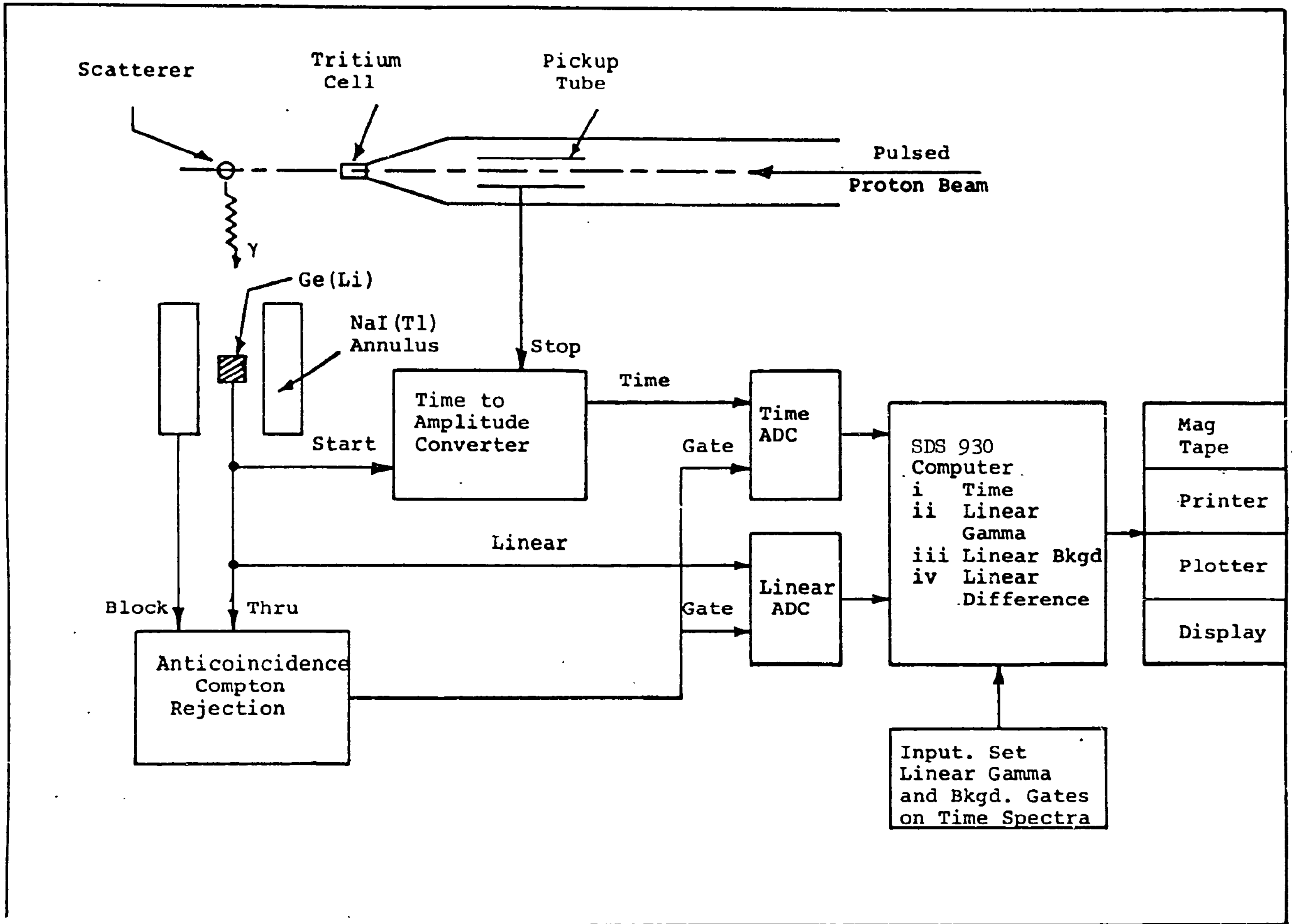

Scatterer
Tritium Cell
Pickup Tube
Pulsed Proton Beam
γ
Ge(Li)
NaI(Tl) Annulus
Stop
Time
Time to Amplitude Converter
Start
Time ADC
Gate
SDS 930 Computer
i Time
ii Linear Gamma
iii Linear Bkgd
iv Linear Difference
Mag Tape
Printer
Plotter
Display
Linear
Linear ADC
Gate
Block
Thru
Anticoincidence Compton Rejection
Input. Set Linear Gamma and Bkgd. Gates on Time Spectra

Fig. 22

Fig. 23. The 55° gamma-ray spectrum, taken at LASL, from natural silicon bombarded by 9-MeV neutrons.

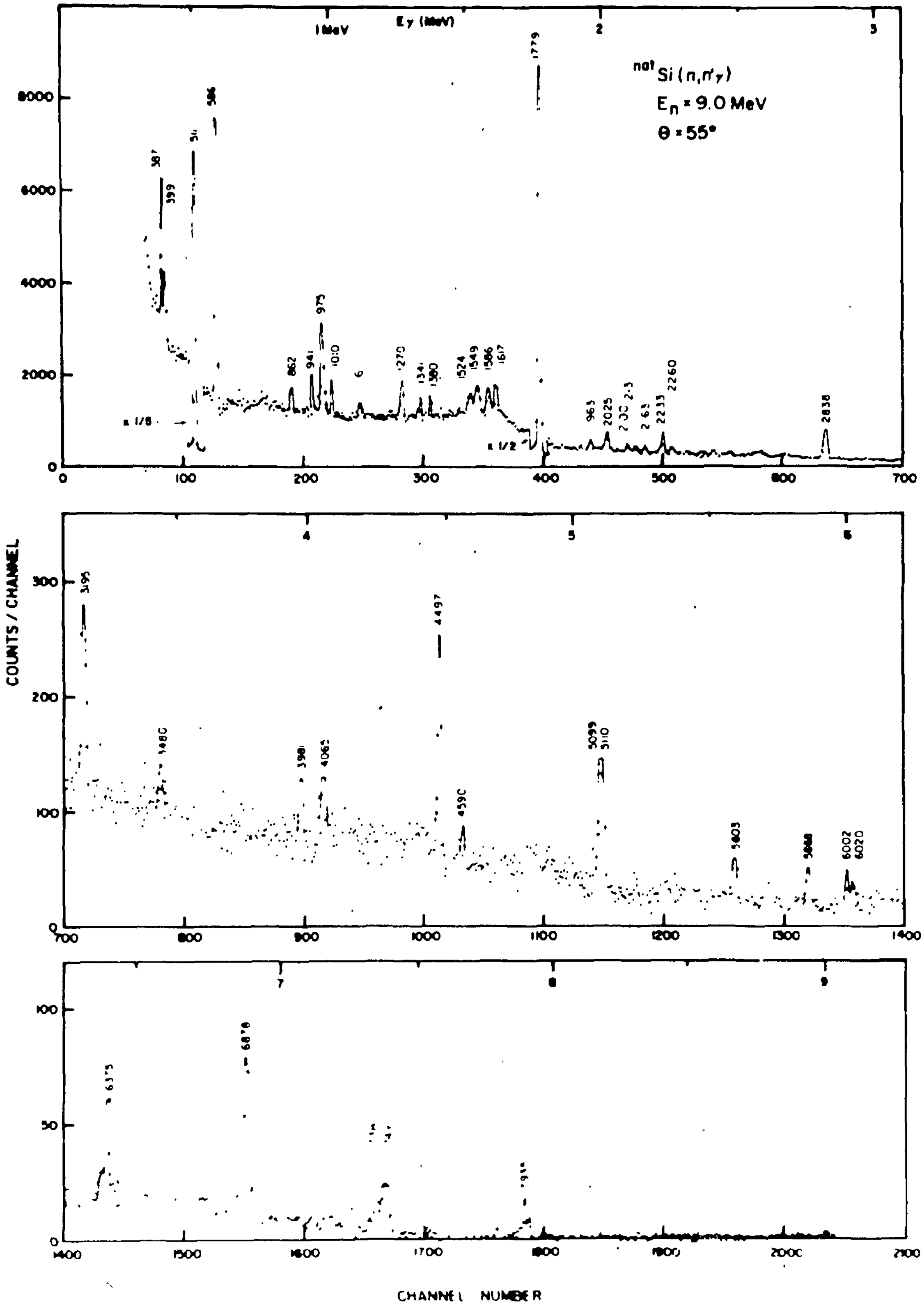

Fig. 23

Fig. 24. The cross sections for inelastic neutron scattering from the 4.44-MeV level of ^{12}C as a function of neutron energy are shown in the middle. The levels in the compound nucleus ^{13}C are shown on the left. Gamma-ray angular distributions for four incident neutron energies are shown on the right.

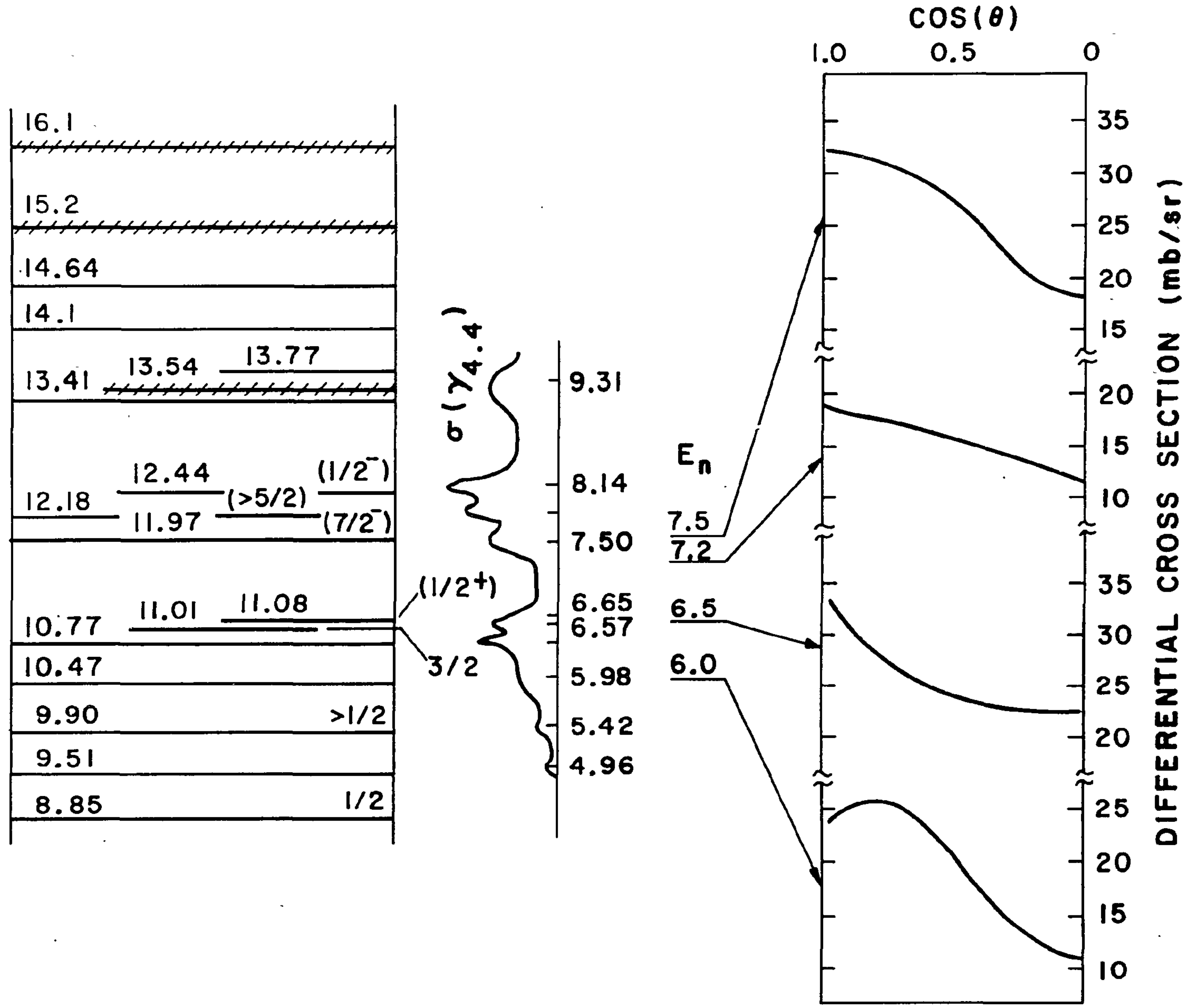

16.1
15.2
14.64
14.1
13.41
13.54
13.77
12.18
12.44
11.97
(>5/2)
(1/2⁻)
(7/2⁻)
10.77
11.01
11.08
(1/2+)
3/2
10.47
9.90
>1/2
9.51
8.85
1/2
σ(γ4.4)
9.31
8.14
7.50
6.65
6.57
5.98
5.42
4.96
En
7.5
7.2
6.5
6.0
COS(θ)
1.0
0.5
0
DIFFERENTIAL CROSS SECTION (mb/sr)

Fig. 24

This, of course, is particularly important for experiments involving high-energy neutrons and complicated gamma-ray spectra.

Figure 22 shows a simplified electronics block diagram. Time and energy spectra are recorded and stored by an on-line SDS 930 computer.

Figure 23 shows an example of the gamma-ray spectrum at 55° from natural silicon bombarded by 9-MeV neutrons.* More than 40 gamma rays are clearly resolved and there are indications of several others. The purpose of this slide is to show how clean these spectra really are, and to emphasize that the Ge detectors provide a very powerful tool.

Several of these gamma rays do not result from $(n,n'\gamma)$ reactions. The $^{28}Si(n,p\gamma)^{28}Al$ and $^{28}Si(n,\alpha\gamma)^{25}Mg$ reactions are energetically allowed, and a number of gamma rays have been attributed to transitions in the final nuclei ^{28}Al and ^{25}Mg. Notice that this technique can be used to study the (n,charged particle) reactions discussed previously.

An experiment designed to study levels in the compound system will now be discussed.

D. M. Drake, at LASL, has used the angular distribution of the gamma radiation from the 4.44-MeV level in ^{12}C to deduce spins of levels in the compound nucleus ^{13}C.

Figure 24 shows the cross sections for inelastic neutron scattering from the 4.44-MeV level of ^{12}C as a function of neutron energy. The left side shows the locations of various levels, while the right-hand side shows the differential cross sections for the 4.44-MeV gamma radiation for 4 different incident neutron energies. The 6-MeV data will be used as an example for the analysis.

*These data were taken at LASL in collaboration with the Texas Nuclear Corporation.

The ^{12}C ground state is 0^+ and the first excited state at 4.44 MeV is 2^+. Since 6 MeV is only about 1 MeV above the threshold for excitation of the 4.44-MeV state, the most probable orbital angular momenta for the incident and scattered neutrons are $\ell = 2$ and $\ell = 0$, respectively. This requires j to be either 5/2 or 3/2 for the incident neutron and j = 1/2 for the scattered neutron. The orbital angular momentum has no component along the direction of the beam, and only the neutron spin can give the projection m a nonzero value. The following table summarizes the restrictions.

	j	m		j	m
incident neutron	$5/2^+$	, ±1/2	or	$3/2^+$	, ±1/2
scattered neutron	$1/2^+$	, ±1/2		$1/2^+$	, ±1/2

The calculated angular distributions resulting from each of these possibilities are shown in Fig. 25 along with the measured gamma-ray angular distribution.

A similar computation can be done employing the 6.13-MeV 3^- level of ^{16}O, assuming $\ell = 3$ for the incident neutron and $\ell = 0$ for the outgoing neutron. This requires the ^{17}O compound state to be either $7/2^-$ or $5/2^-$. The two distributions corresponding to these choices for the spin and parity of the compound nucleus level are shown in the right-hand side of Fig. 26. A comparison with the observed distribution, shown on the left side of Fig. 26, indicates that the compound system ^{17}O is largely $7/2^-$ for 7.5-MeV incident neutrons.

It should be pointed out that if a differential cross section is measured at only one angle, and the integrated cross section obtained by multiplying that one result by 4π, then the optimum choice of angle is usually 55° (or 125°) where $P_2(\cos\theta) = 0$.

For example, suppose

Fig. 25. The calculated angular distributions for the 4.44-MeV gamma-ray ^{12}C bombarded by 6-MeV neutrons. The various angular distributions are for various spins of the compound nucleus ^{13}C.

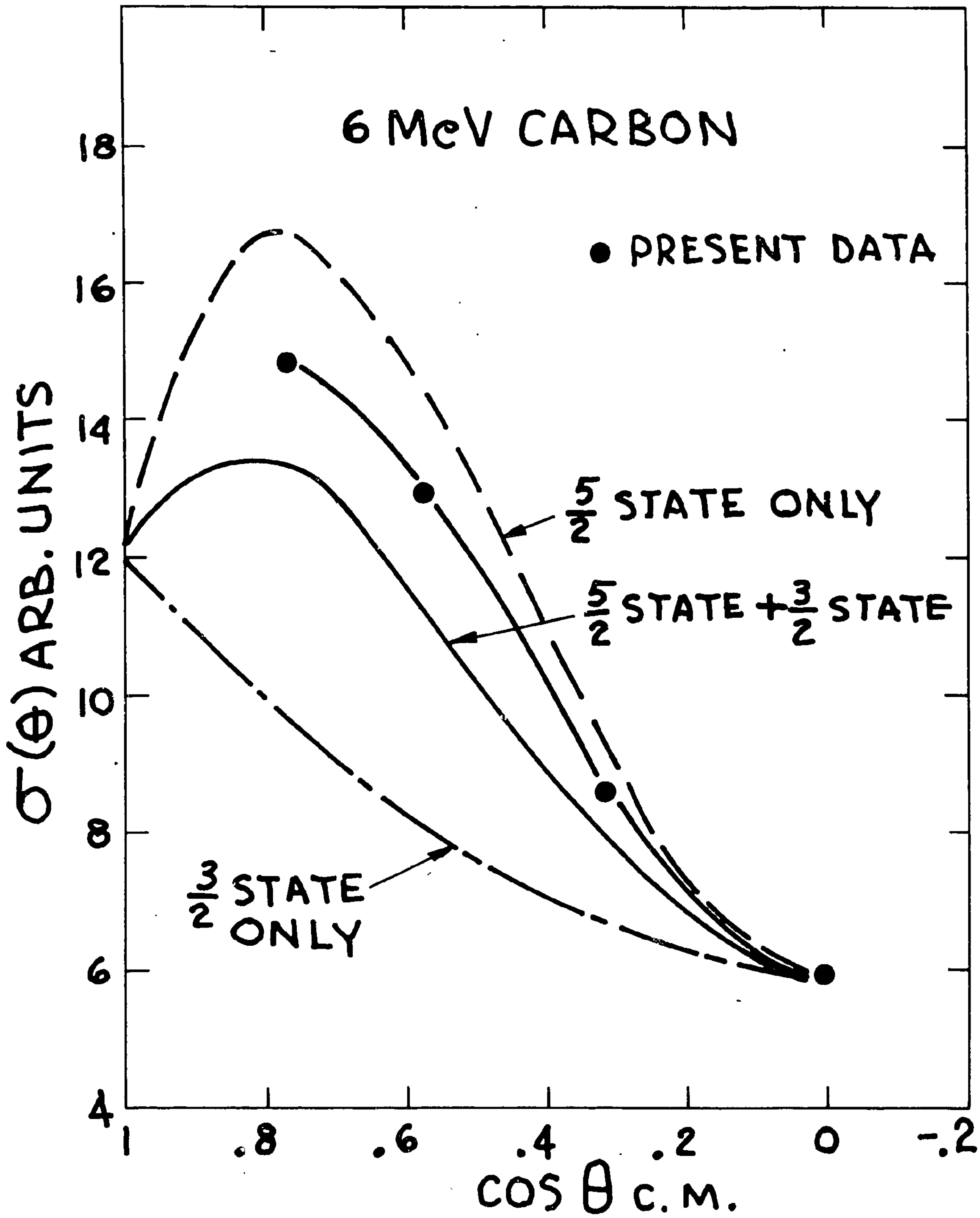

6 MeV CARBON
• PRESENT DATA
5/2 STATE ONLY
5/2 STATE + 3/2 STATE
3/2 STATE ONLY
σ(Φ) ARB. UNITS
18
16
14
12
10
8
6
4
1
.8
.6
.4
.2
0
-.2
COS θ C.M.

Fig. 25

$$\sigma(\theta) = a_o + a_2 P_2(\theta) + a_4 P_4(\theta) .$$

Usually $a_4 << a_2$. Consequently, at 55° or 125° $\sigma(55°) \approx a_o$. The cross section, integrated over angle, is $4\pi a_o$.

Occasionally 55° is not a good choice, as shown in Fig. 26. This is, however, a far better procedure than to arbitrarily assume that the 90° cross section equals a_o.

A technique developed by Drake (Dr 69a) for the extraction of neutron inelastic scattering cross sections for fissionable nuclei will now be described.

Measurements of inelastic neutron scattering from fissionable isotopes are difficult since they usually involve subtracting the spectrum of prompt neutrons emitted by the fission fragments from a measured spectrum that includes elastic, inelastic, and fission neutrons. Drake's technique is to deduce these cross sections from measurements of neutron-induced gamma-ray production.

Essentially the idea involves measuring the average total gamma-ray energy per nonelastic collision and equating this to the energy per fission times the fraction of fissions, plus the energy per inelastic scattering times the unknown fraction of inelastic collisions. The appropriate expression for this energy balance can be solved for the unknown fraction of inelastic collisions. This then can be directly related to the inelastic scattering cross sections.

Drake has compared the results obtained from his theory with experimental measurements made at LASL and elsewhere. The agreement is usually very good.

C. Texas Nuclear Corporation

The facilities and experimental programs of the Texas Nuclear Corporation will now be discussed.

Their experimental arrangement is shown in Fig. 27 (Mo 69). They have used both NaI(Tl) and Li-drifted Ge detectors surrounded by a NaI(Tl) anti-coincidence annulus. A germanium detector is pictured here along with the required liquid-nitrogen cooling system.

Figure 28 shows two time spectra taken with a 34 cc Ge(Li) detector. The top spectrum was taken without the anti-coincidence feature. The bottom spectrum was taken with the NaI annulus in anti-coincidence. This figure also demonstrates the channels used for the foreground and background, labeled "add" and "subtract," respectively.

Figure 29 shows the gamma-ray spectra from the $^{12}C(d,p\gamma)^{13}C$ reaction. The top spectrum was taken in the ungated configuration. The middle spectrum was taken with the anti-coincidence gate, and the bottom spectrum was taken with anti-coincidence and time-of-flight gating. There is only one gamma ray present, with an energy of 3.09 MeV. Notice, however, all of the structure associated with the ungated spectrum. Obviously anti-coincidence gating is a great help in unravelling complicated spectra.

Figure 30 shows a similar set of spectra resulting from the $^{56}Fe(n,n'\gamma)$ reaction. In this case, however, the ungated spectrum was not even worth showing. The top spectrum was taken in the anti-coincidence mode. The middle spectrum was taken with the anti-coincidence gating and time-of-flight gating. Notice the substantial improvement due to time-of-flight gating when neutron scattering is involved. The bottom spectrum resulted from the subtraction of a background run from the spectrum pictured in the middle.

Fig. 26. The right side shows two theoretical 6.13-MeV gamma-ray angular distributions corresponding to the excitation of a $5/2^-$ or a $7/2^-$ compound state in ^{17}O by 7.5-MeV neutrons. On the left side is the observed angular distribution which indicates that the compound system is largely $7/2^-$.

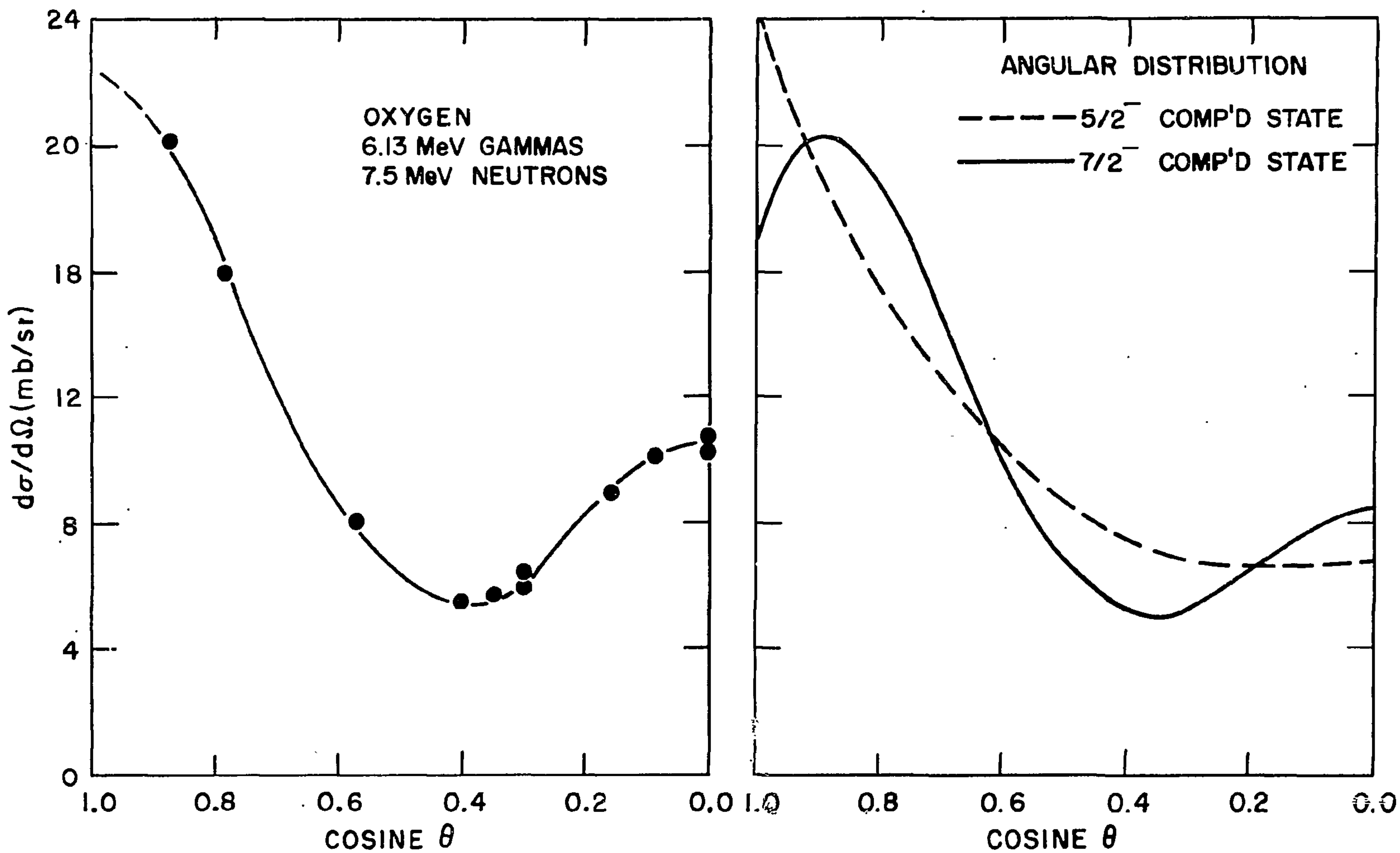

24
20
18
12
8
4
0
1.0
0.8
0.6
0.4
0.2
0.0
COSINE θ
dσ/dΩ (mb/sr)
OXYGEN
6.13 MeV GAMMAS
7.5 MeV NEUTRONS
ANGULAR DISTRIBUTION
5/2⁻ COMP'D STATE
7/2⁻ COMP'D STATE

Fig. 26

Fig. 27. The experimental arrangement used by the Texas Nuclear Corporation for studies of the $(n,x\gamma)$ reaction.

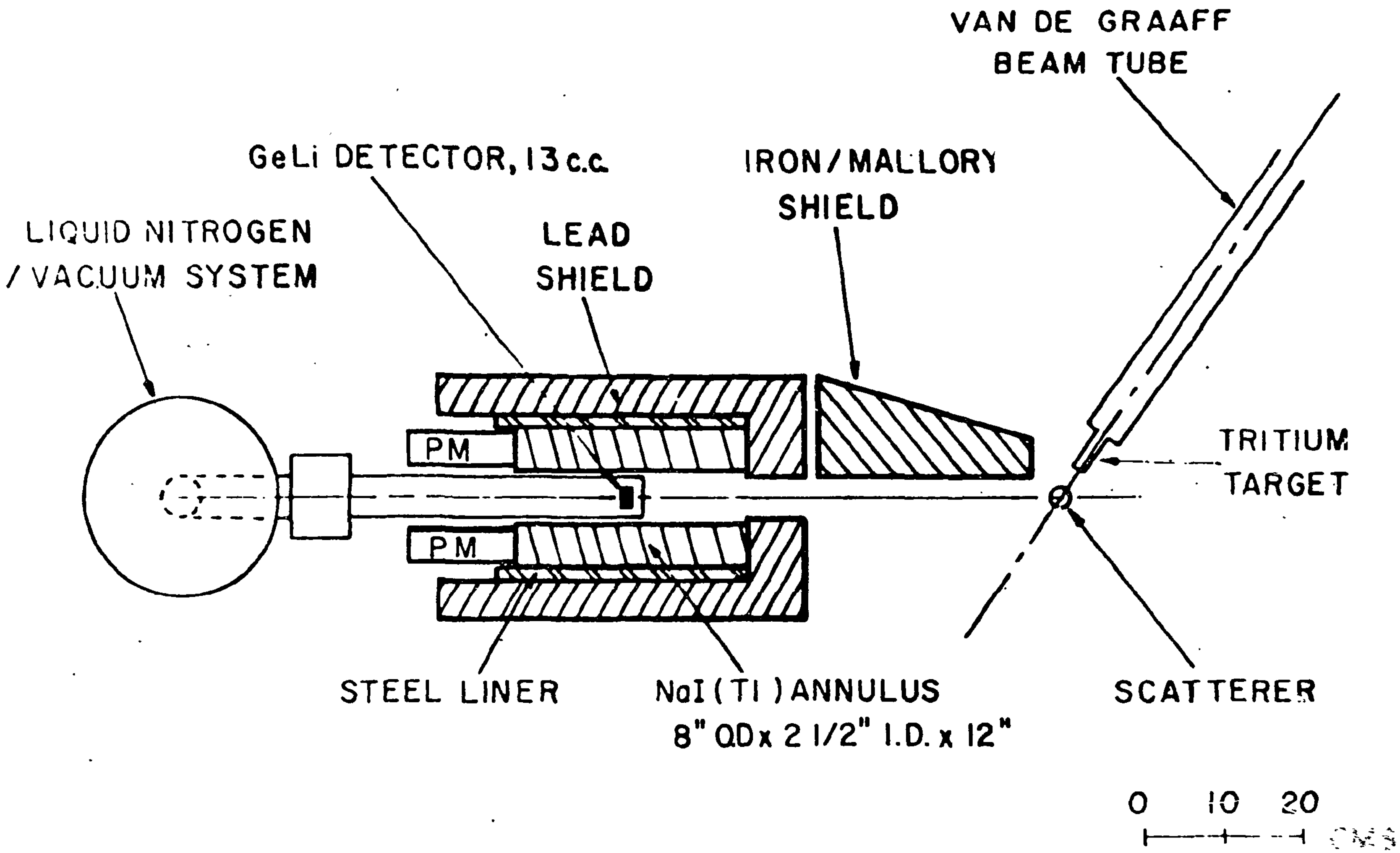

GE(LI) SPECTROMETER SYSTEM FOR $(n,n'\gamma)$ MEASUREMENTS

Fig. 2

Fig. 28. Two time spectra taken with a 34-cc Ge(Li) detector by the Texas Nuclear Corporation. The top spectrum was taken without the anti-coincidence feature. The bottom spectrum was taken with the NaI annulus in anti-coincidence.

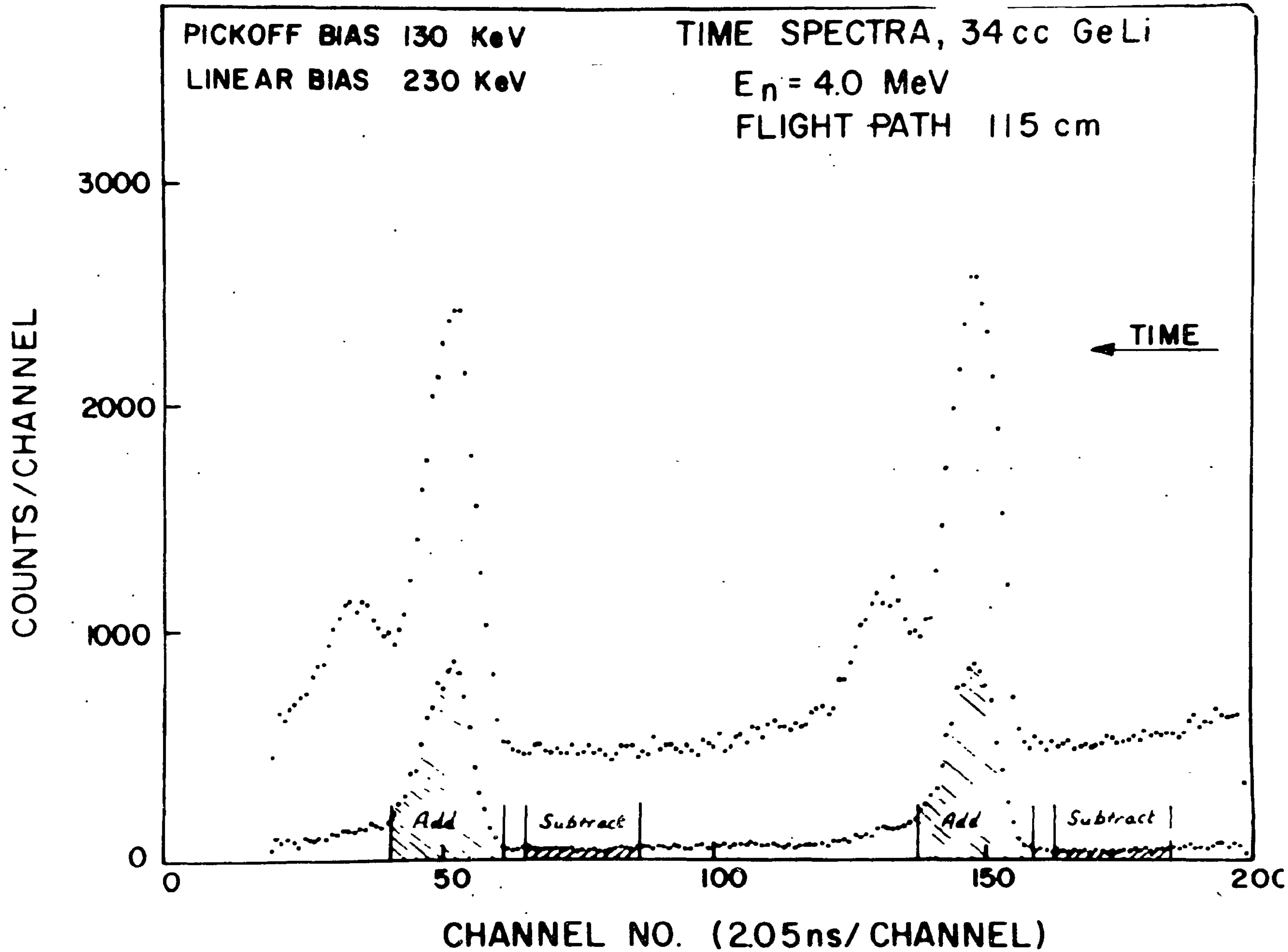
PICKOFF BIAS 130 KeV
LINEAR BIAS 230 KeV
TIME SPECTRA, 34 cc GeLi
E_n = 4.0 MeV
FLIGHT PATH 115 cm
TIME
Add
Subtract
Add
Subtract
COUNTS/CHANNEL
3000
2000
1000
0
0
50
100
150
200
CHANNEL NO. (2.05 ns/CHANNEL)

Fig. 28

Fig. 29. The gamma-ray spectra from the $^{12}C(d,p\gamma)^{13}C$ reaction (taken by the Texas Nuclear Corporation).

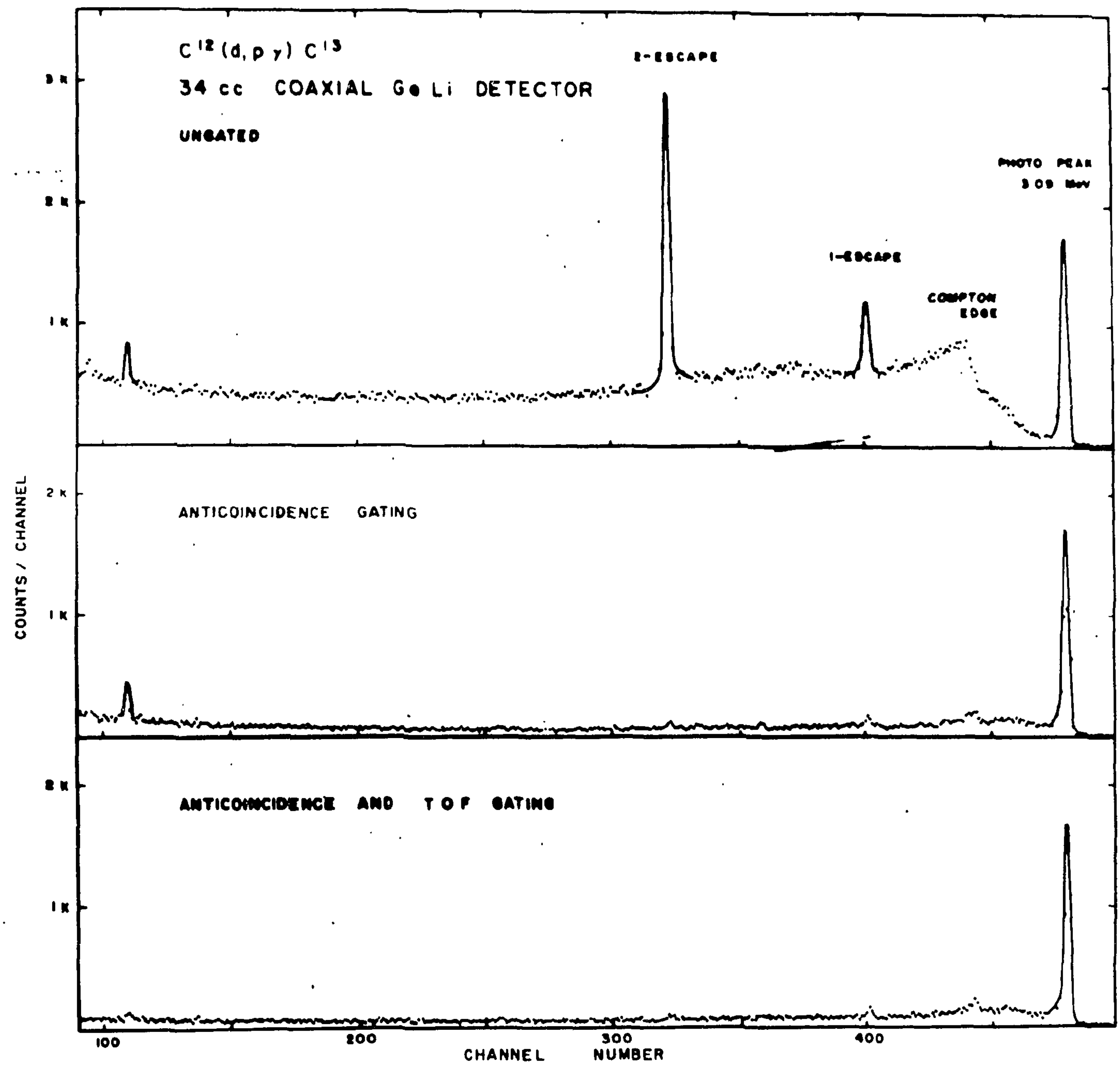

$C^{12}(d,p\gamma)C^{13}$
34 cc COAXIAL Ge Li DETECTOR
UNGATED
2-ESCAPE
1-ESCAPE
COMPTON EDGE
PHOTO PEAK
3.09 MeV
ANTICOINCIDENCE GATING
ANTICOINCIDENCE AND T O F GATING
COUNTS / CHANNEL
3 K
2 K
1 K
100
200
300
400
CHANNEL NUMBER

Fig. 29

Fig. 30. The gamma-ray spectra resulting from the $^{56}Fe(n,n'\gamma)$ reaction (taken by the Texas Nuclear Corporation).

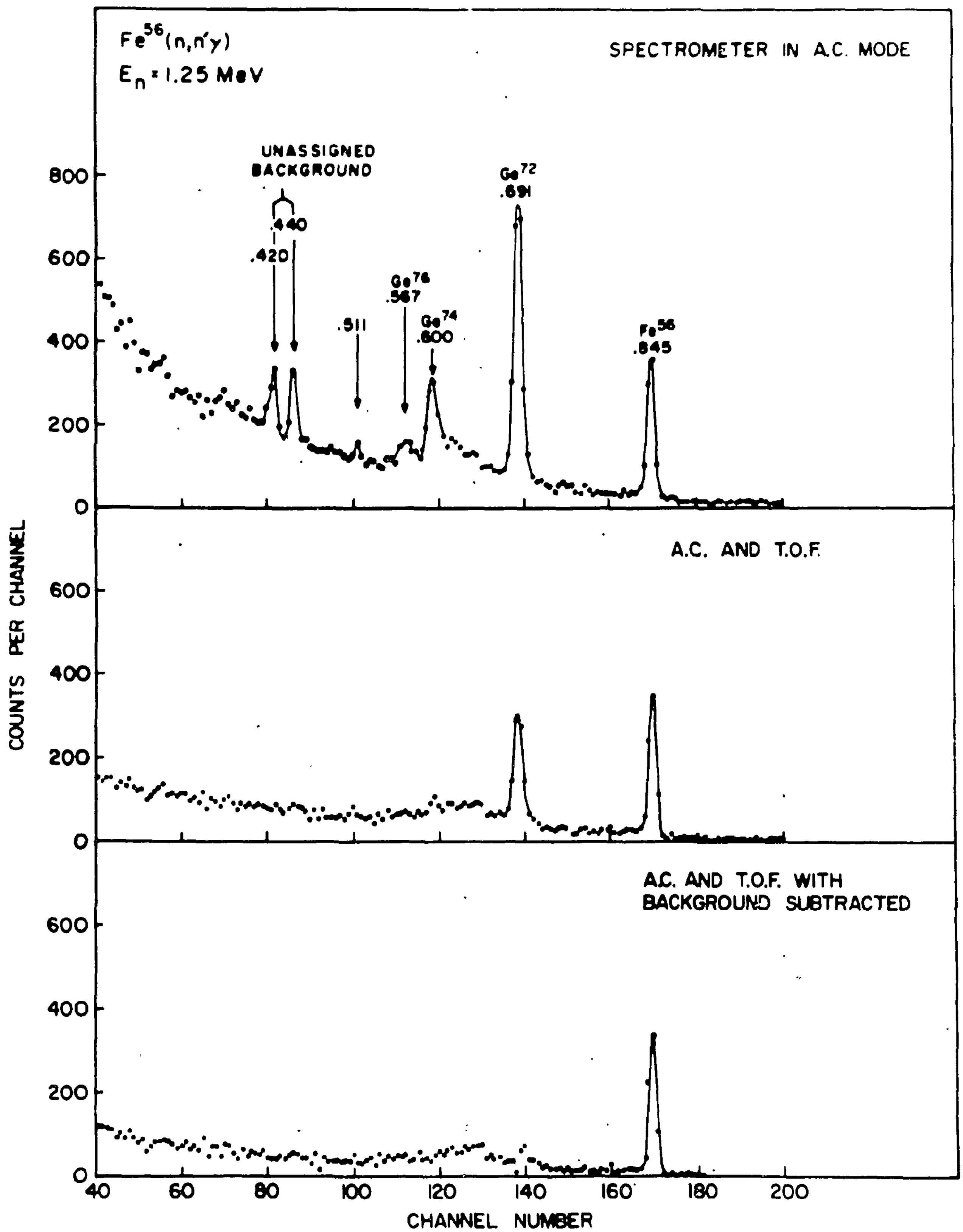
Fe56(n,n'γ)
En = 1.25 MeV
SPECTROMETER IN A.C. MODE
UNASSIGNED BACKGROUND
.420
.440
.511
Ge76
.567
Ge74
.600
Ge72
.691
Fe56
.845
A.C. AND T.O.F.
A.C. AND T.O.F. WITH BACKGROUND SUBTRACTED
COUNTS PER CHANNEL
CHANNEL NUMBER
0
200
400
600
800
40
60
80
100
120
140
160
180
200

Fig. 30

Fig. 31. The angular distribution of the 0.845-MeV gamma ray from the first excited state ($2^+ \rightarrow 0^+$) of ^{56}Fe for various incident neutron energies.

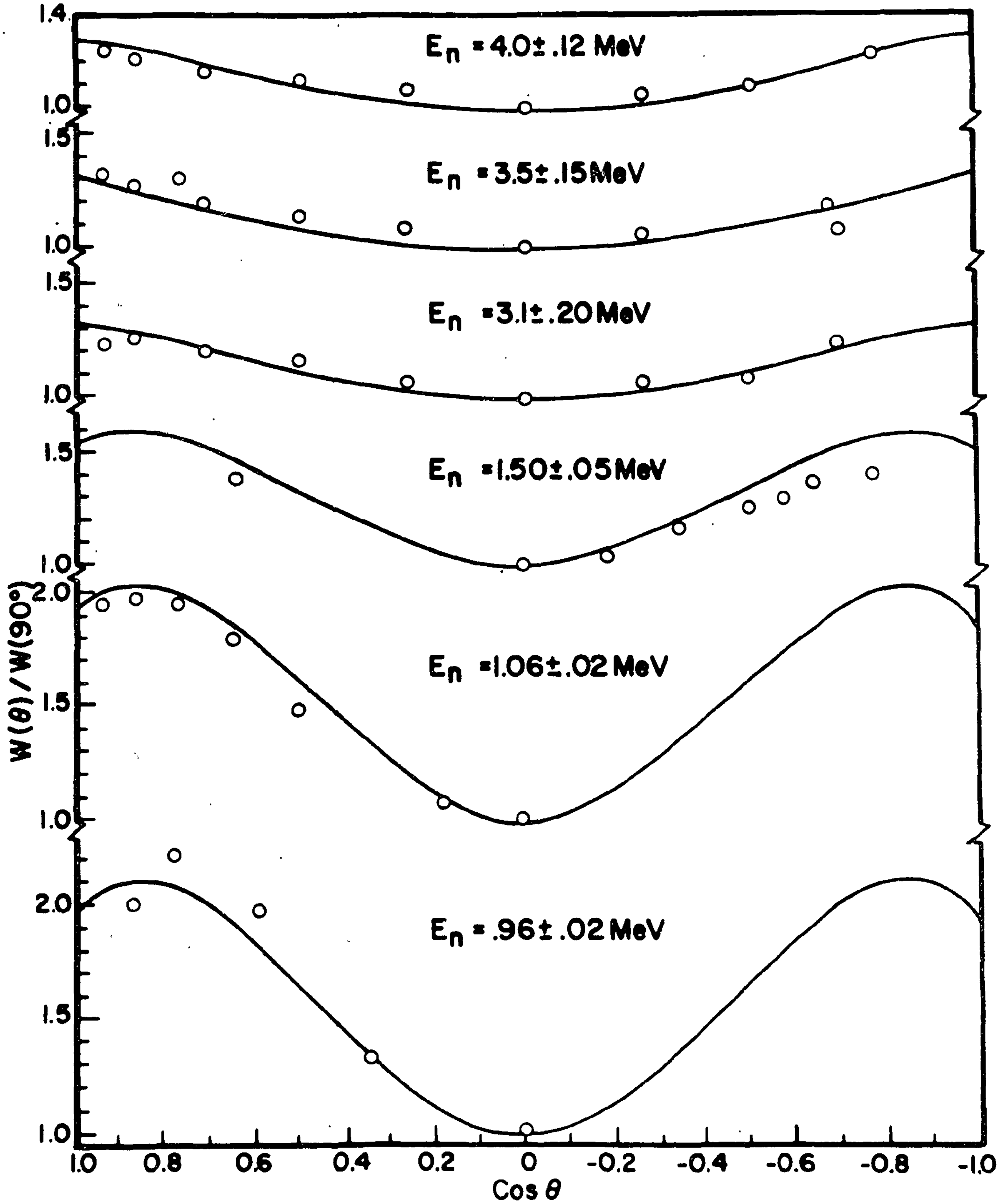

$E_n = 4.0 \pm .12$ MeV
$E_n = 3.5 \pm .15$ MeV
$E_n = 3.1 \pm .20$ MeV
$E_n = 1.50 \pm .05$ MeV
$E_n = 1.06 \pm .02$ MeV
$E_n = .96 \pm .02$ MeV
W(θ)/W(90°)
Cos θ
1.4
1.0
1.5
2.0
1.0 0.8 0.6 0.4 0.2 0 -0.2 -0.4 -0.6 -0.8 -1.0

Fig. 31

Fig. 32. The spectrum of gamma rays from the $^{89}Y(n,n'\gamma)^{89}Y$ reaction taken with a NaI(Tl) detector by the Texas Nuclear Corporation.

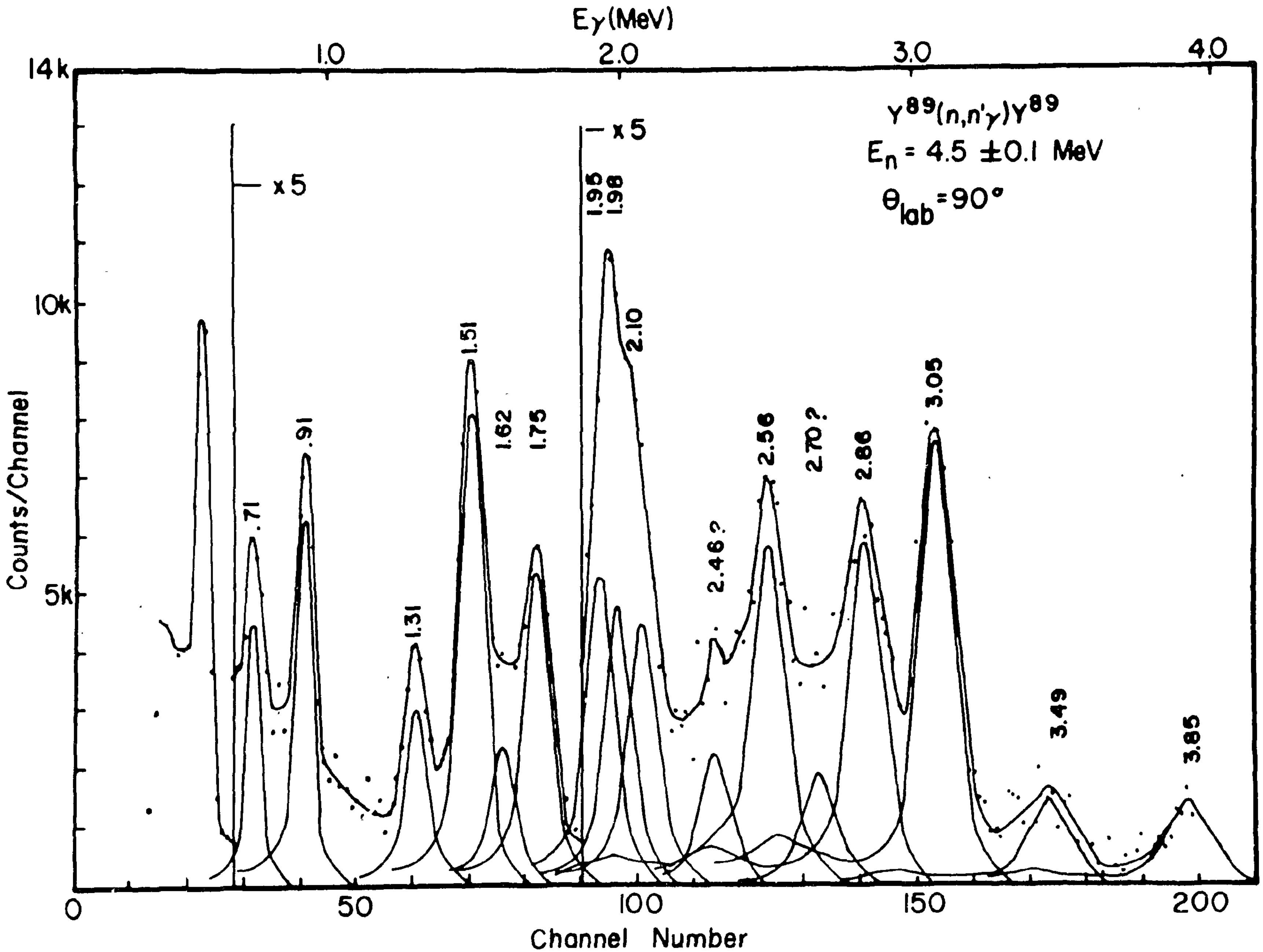

Eγ(MeV)
1.0
2.0
3.0
4.0
14k
10k
5k
Counts/Channel
Y89(n,n'γ)Y89
En = 4.5 ±0.1 MeV
θlab=90°
x5
x5
.71
.91
1.31
1.51
1.62
1.75
1.95
1.98
2.10
2.46?
2.56
2.70?
2.86
3.05
3.49
3.85
0
50
100
150
200
Channel Number

Fig. 32

Fig. 33. The spectrum of gamma rays from the $^{89}Y(n,n'\gamma)^{89}Y$ reaction taken with a Ge(Li) detector by the Texas Nuclear Corporation.

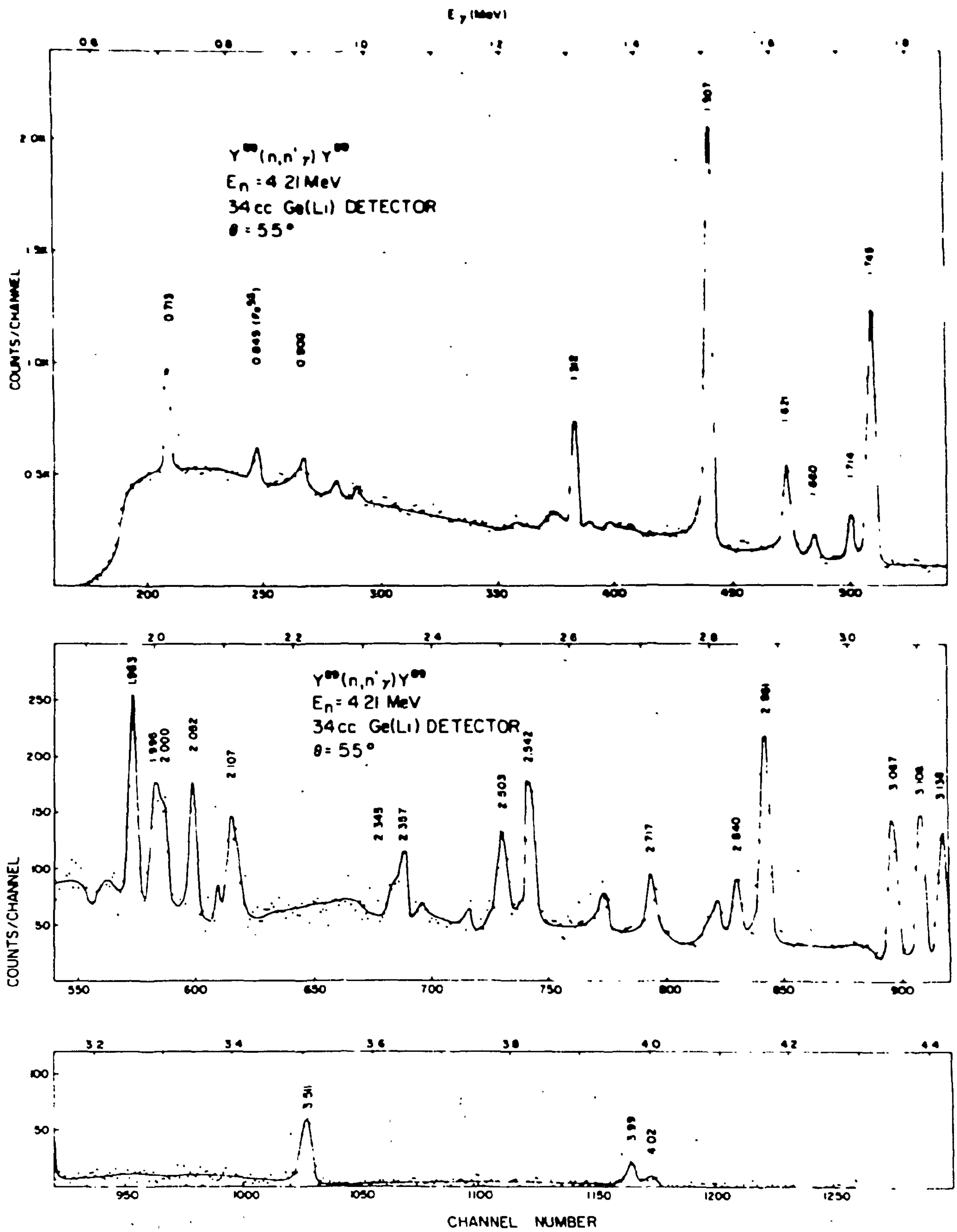
E_γ (MeV)
$Y^{89}(n,n'\gamma)Y^{89}$
E_n = 4.21 MeV
34cc Ge(Li) DETECTOR
θ = 55°
COUNTS/CHANNEL
CHANNEL NUMBER

Fig. 33

Fig. 34. The level schemes of ^{89}Y as determined with the help of gamma-ray spectra obtained with a NaI(Tl) detector and a Ge(Li) detector by the Texas Nuclear Corporation.

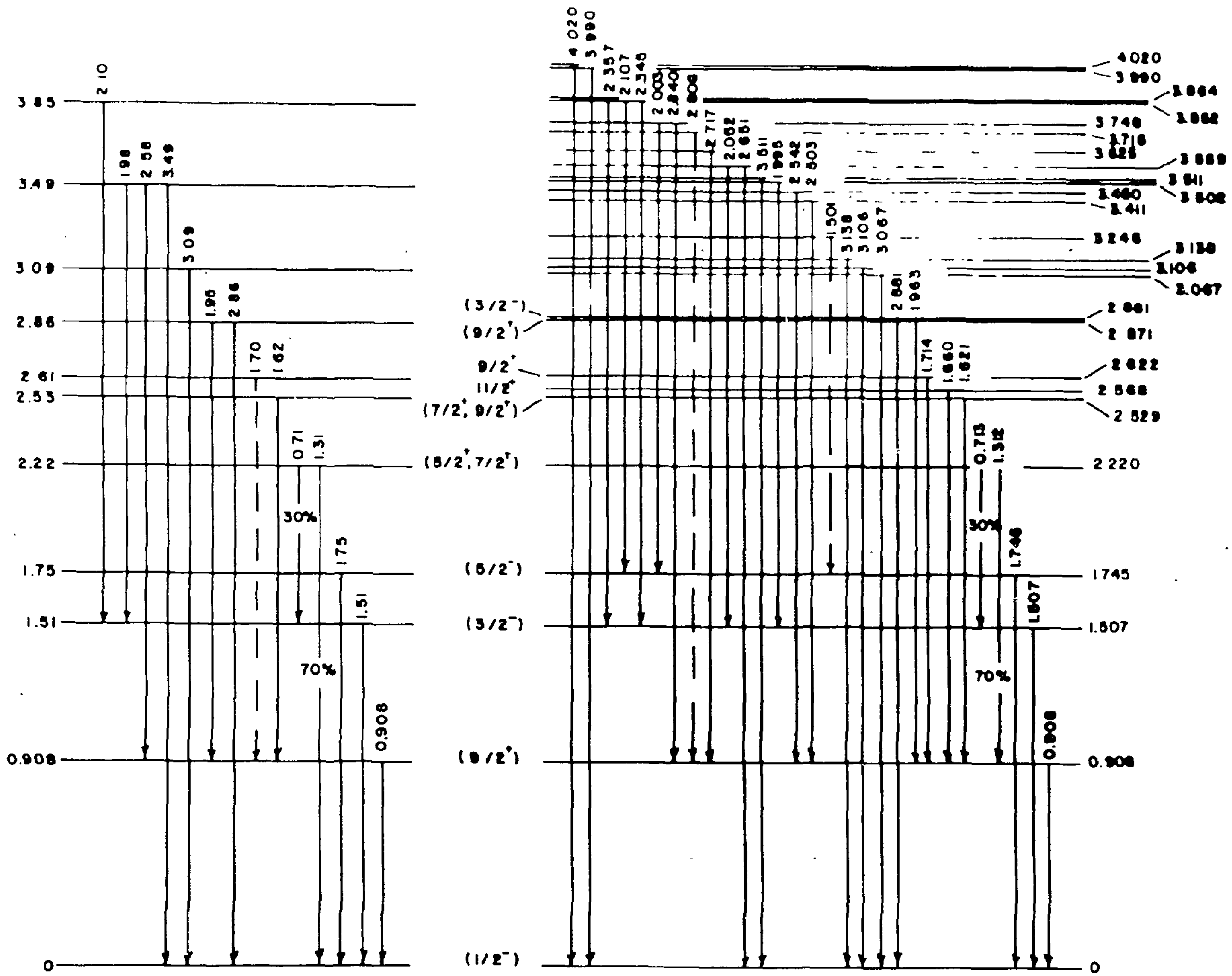

FROM NaI (Tl) DETECTOR SPECTRA FROM GeLi DETECTOR SPECTRA

Y^{89}

Fig. 34

Fig. 35. The Oak Ridge National Laboratory arrangement for the study of $(n,x\gamma)$ reactions.

Fig. 35

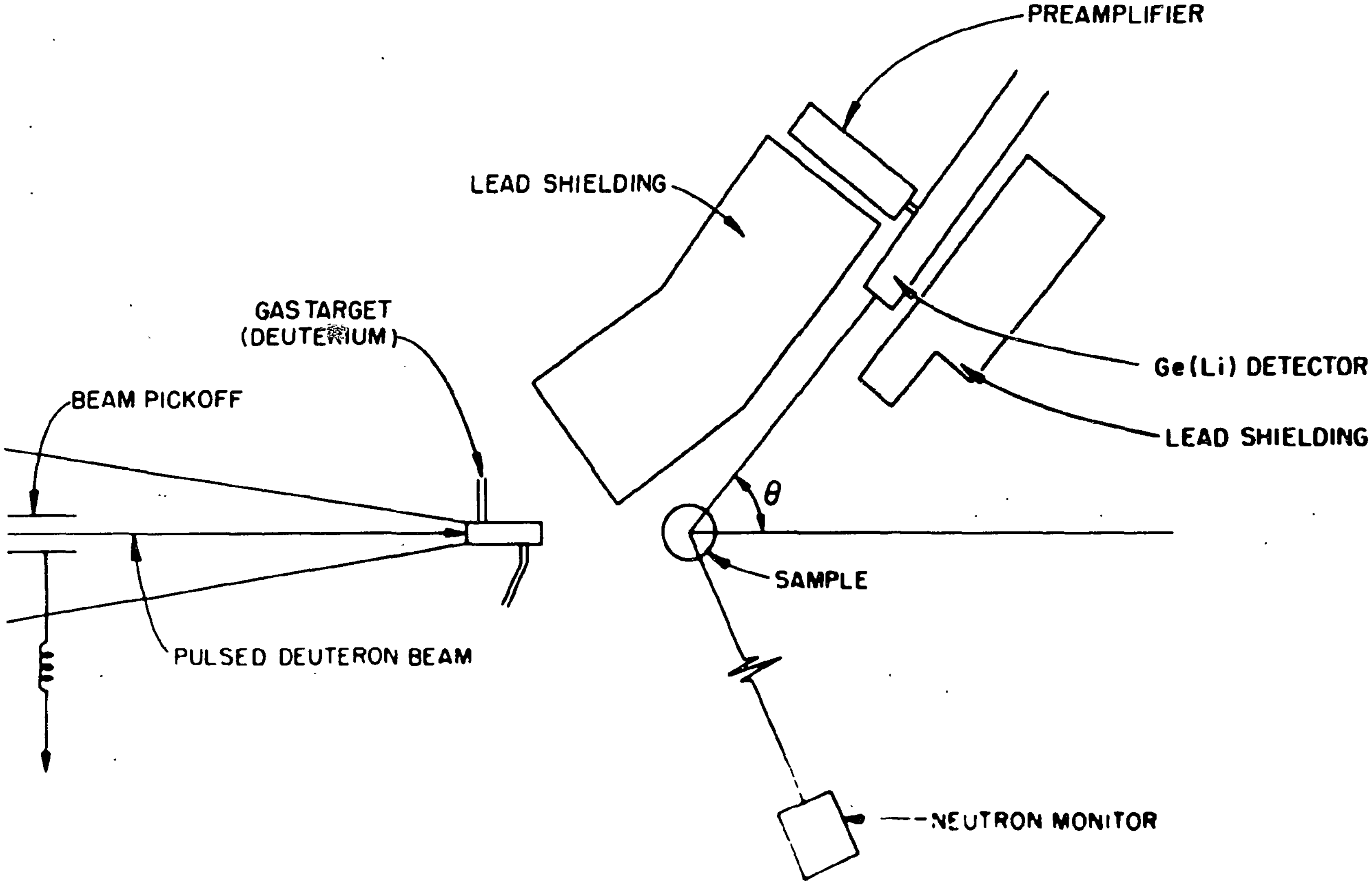

Experimental Arrangement

Figure 31 shows the angular distribution of the 0.845-MeV gamma ray from the first excited state ($2^+ \rightarrow 0^+$) of ^{56}Fe for various incident neutron energies. There are two features that should be noticed. The first is that the angular distribution becomes more isotropic as the incident neutron energy is raised. The second is that a measurement at cos 55° = 0.574 yields a reasonably good average cross section. Obviously 90° is not the place to measure an average cross section.

The next few figures show examples of nuclear spectroscopy of the ^{89}Y(n,n'γ)^{89}Y reaction as done first with a NaI(Tl) detector and then with a lithium-drifted germanium detector.

The first example, in Fig. 32, shows the gamma-ray spectrum at 90° taken with a NaI(Tl) detector. The incident neutron energy was 4.5 MeV. Notice that the full width at half maximum of the peaks is about 150 keV at 3 MeV. This corresponds to 5% energy resolution, which is good for NaI.

A comparable spectrum taken with a Ge(Li) detector is shown in Fig. 33. Notice that the single peak at 3 MeV is shown there as a triplet. The full widths at half maxima are now about 15 keV at 3 MeV for an energy resolution of 0.5%.

Figure 34 shows the impact of this improved resolution on the ^{89}Y level scheme. The number of levels jumped from 11 to 26 and the number of transitions increased from 13 to 27 for incident energies up to approximately 4.1 MeV. The final analysis of ^{89}Y has not been completed. It will probably end up even more complicated than pictured here.

The Texas Nuclear group has made extensive measurements of many different isotopes (As 66, Tu 68, Be 67c). They have also made substantial contributions to the theoretical understanding of the observed spectra (Ma 67). The have, for example, developed new computer codes and modified existing computer codes to calculate gamma-ray spectra from (n,xγ) reactions, incorporating the Satchler formalism (Sa 53, Sa 54, Sa 56b, Sa 58), with the inclusion of the Moldauer, Engelbricht, and Duffey NEARREX code for width fluctuation and resonance interference corrections (Mo 64a).

D. Oak Ridge National Laboratory

The Oak Ridge National Laboratory gamma-ray studies will now be discussed.

They have used the ORNL 6-MeV Van de Graaff accelerator to investigate (n,xγ) reactions on various nuclei. They have published their results on the ^{14}N(n,xγ) reaction for incident neutron energies between 5.8 and 8.6 MeV (Di 69).

The ORNL experimental arrangement shown in Fig. 35 is similar to those used at LASL and at Texas Nuclear except that the Oak Ridge group does not use an anti-coincidence shield. They do, however, have a rather sophisticated setup incorporating fast timing and an on-line PDP 7 computer.

A spectrum of the gamma radiation from the ^{14}N(n,xγ) reactions for an incident neutron energy of 7.4 MeV is shown in Fig. 4 of (Di 69).

E. University of Kentucky

A brief discussion of the program at the University of Kentucky will now be presented. They have used both the anti-coincidence scheme, similar to the LASL and Texas Nuclear arrangements, and the single-detector technique as used at Oak Ridge.

The Kentucky group has made an extensive series of measurements over a number of years (Ni 66, Ba 68b, Ni 68, Ch 68, Ve 69). The motivation for most of their work has been the determination of level structures and decay schemes, including branching ratio measurements.

Brandenberger at Kentucky has developed a method of obtaining improved time resolution from coincidence measurements utilizing large volume Ge(Li) detectors (Br 69a).

Essentially the technique involves the measurement of the pulse rise time between two appropriate discriminator levels. The time of arrival then is corrected for this rise time difference. Using a 15-cm^3 coaxial Ge(Li) detector, with a 100-keV side channel, Brandenberger gets a time resolution of 4 nsec. The time resolution without the rise time correction was 14 nsec. This is a rather simple technique providing a very substantial improvement.

F. Gulf General Atomic Inc.

A completely different technique for the measurement of (n,xγ) reactions will now be discussed. This technique was developed at the Gulf General Atomic Laboratory and involves the electron linac and white neutron source described previously (Or 68, Or 69).

Figure 10 shows the experimental arrangement. A pulsed beam of neutrons is scattered from the ring sample shown on the far right. A lithium-drifted germanium detector is placed on the axis of the beam line, but shielded from the direct incident neutrons. The gamma-ray detector is placed upstream from the scattering sample to reduce the flux of scattered neutrons at the detector position.

The unique feature of the Gulf General Atomic arrangement is the ability to accumulate energy spectra as a function of time, or energy, of the incident neutrons. An example of the time spectrum is shown in Fig. 8 of (Or 69). The scattering sample is oxygen. The upper curve is generated from all detected gamma-ray events and the lower curve is for only those pulse heights in the range of the double-escape peak of the 6.128-MeV gamma ray. Obviously this feature could be quite useful in deducing the position of a particular gamma ray in an energy level scheme.

The numbers 1, 2, and 3 at the top of this figure correspond to time channels selected for the particular gamma-ray spectra shown in Fig. 9 of (Or 69). The gamma-ray energy resolution at 6.128 MeV was about 11-keV full width at half maximum.

A measurement of the gamma-production cross section necessitates a knowledge of the incident neutron flux and the detection efficiency of the Ge(Li) detector. These are more serious problems under the circumstance described here than they are for the monoenergetic Van de Graaff neutron sources.

Another difficulty arises from the placement of the detector in the incident neutron beam channel, where it is subjected to a neutron flux and the intense gamma flash from the machine.

This is a new and powerful technique, and the problems are just beginning to be solved. With the present ring scattering geometry the method is probably not as satisfactory as that used by the Van de Graaff accelerator groups. The disadvantages are that the spectra are not as clean as can be obtained with the anti-coincidence systems and also the ring scattering geometry does not lend itself to convenient angular distribution measurements.

On the other hand, if a very intense LINAC source could be combined with a well-shielded anti-coincidence detector arrangement as used by LASL, Texas Nuclear, and others, as they propose (Or 68), there could result the optimum gamma-ray production facility.

G. Angular Correlation Studies

This section will be concluded with a few brief comments on neutron-gamma ray angular correlations measurements.

The whole field of angular correlation studies in inelastic nucleon scattering has been reviewed by Sheldon (Sh 63). There has been a fair amount of work with charged particles, but for obvious reasons neutron-gamma ray angular correlation studies are sparse (Be 63, Ni 63).

Sheldon (Sh 63) points out that future experimental investigations of correlation should aim at securing accurate absolute results for the double differential cross section over a wide range of angles to test symmetry characteristics in addition to providing data for stringent comparison with theory. He also stresses the desirability of extending the correlation studies to absolute measurement of the correlations between neutron and gamma ray for particular nucleon exit channels populating the first level and for channels inducing population of the second or higher excited states of the target nucleus.

For studies of heavier nuclei ($A \gtrsim 70$) the use of neutrons, rather than protons, would be preferred for two reasons. The first is that there are no Coulomb barrier penetration problems. The second is that there would be no Coulomb excitation to complicate the analysis.

Measurements upon families of isotopes for a given target element at a given energy might be expected to shed some light on the regions of applicability of different reaction mechanisms.

The whole field of neutron-gamma ray correlations deserves a great deal more work. There is a very substantial need for accurate, careful experimentation.

III-8. Polarization

A. General Comments

Measurements of the scattering of polarized neutrons from nuclei provide direct information regarding the spin dependence of nuclear reactions.

Consider the scattering of spin-1/2 particles from a spinless target. The asymtotic form of the scattered wave can be written (Wu 62)

$$\psi = e^{ikZ} \chi^{m_{si}} + \frac{e^{ikr}}{r} \sum f_{ij} (\theta,\phi) \chi^{m_{sj}} ,$$

where $\chi^{m_{si}}$ and $\chi^{m_{sj}}$ (m_{si}, m_{sj} = ±1/2) denote the spin state of the incident and scattered particles, respectively.

The scattering amplitudes f_{ij} are the matrix elements of a 2 × 2 matrix f that can be expressed in terms of the Pauli matrices σ_x, σ_y, σ_z, and the unit matrix $\vec{E}$.

$$f = g \vec{E} + (\vec{h} \cdot \vec{\sigma}) .$$

The g corresponds to the spin-independent part and h to the spin-dependent part of the interaction. The g and h are functions of the angle θ. The scattering amplitude can be written

$$f(\theta) = g(\theta) \vec{E} + h(\theta) (\vec{n} \cdot \vec{\sigma}) .$$

The differential cross section can then be written as

$$\sigma(\theta) = |g(\theta)|^2 + |h(\theta)|^2 ,$$

and the polarization as

$$P(\theta) = \frac{2Re(g^*h)}{\sigma(\theta)} .$$

Usually h << g in which case the differential cross section provides a good determination of g, but not of h. On the other hand, the polarization, which is a product of g and h, provides a sensitive measure of h.

Rodberg (Ro 59) has shown that the polarization is approximately proportional to the derivative, with respect to angle, of the differential cross section. The polarization is zero at the maxima and minima of the angular distribution, and maximum in between. This result is strictly an approximation (Hü 65b, De 66). It is, however, a useful tool in the estimation of effects to be observed experimentally.

Polarization measurements are performed in two ways. One involves the measurement of the polarization produced in an unpolarized incident beam of neutrons scattered from a sample. The other technique is to measure the asymmetry in the scattering of a polarized beam of neutrons. Actually the quantity measured using the first method is called the polarization whereas the quantity measured using the second method is called the analyzing power. For elastic scattering these two quantities are the same, provided time reversal invariance holds, for the same incident neutron energies.

For the present discussion inelastic scattering will be neglected and the polarization and the analyzing power will be considered as the same number.

B. Few-Body Systems and Light Nuclei

Light nuclei and the few-body problems will be discussed separately. In this mass region a phase-shift analysis is particularly convenient and useful.

Polarization in the 3-body system was reviewed by Haeberli at the 1969 Birmingham Conference (Ha 69). Seagrave summarized the neutron polarization data for deuterium, tritium, and ^{3}He at the 1967 Brela Conference (Se 67). H. H. Barschall reviewed the polarization data for the 3-, 4-, and 5-nucleon systems at the 1965 Karlsruhe Conference (Ba 65).

The availability of these reviews precludes the usefulness of yet another survey. The objective here will be just to convey an idea of the general trends in the data.

The polarization produced in the n-D scattering is approximately zero at all angles for incident neutron energies below 10 MeV as shown in Fig. 16 of (Se 67). Above 10 MeV the polarization grows slowly until, in the neighborhood of 20 MeV, the polarization reaches $\sim$+5% at the forward angles, $\sim$−10% in the vicinity of 90°, and $\sim$+20% at backward angles; at 0° and at 180°, of course, the polarizations are zero.

Figure 22 of (Se 67) shows the n-T polarization data. The general trend at low energies is for the polarization to be predominantly positive while at higher energies the polarization is negative at forward angles and positive at back angles. We have made extensive n-T polarization and differential cross section measurements at LASL and expect, eventually, to define the phase shifts in this region in some detail.

Figure 36 shows a contour plot of the polarization of neutrons scattered by ^{4}He (Ba 65). The neutron energies and scattering angles are in the laboratory system. Notice the region of the ^{4}He(n,d)T resonance just above 22 MeV. This figure shows why ^{4}He is a good polarization analyzer in the energy region of 4 to 21 MeV.

The polarization times the differential cross section can be expressed as a sum over associated Legendre polynomials

$$\sigma(\theta)\ P(\theta) = \sum_{L=1}^{L_{max}} a_L\ P_L^1(\cos\theta)\ .$$

An expression of this form can be fitted to the data to obtain an estimate of the s, p, or d wave contribution to the polarization (Be 66). If a sufficient amount of data are available, however, a complete phase-shift analysis is the most satisfactory. This has been done on the n-α system by various groups (for example, Ho 66, Mo 68b) and tentatively on the n-^{3}He system (Bü 69).

Fig. 36. Contour plot of the polarization of neutrons scattered by ^{4}He in the laboratory system.

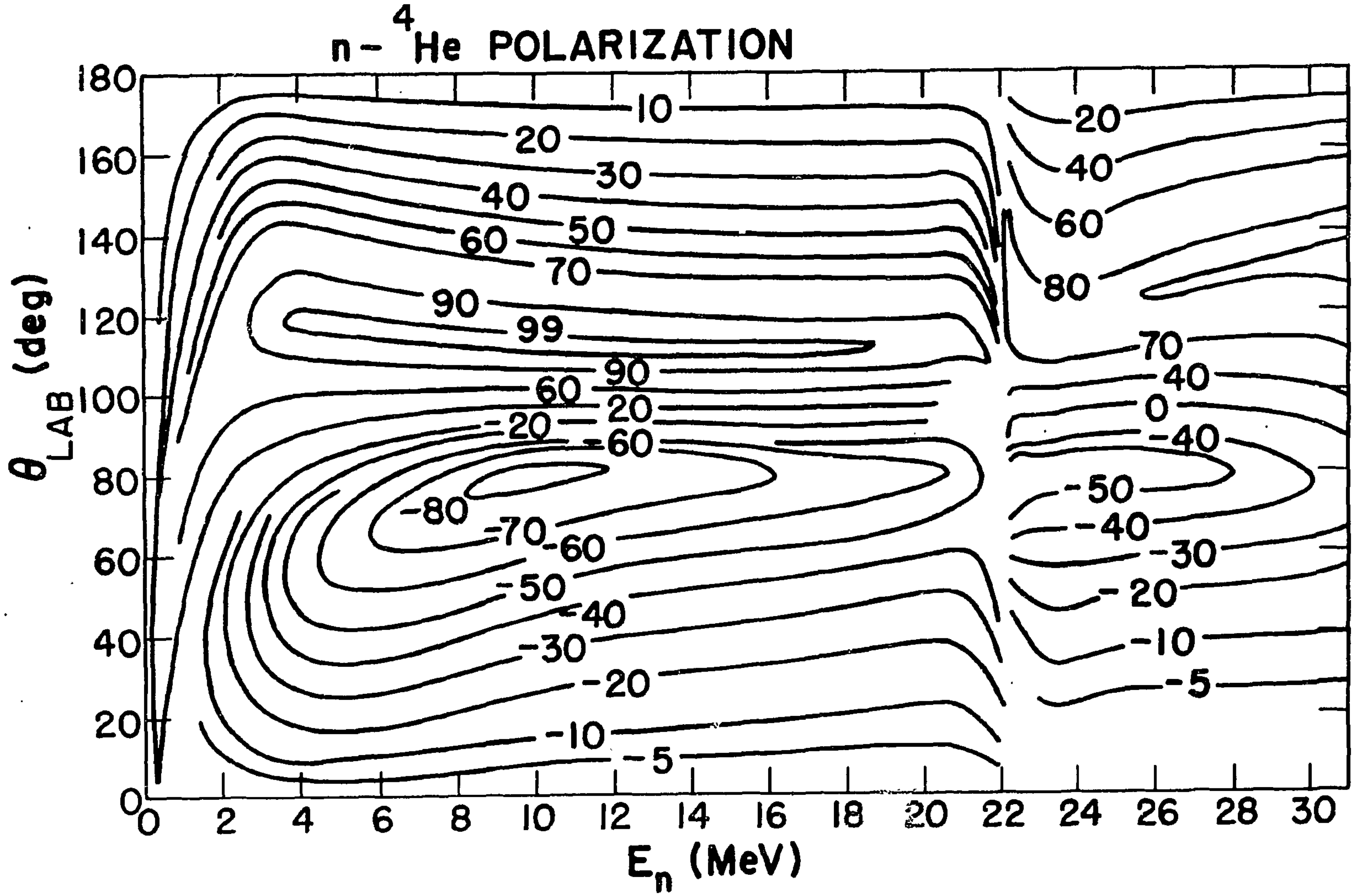
n-4He POLARIZATION
θ_{LAB} (deg)
E_n (MeV)
180
160
140
120
100
80
60
40
20
0
0
2
4
6
8
10
12
14
16
18
20
22
24
26
28
30
10
20
30
40
50
60
70
90
99
90
60
20
-20
-60
-80
-70
-60
-50
-40
-30
-20
-10
-5
20
40
60
80
70
40
0
-40
-50
-40
-30
-20
-10
-5

Fig. 36

Several analyses have been done by using the proton data for the mirror reaction with the Coulomb potential turned off (Va 67b). There are preliminary indications, however, that this is not a proper approach.

Polarization results on light nuclei can occasionally be analyzed in terms of the optical model, as was done for ^{6}Li and ^{7}Li (La 64a) with some success. Often they are parameterized in terms of phase shifts (Mi 69, We 65).

A number of different theoretical approaches have been examined by the Argonne group in their extensive investigations at neutron energies below 2 MeV (see, for example, La 64b, El 62). There will be no discussion of these here except to comment that the objectives were usually to extract nuclear structure information. For example, they have been able to make spin and parity assignments to levels of the compound nucleus using a 2-channel R-matrix theory.

Recently the Argonne group, in collaboration with a group from Ohio University, has been analyzing the low energy ^{12}C differential cross section and polarization data in terms of the R-matrix formalism (La 69a). Similar efforts have been made by a group from the Knolls Laboratory (Re 68b) using a coupled-channel calculation. Both groups have been very successful in obtaining detailed fits to the data.

C. Medium and Heavy Nuclei--Optical Model Studies

Virtually all of the polarization investigations on medium and heavy nuclei were designed to determine optical model parameters.

Rosen, Beery, Goldhaber, and Auerbach (Ro 65b) have made several of the most comprehensive studies of the polarizations and differential cross sections to be expected from a particular set of parameters. Their studies are of interest to the users who wish to plan experiments or to perform some calculation requiring cross section or polarization values.

The Rosen parameters were obtained from a systematic study of the elastic scattering of polarized protons and from the fitting of 14-MeV neutron elastic scattering data.

They used a potential of the form:

$$V(r) = -V\ f(r) - iW\ g(r) - V_S\ h(r)\ \vec{\sigma} \cdot \vec{\ell}\ .$$

The real central potential is assumed to have the Saxon-Woods radial dependence (Wo 54) with radius R and diffuseness a:

$$f(r) = [1 + \exp\ (\frac{r-R}{a})]^{-1}\ ,$$

where $R = r_o A^{1/3}$.

The imaginary part of the potential is peaked at the surface and is characterized by a radius R and a width b. It has the form

$$g(r) = -4b\ \frac{d}{dr}\ [1 + \exp\ (\frac{r-R}{a})]^{-1}\ .$$

The spin-orbit term is of the form

$$h(r) = -\lambda_\pi^2\ \frac{1}{r}\ \frac{df(r)}{dr}\ ,$$

where λ_π is the pion Compton wavelength, $\hbar/mc$; $\vec{\sigma}$ is the Pauli matrix for the nucleon, with $s = (\hbar/2)\sigma$; and $\vec{\ell}$ is the orbital angular momentum in units of $\hbar$.

The average parameters were found to be the following:

$V = 49.3 - 0.33\ E$ (MeV) where E is the neutron energy in the center-of-mass system

$W = 5.75$ MeV

$r_o = 1.25$ fm

$a = 0.65$ fm

$b = 0.70$ fm

$V_S = 5.5$ MeV

Compound elastic scattering was calculated using the Hauser-Feshbach theory. It was assumed, however, that only shape elastic scattering contributed to the polarization.

Using these parameters Beery, Harper, Stovall, and Rosen calculated the differential polarization for 41 nuclides between ^{6}Li and ^{240}Pu for incident neutrons with energies between 1 and 16 MeV (Be 68).

There have been numerous other studies of the spin-orbit term in the optical model (Ro 65a, El 64, Cl 58). Other references are to be found in the proceedings of the 2nd International Symposium on Polarization Phenomena of Nucleons, Karlsruhe, 1965 (Hu 65a).

So far, everything that has been mentioned in this discussion applies only to elastic scattering. Compound elastic and compound nuclear inelastic scattering are expected to exhibit zero polarization. This is what was found when the polarization was measured for 1.95-MeV neutrons scattered from the 0.845-MeV level of ^{56}Fe (br 64). Some polarization would probably be expected from direct inelastic scattering to individual levels. This, however, has not been investigated in any detail.

There are two different effects that can be studied with oriented targets. Oriented ^{165}Ho, which has a large nuclear deformation, has received most of the attention.

If the total cross sections of oriented and unoriented ^{165}Ho are subtracted, one gets what is called the deformation effect:

$$\Delta\sigma_{def} = \sigma_{oriented} - \sigma_{unoriented}.$$

This has been studied by a number of groups (Wa 65a, Mc 68, Ma 68, Fi 67).

There is a good theoretical understanding of the behavior of $\Delta\sigma_{def}$ in terms of a coupled-channel analysis. Marshak et al. (Ma 68d) have also provided an instructive semiclassical explanation employing some concepts of the black-nucleus model and the nuclear Ramsauer effect. The essential features of their model are really quite simple. If the nuclei are aligned with the symmetry axis parallel to the beam, then the classical area, or cross section, presented to the beam is smaller than for unaligned nuclei. Also there is a corresponding increase in the path length through the nuclei. The decrease in the cross section corresponds to the deformation effect while the increased length results in a shift of the locations, on an energy scale, of the cross section maxima and minima. This is the Ramsauer effect. Marshak et al. have made quantitative calculations with these very simple models and are able to get good agreement with the data.

The possibility of a spin-spin interaction term in the optical potential has been suggested many times. If such a term does indeed have any importance, it will manifest itself in the scattering of polarized neutrons from oriented ^{165}Ho (Fi 67, Wa 65, Fi 69a). The term to be added to the potential might have the form

$$-V_{SS}\ f(r)\ [\frac{\vec{I}\cdot\vec{\sigma}}{I}] ,$$

where $\vec{\sigma}$ is the neutron spin and $\vec{I}$ is the nuclear spin.

The measured quantity has been defined as

$$\Delta\sigma = \sigma_t^{\uparrow\uparrow} - \sigma_t^{\uparrow\downarrow} ,$$

where $\sigma_t^{\uparrow\uparrow}$ is the total cross section for neutron and target spins parallel and $\sigma_t^{\uparrow\downarrow}$ is the total cross section for neutron and target spins antiparallel.

The best limit on $|V_{SS}|$ now is $|V_{SS}| < 300$ keV (Fi 69b).

The Lockheed group hopes to extend these measurements to other nuclei in the near future (Fi 69b).

III-9. Electromagnetic Neutron-Nucleus Interaction

The interaction of the neutron magnetic moment with the Coulomb field of a nucleus was first investigated by Schwinger in 1948 (Sc 48). This is by far the most important one of several electromagnetic neutron-nucleus interactions. For several years there were peculiar anomalies in the experimental data which lead to theoretical searches for additional effects. Fortunately, they were not found to be significant because it turned out that the experiments, which are exceedingly difficult, were wrong. On the other hand, these anomalous results encouraged additional work on the so-called Schwinger scattering and now it turns out that this interaction possesses some particularly interesting and useful properties.

The history of the field will be outlined and the story unfolded in more or less chronological order. Examples of various studies will be selected mainly for comparison between theory and experiment.

Schwinger scattering shows up at small angles, in the form of a substantial enhancement of the differential cross section very close to zero degrees.

The differential cross section can be written as (Fo 63)

$$\sigma(\theta) = \sigma_N(\theta) + \sigma_C(\theta)$$

where $\sigma_C(\theta)$ is the Schwinger scattering cross section and $\sigma_N(\theta)$ is the scattering cross section due to the nuclear potential. There are no interference terms for an unpolarized incident neutron beam.

$$\sigma_C(\theta) = \gamma^2 \cot^2 (\tfrac{1}{2}\theta)$$

or for small angles

$$\sigma_C(\theta) = \frac{4\gamma^2}{\theta^2} ,$$

where

$$\gamma = \frac{1}{2}\mu_n \frac{Ze^2}{Mc^2}$$

μ_n = magnetic moment of the neutron,

M = mass of the neutron,

Z = atomic number of the target nucleus.

The last expression demonstrates the very rapid increase in $\sigma_C(\theta)$ with decreasing angle.

Schwinger scattering is spin dependent. Consequently, there is a spike in the polarization near zero degrees. Without Schwinger scattering the polarization drops smoothly to zero at zero degrees. With Schwinger scattering the polarization heads toward zero at zero degrees, then at small angles undergoes a radical change in magnitude and returns to zero at zero degrees. The expression for the polarization is (Sc 48, Ha 63b)

$$P = \frac{\gamma\cot\frac{\theta}{2}\,\mathrm{Im}\ f_o(\theta)}{|f_o(\theta)|^2 + \gamma^2\cos^2\frac{\theta}{2}} \quad ,$$

where $f_o(\theta)$ is the scattering amplitude.

The denominator is the scattering cross section. The optical theorem relates the $\mathrm{Im}f_o(0°)$ to the total cross section (see Section III-4).

$$\mathrm{Im}f_o(0°) = \frac{k\sigma_T}{4\pi} \quad .$$

Some examples of this will be seen later.

The differential cross section and polarization were investigated with 100-MeV neutrons from the AERE cyclotron (Vo 56). The neutrons were scattered from uranium at several angles between 1/4° and 1°. The results were compared with Schwinger scattering theory and found to agree within the experimental uncertainties (for example, asymmetry at $1/3^{\circ} \sim (7\pm1)\%$). The results were used to determine the sign and magnitude of the polarization of the neutron beam.

Detailed calculations were performed of the scattering of 3.1-MeV polarized neutrons at small angles from les (Sa 56a). The purpose of this examination was to study the effects of treating the problem with perturbation theory, using wave functions obtained from hard-sphere scattering as the zero-order approximation. The results are consistent with the results of other calculations (Ho 69a).

Schwinger scattering may not be the only result of the electromagnetic neutron-nucleus interaction. In an electric field there may be induced in the neutron an electric dipole moment parallel to the inducing field.

Let $\vec{p}$ be the induced dipole moment. Then

$$\vec{p} = \alpha \vec{E} ,$$

where α is the polarizability and $\vec{E}$ is the electric field vector. The perturbing Hamiltonian due to the dipole-moment Coulomb-field interaction is

$$H' = -\frac{1}{2} \vec{p} \cdot \vec{E} = -\frac{1}{2} \alpha E^2 .$$

In the field of a nucleus of charge Z

$$H'_{(r)} = -\frac{1}{2} \alpha Z^2 e^2/r^4 \qquad \text{for} \qquad r > R ,$$

where R is the nucleus radius. Inside the nucleus this effect is trivial compared to the nuclear effect.

It has been suggested that deviations from nuclear plus Schwinger scattering might be interpreted in terms of electric polarizability of the neutron

(Al 56, Al 57). Thaler examined various experiments and obtained an estimate of the upper limit of $\sim 1 \times 10^{-41}$ cm^3 (Th 59). This can be compared with the value obtained from meson theory of 2×10^{-42} cm^3 (Th 59).

Breit and Rustig (Br 59) deduced an upper limit of 2×10^{-42} cm^3 from data on the photoproduction of pions from hydrogen. They also considered several more exotic effects, including the interaction of the neutron magnetic moment with the vacuum polarization charge and with the electric charge density at the nuclear surface. These latter effects are small.

The long range nuclear potential has been considered in detail by Fox (Fo 63). The effect on the differential cross section of this potential, however, extends to much greater angles than do the effects of the electromangetic interactions. For example, the long range potential tail necessary to fit 100-MeV data for carbon modifies the differential cross section out to 15° whereas the electromagnetic effects are insignificant beyond a few degrees (Fo 63). Calculations including polarization were carried out by Monahan and Elwyn (Mo 64b).

Fossan and Walt made a careful measurement of the differential scattering cross section of 570-keV neutrons by uranium and set an upper limit of $\sim 2 \times 10^{-40}$ cm^3 on α (Fo 64, Wa 65b). This was in conflict with some of the data of Aleksandrov et al. that they analyzed (Wa 65).

The Argonne group (El 66) also made a careful measurement and analysis with the result that they set a lower limit of 4×10^{-40} cm^3 for α. They suggested that this anomalous behavior may be related to the fission process.

In 1966, Aleksandrov et al. (Al 66) used the JINR pulsed reactor to obtain 1-26 keV neutrons, which they scattered from lead. They measured the differential cross section and extracted limits on the value of α.

$$-4.7 \times 10^{-42}\ \text{cm}^3 < \alpha < 6.1 \times 10^{-42}\ \text{cm}^3$$

Fig. 37a-h. Differential cross sections or polarizations calculated with and without the Mott-Schwinger (MS) interaction (Ho 69b).

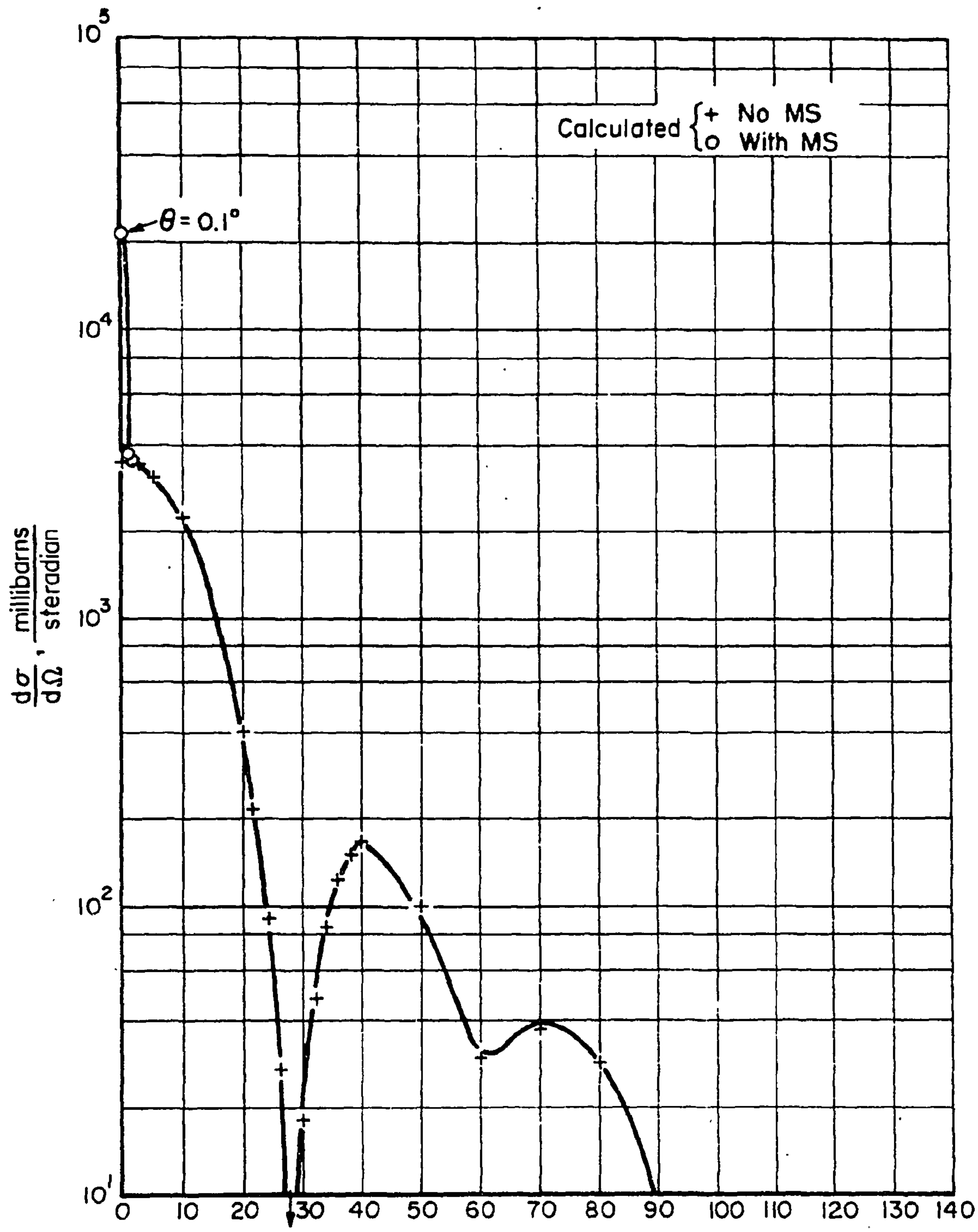

DIFFERENTIAL CROSS SECTION FOR 24 MEV NEUTRONS SCATTERED BY Mn

Fig. 37a

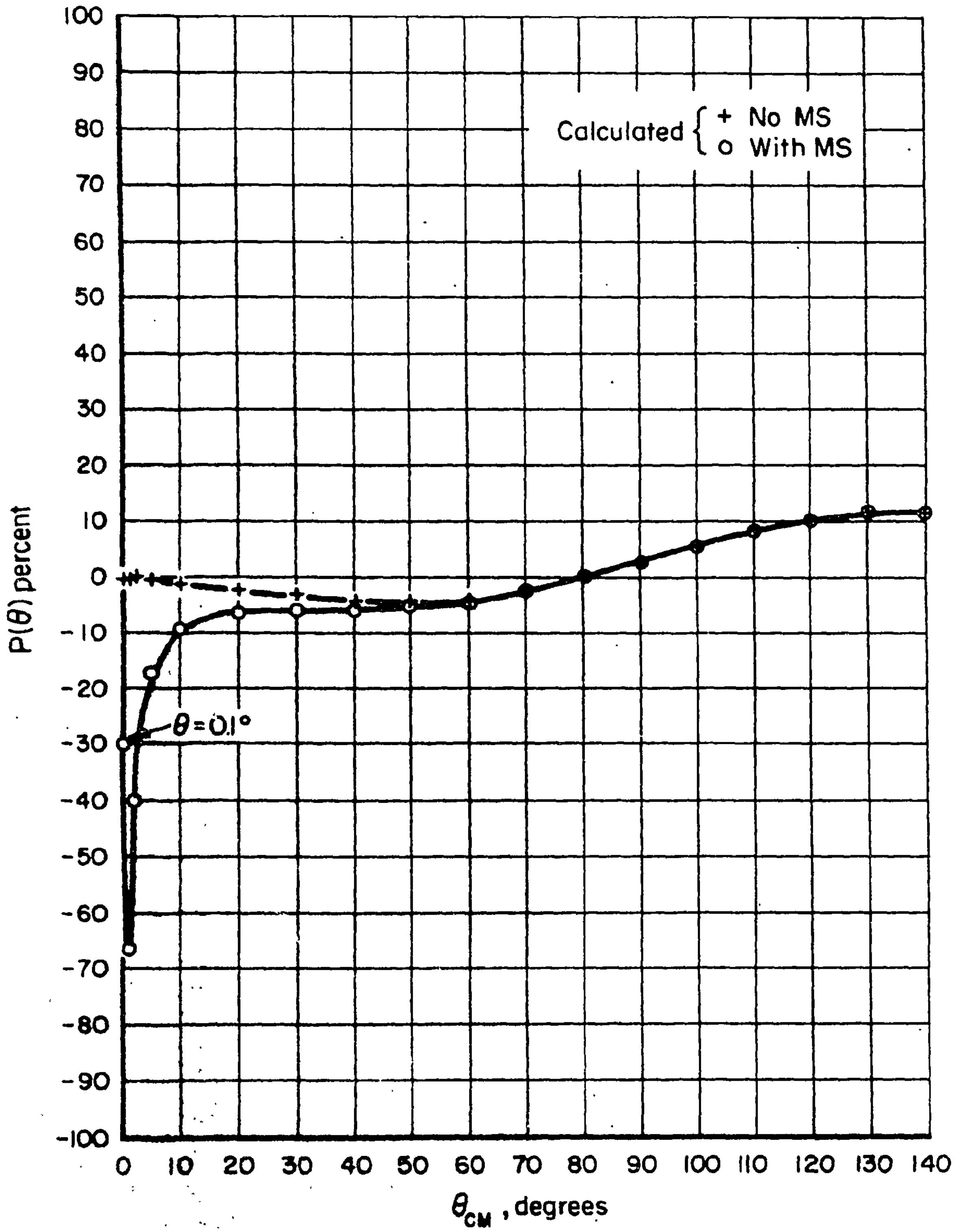

POLARIZATION OF 1 MEV NEUTRONS SCATTERED BY Mn

Fig. 37b

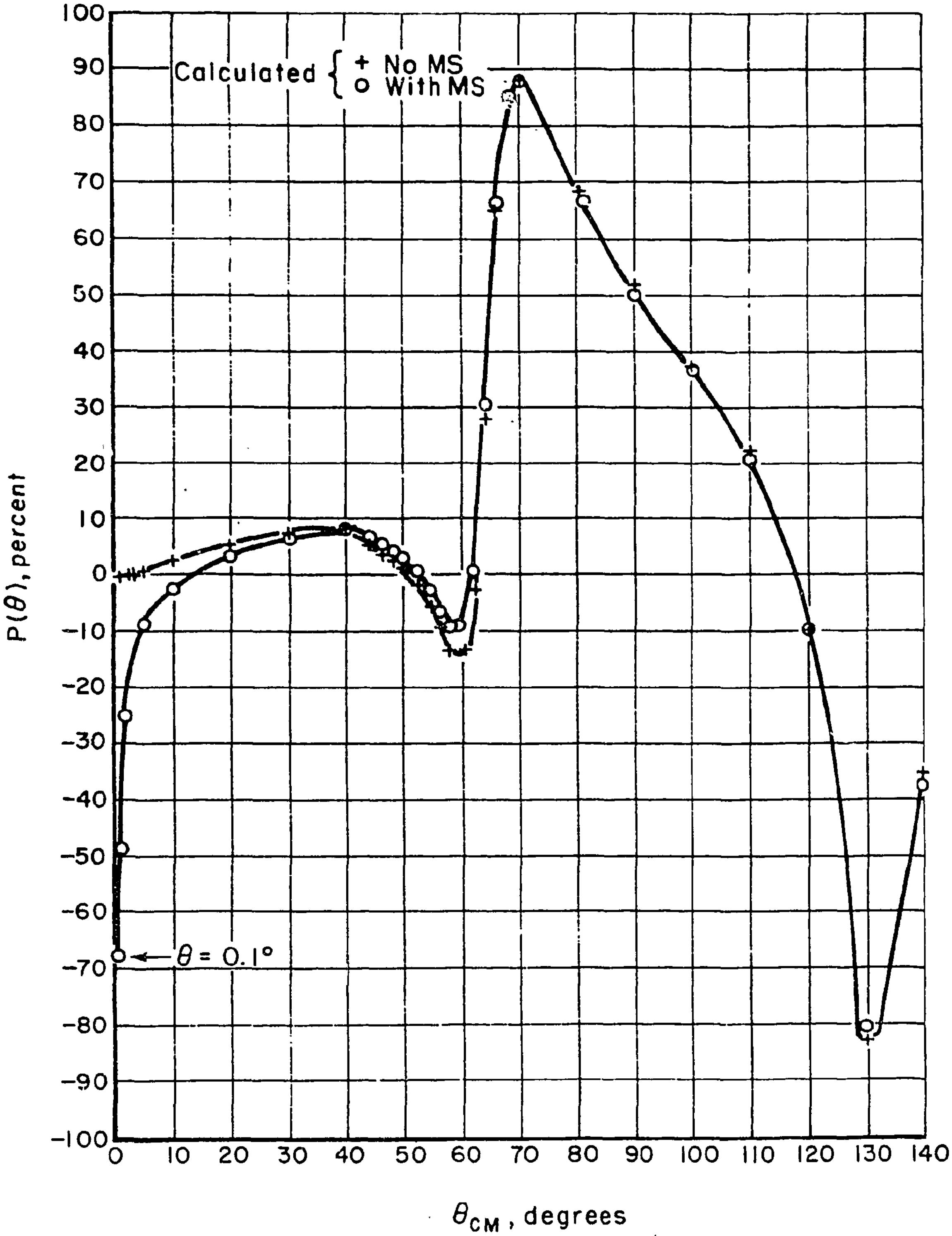

POLARIZATION OF 7 MEV NEUTRONS
SCATTERED BY Mn

Fig. 37c

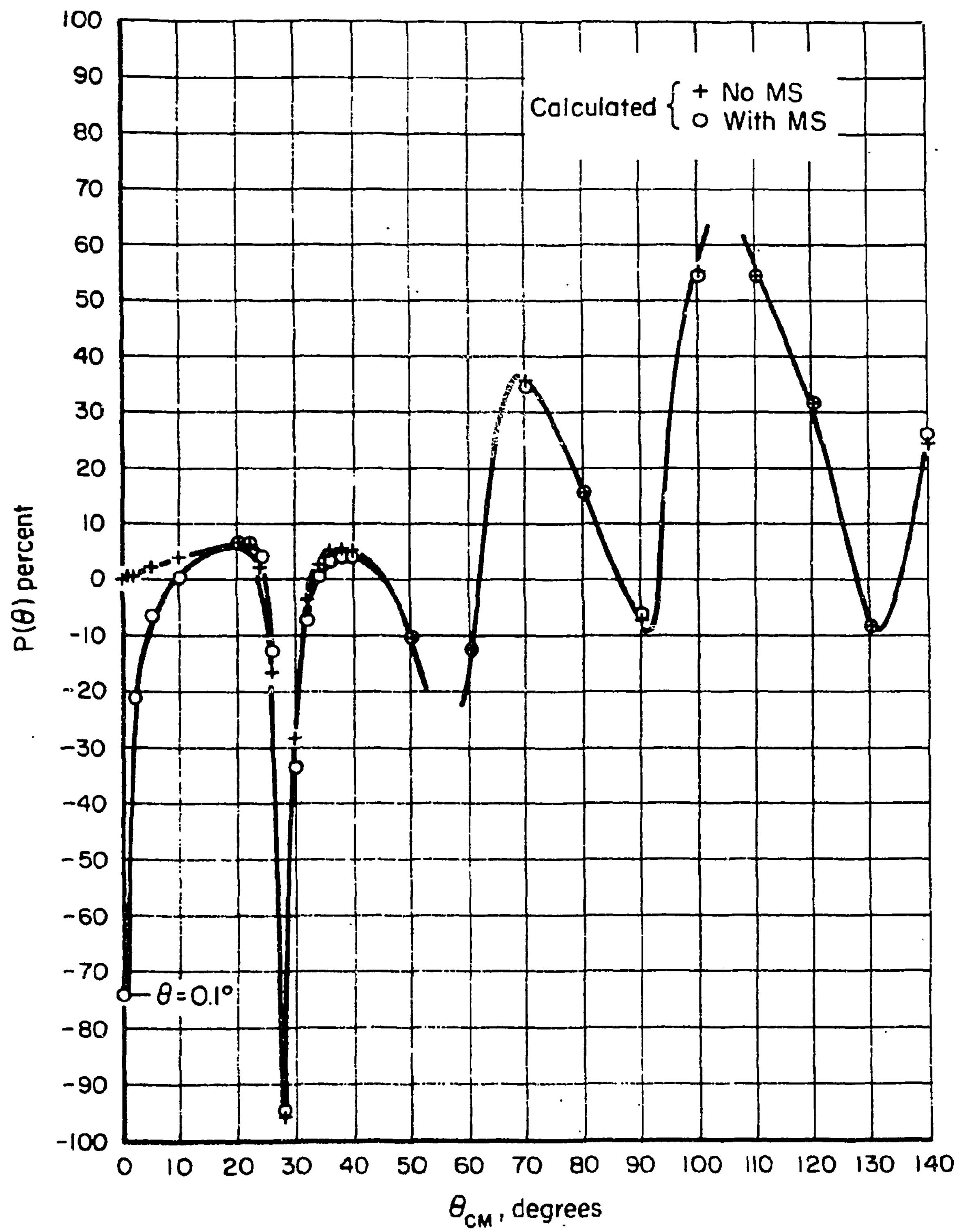

POLARIZATION OF 24 MEV NEUTRONS
SCATTERED BY Mn

Fig. 37d

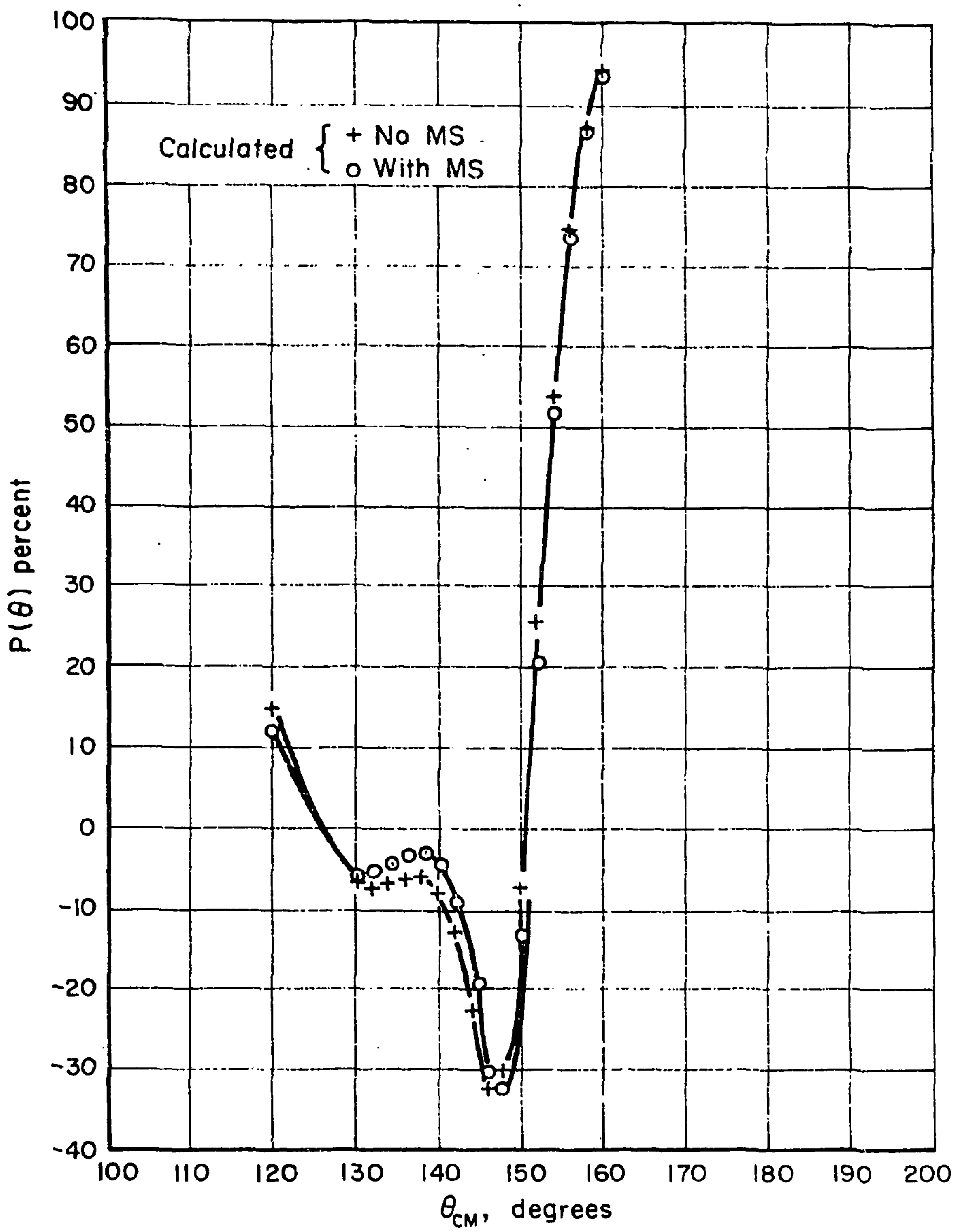

LARGE ANGLE POLARIZATION OF 7 MEV NEUTRONS SCATTERED BY Bi

Fig. 37e

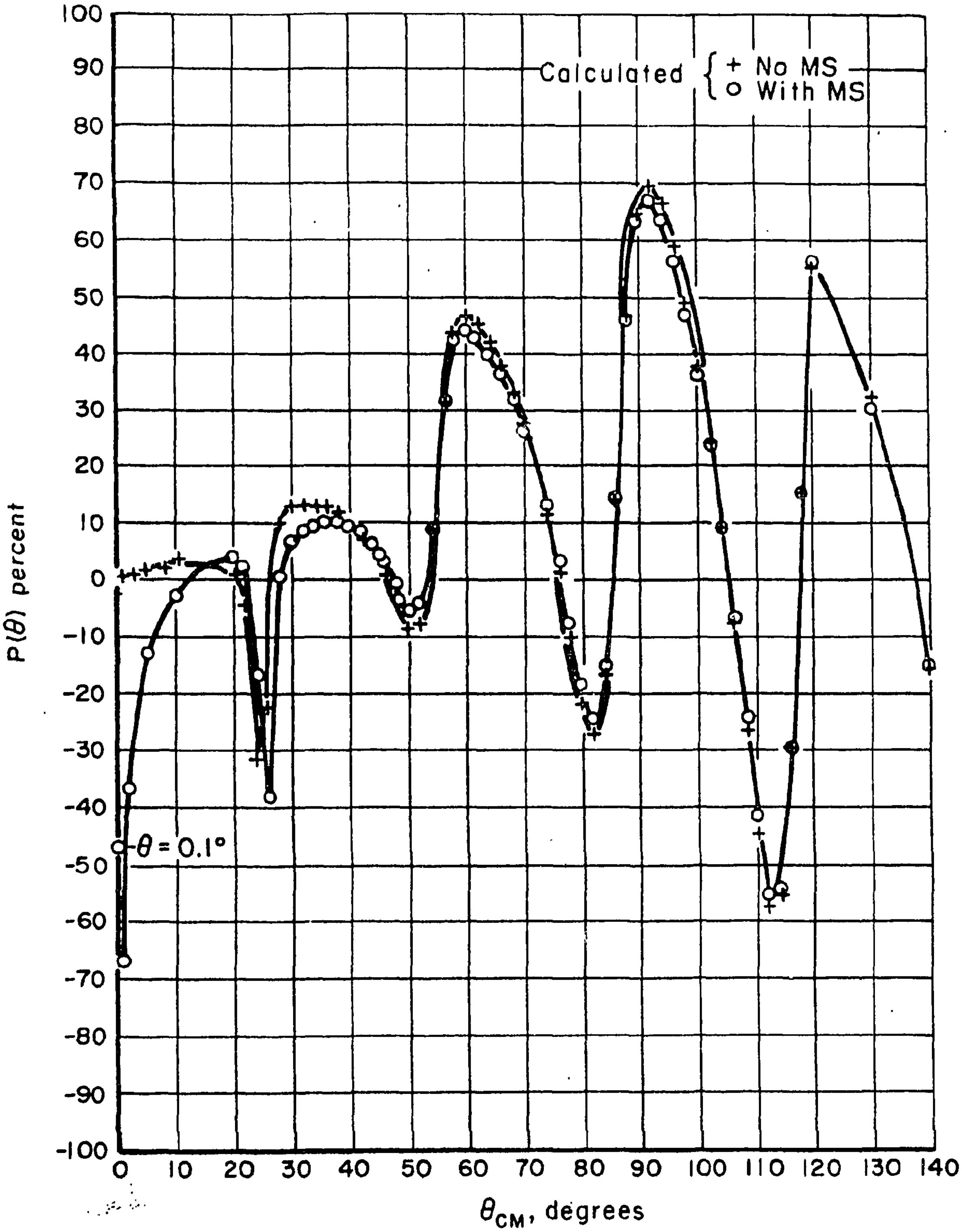

POLARIZATION OF 14.5 MEV NEUTRONS
SCATTERED BY Bi

Fig. 37f

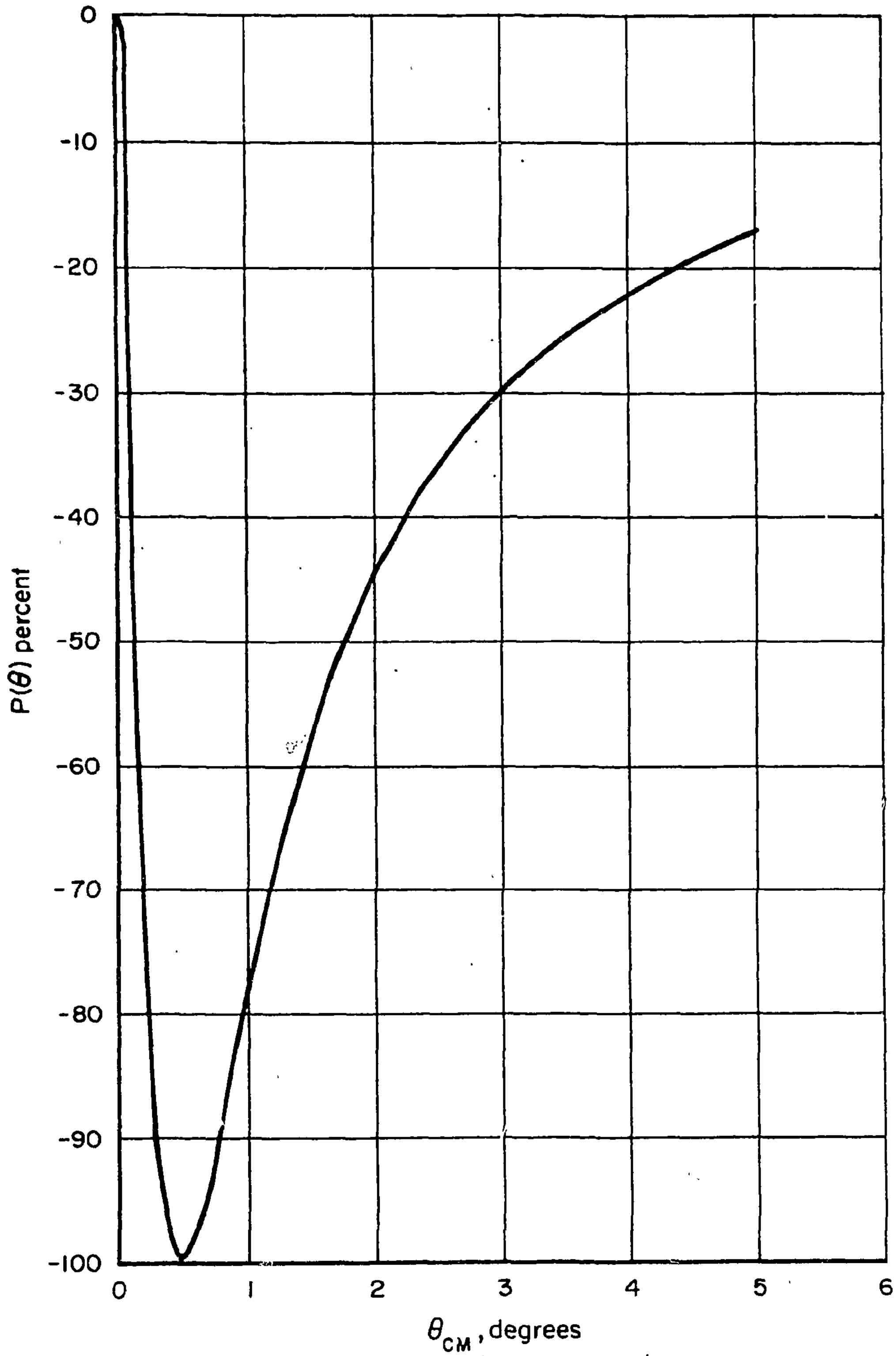

SMALL ANGLE POLARIZATION OF 7 MEV NEUTRONS SCATTERED BY Bi (WITH M-S)

Fig. 37g

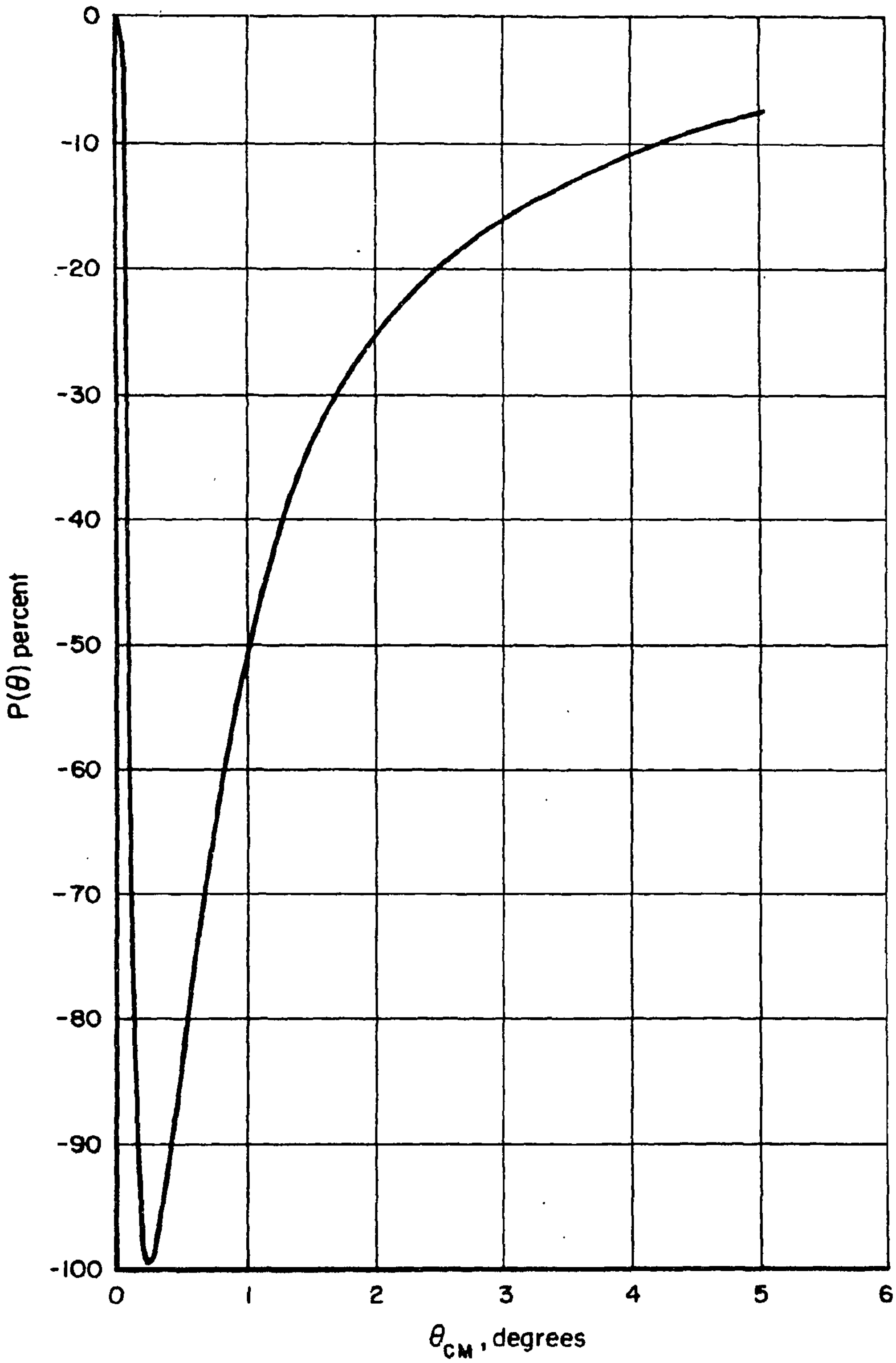

SMALL ANGLE POLARIZATION OF 24 MEV NEUTRONS SCATTERED BY Bi (WITH M-S) with a probability of 68%.

Gorlov *et al*. (Go 67) measured the elastic scattering of 4-MeV neutrons by Cu, In, Sn, Pb, Bi, and U at scattering angles between 2 and 21°. They concluded that their results could be well described under the assumption that only nuclear and Schwinger scattering exist.

The Argonne group re-examined the small angle neutron scattering from U, Th, Pb, Au, W, and Cd (Ku 68). These polarization and differential scattering measurements now revealed that there was no anomalous small angle scattering. They feel that their previous conclusion was wrong and that their results are now consistent with a value of $\alpha < 4 \times 10^{-40}$ cm^3.

The situation can be summarized with regard to the polarizability by reporting that it is reasonably well understood. There does not seem to be any anomalous scattering and all results can be explained with only nuclear and Schwinger scattering. In other words, the polarizability is small enough so that it cannot be deduced from an examination of neutron-nucleus scattering. Consequently, it is sufficiently small to be consistent with theoretical predictions.

Recently Hogan and Seyler have developed a formalism whereby the Schwinger interaction can be treated exactly in optical model calculations (Ho 69a). In their investigations they made the discovery that polarizations can be influenced at angles much greater than had been previously considered. This is particular evident at angles which lie near minima in the cross section curve. Examples of such effects from their calculations with and without Schwinger (sometimes called Mott-Schwinger or MS) scattering are shown in Figs. 37a-h for the differential cross sections and polarizations (Ho 69b).

They also make the point that since the effect of Schwinger scattering extends to large angles it should be considered in any optical model study which attempts to fit polarization data.

We have seen that Schwinger scattering results in an enhancement of both the polarization and the differential cross section at small angles. For example, at 0.2° for 24-MeV neutrons scattered by Bi the polarization is -100% and the differential cross section is about twice the non-Schwinger optical model cross section (Ho 69a). Several groups have already made use of this small-angle polarization (Vo 56, Ku 68). Usually the polarization is large where the cross section is small. This is the one case where the polarization is large where the cross section is large.

III-10. Fissian

A. Introduction

Fission induced by fast neutrons will now be discussed.

By selecting a low energy cutoff of 500 keV, this survey almost eliminated the most exciting discovery in the field of fission physics in many years. This, of course, is the discovery of the double-humped fission barrier.

For completeness it is necessary to provide a brief outline of the significance of this phenomenon and the appropriate references for further study. After a brief review of the consequences of the double-humped fission barrier, a few comments will be made about other aspects of fast-neutron induced fission. These last topics have a very substantial amount of applied interest.

B. Manifestations of the Double-Humped Fission Barrier

Strutinsky (St 67) in 1967 showed that a second minimum, not so deep as the minimum at the normal equilibrium deformation, should exist in the potential energy curve of the transuranic nuclei. An approximation to a plot of ENERGY OF DEFORMATION VS DEFORMATION (St 68) appears as

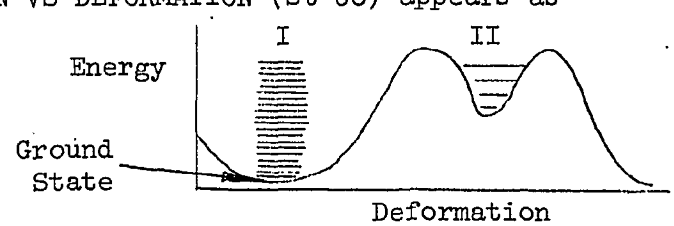

The two regions are labeled I and II.

A nucleus in the lowest class II state will be one of the now familiar fissioning isomers. It can only decay by barrier penetration.

Class II states mix with Class I states, particularly at the higher energies where the penetrability is higher. The level spacings in region II are much greater than the level spacings in region I.

The effect of the mixing of states between regions I and II is to produce enhancements in cross sections at energies corresponding to states in region II. Qualitatively, the fission cross section vs the incident neutron energy would look something like this:

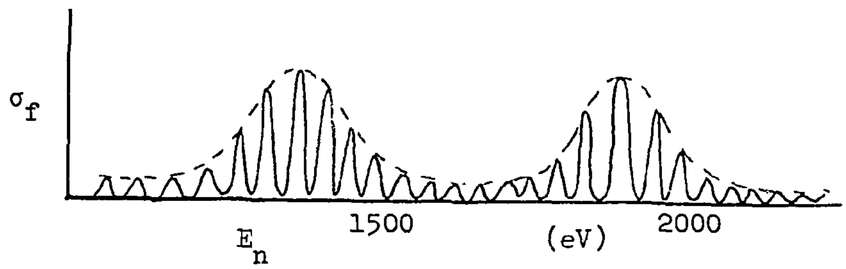

This was indeed observed at Geel for ^{240}Pu (Z=94, N=146) (Ma 68c).

The broad, well separated structure is due to the states in region II. The narrow closely spaced peaks are the compound nucleus states of region I.

Lynn (Ly 68) has examined these and many other arguments in a quantitative fashion. He also has an excellent summary of the experimental situation as it existed in the late summer of 1968. Other recent references include a survey article by Michaudon presented at the 1968 Washington, D. C., Cross Section Conference (Mi 68a) (several other papers on this subject were also presented at the same conference), the 1968 Dubna Conference on Nuclear Structure (see St 68), and the July 1969 Vienna Conference on Fission (Vi 69).

C. Other Aspects of Fast-Neutron Induced Fission

The experiments that will be mentioned now have lost the limelight to sub-threshold fission studies. Nevertheless they have lost none of their importance to the atomic energy industry. These are immediately useful experiments that play major roles in reactor design and development. Such bizarre applications as personnel shielding for deep space missions involving nuclear reactor propulsion, and of course the reactor itself, depend upon the crucial nuclear properties of the materials involved.

The quantities of interest to fast-neutron physicists include the following:

1) Fission cross sections
2) $\bar{\nu}$, the average number of neutrons emitted per fission
3) $P(\nu)$, the neutron distribution function
4) α, the capture to fission cross section ratio
5) Angular distributions of fragments
6) Information on delayed neutrons and delayed gamma rays
7) Alpha and heavy particle emission
8) Ternary fission
9) Mass distributions of fragments
10) Charge distributions of fragments

These fields have been extensively reviewed. A partial list includes an excellent book by Keepin (Ke 65), the 1966 Paris Conference (Pa 66), the 1967 Brussels Panel (Br 67b), the 1968 Washington Conference (Wa 68), and the 1969 Vienna Conference (Vi 69). The proceedings of these conferences either have been or will be published.

Qualitatively, the fields are in good order. The general behavior of all of the quantities is reasonably well understood. Barring any major experimental or theoretical breakthroughs, or the discovery of some new facet such as the

Fig. 38. Block diagram of the LAMPF accelerator.

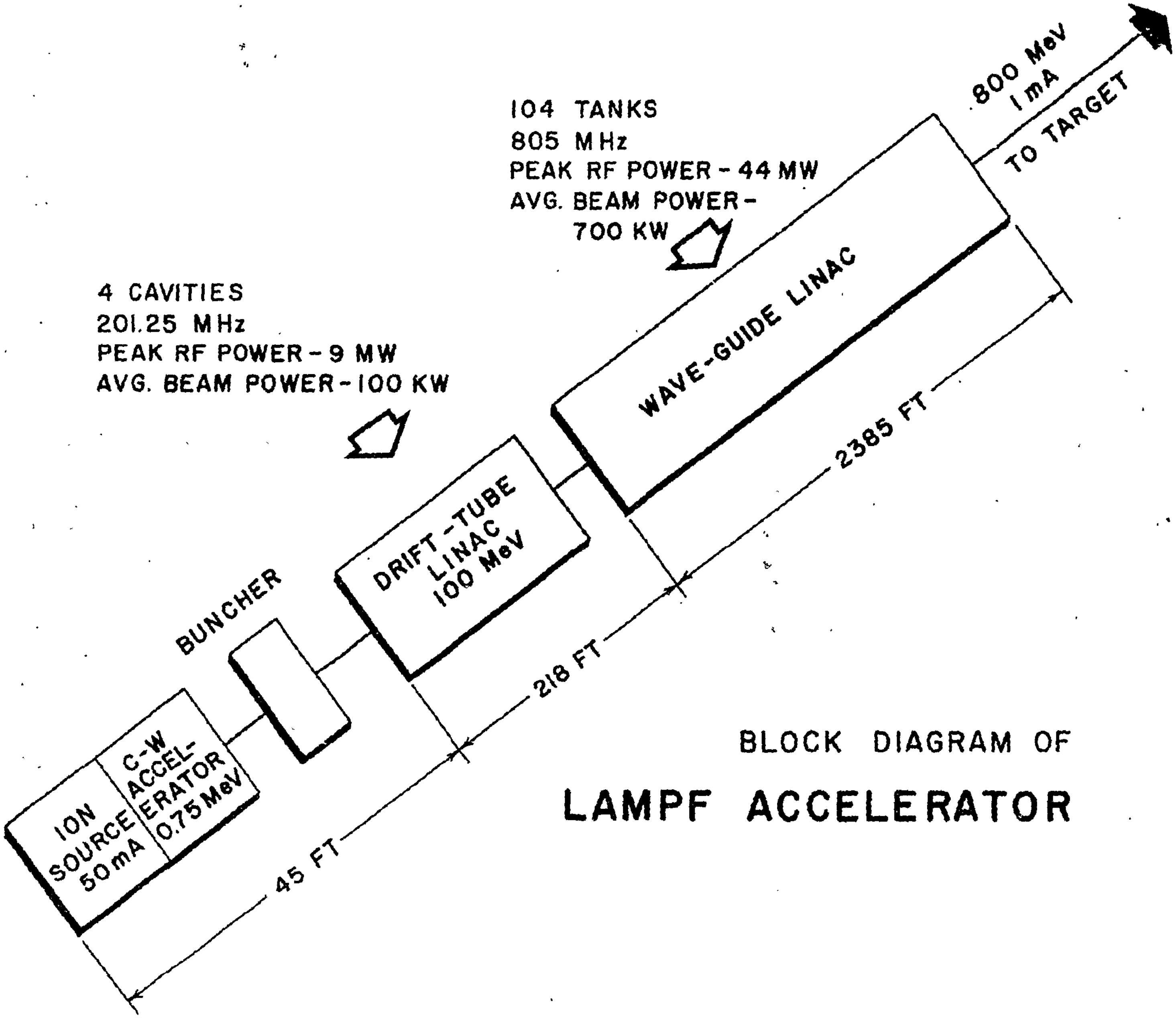

BLOCK DIAGRAM OF

LAMPF ACCELERATOR

Fig. 38

double-humped fission barriers, there will be just a slow steady refinement of the various numbers. It seems clear that the values are not as well established as some designers would wish. On the other hand, there seems to be no great clamor for a crash program to push the accuracy to one more decimal place.

Probably the most fascinating feature of some fast-neutron fission experiments is the practical use of nuclear explosions as very intense sources of neutrons. The underground "pipe shots" at the Nevada Test Site are well known (He 66a, He 68, Br 69b), and will not be described here.

The new feature is that Diven and his colleagues are now trying to polarize the neutron beam. They will use a polarized proton filter similar to that described by Shapiro (Sh 65) at Dubna. They hope to obtain $\sim$60% proton polarization resulting in a 64% polarization of the transmitted neutron beam.

The application of nuclear explosions to neutron physics was an experimental breakthrough. The possibilities are immense for performing whole classes of experiments that would be extremely difficult or impossible in the laboratory.

III-11. High Energy

Los Alamos has now completed about 2/3 of the design and construction of a large, very high-intensity, medium-energy, proton linear accelerator. This is called LAMPF, which means Los Alamos Meson Physics Facility (Ro 66, Ro 69a). We intend to use this machine as a high-energy (100-800 MeV) neutron source to study the n-p reaction and various n-nuclear interactions.

The machine is an 800-MeV, 1-mA (average current), proton linear accelerator.

Figure 38 shows a block diagram of the LAMPF accelerator. A 50-mA ion source and a 750-keV Cockroft-Walton accelerator inject positive or negative ions into the 100-MeV Alvarez drift-tube linac through a klystron bunching system. The output of the Alvarez section injects into a Los Alamos designed wave-guide linac which carries the energy from 100 MeV up to a maximum of 800 MeV.

The facility, as now designed, can simultaneously accelerate an H^+ beam with an average current of 1 mA and an H^- beam with an average current of 100 μA. The energy will be variable between 100 MeV and 800 MeV.

The beam time profile will consist of a macrostructure of 120 pulses per second, each one being 500 μsec long. Each macropulse will have a microstructure consisting of a 0.25-nsec burst every 5 nsec. The energy spread will be about 0.4%.

It is expected that sometime after the machine becomes available in late 1972 or 1973 to have a polarized-proton beam. The polarized-proton ion source has not been designed or developed. However, it would be expected to have a greatly reduced intensity (perhaps ≤ 1 μA). We hope to do neutron time-of-flight experiments on LAMPF and are negotiating the characteristics of such a facility with the design scientists.

Figure 39 shows one tentative version of the main LAMPF experimental areas that may be available when the machine turns on.

Area A will contain the pion and muon production and experimentation areas. Area C will contain a 1000-ton ($\sim$1 million kilogram) high-resolution spectrograph, to be used for nuclear physics investigations with charged particles.

Area B, which this discussion will concentrate on, is the fast-neutron area. The building, beam line, shielding, and beam stop are now undergoing design studies.

Fig. 39. One tentative version of the main LAMPF experimental areas. The final design was not complete at the time of writing (summer 1969).

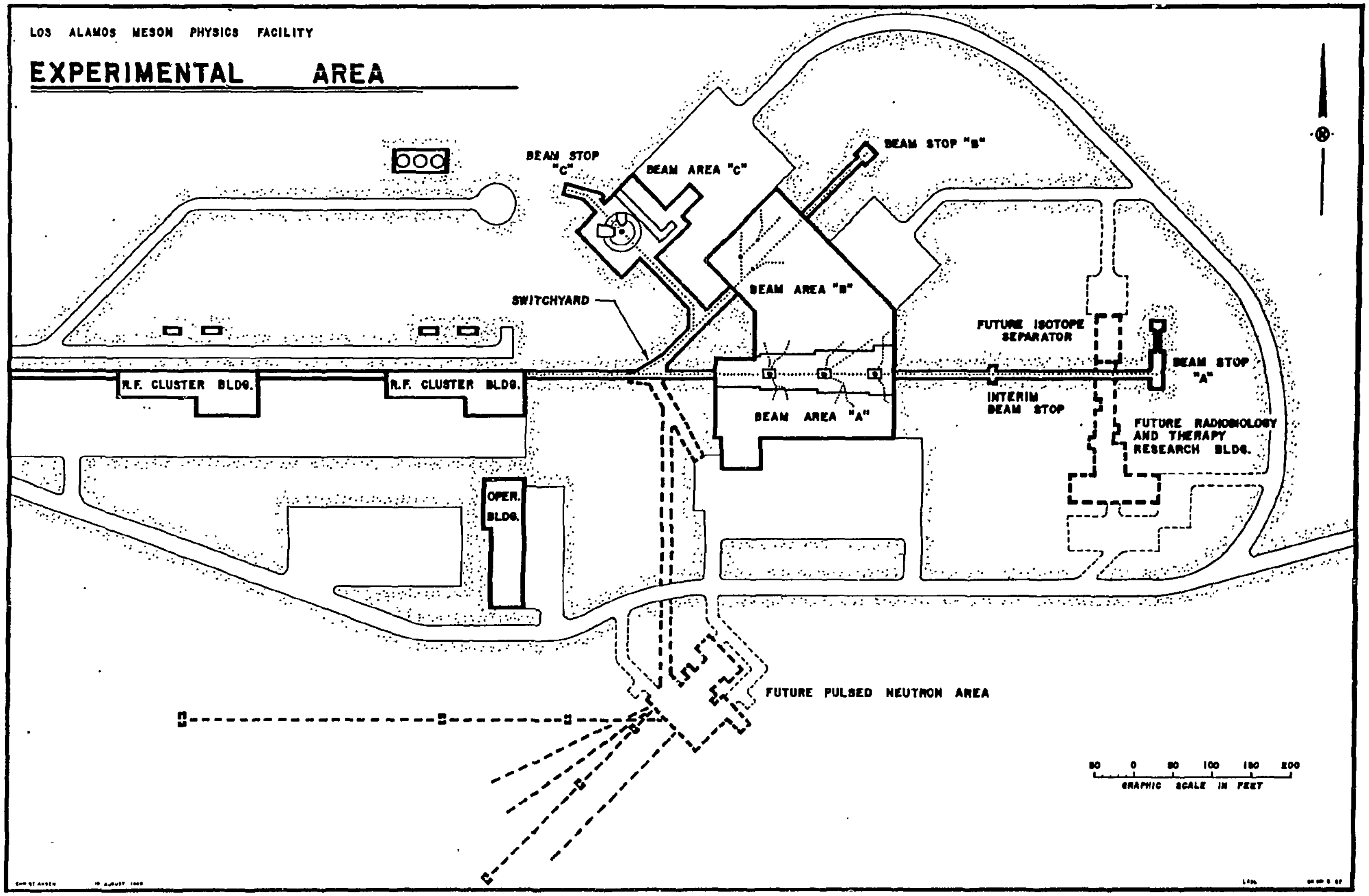
LOS ALAMOS MESON PHYSICS FACILITY
EXPERIMENTAL AREA
BEAM STOP "C"
BEAM AREA "C"
BEAM STOP "B"
BEAM AREA "B"
SWITCHYARD
R.F. CLUSTER BLDG.
R.F. CLUSTER BLDG.
BEAM AREA "A"
FUTURE ISOTOPE SEPARATOR
INTERIM BEAM STOP
BEAM STOP "A"
FUTURE RADIOBIOLOGY AND THERAPY RESEARCH BLDG.
OPER. BLDG.
FUTURE PULSED NEUTRON AREA
50 0 50 100 150 200
GRAPHIC SCALE IN FEET

Fig. 39

For the initial operation the experiments in the neutron area will probably use a large fraction of the H^- beam. In this mode meson experiments, which use all of the very intense H^+ beam, can proceed simultaneously with the charged particle and neutron experiments, which share the H^- beam. Neither of the last two areas could handle the full intensity H^+ beam as they are presently planned.

Actually, there are a number of advantages of the H^- beam. One will be discussed now because it is a good trick and may have numerous applications. This goes by the name of super collimation (Ri 62, Ar 69).

A negative beam, with particles consisting of a proton plus 2 electrons, can be collimated with slits or apertures. All particles striking the slits will be converted from negative to positive and can be swept away with electromagnetic devices. Consequently, slit scattering, the plague of positive beam collimation, is eliminated. This, of course, is a powerful tool for the study of small-angle scattering.

Monoenergetic neutrons, variable in energy between 100 and 800 MeV, will be produced by means of the D(p,n)2p reaction (La 60, Me 66a, La 67). A 15-cm-thick liquid-deuterium target will intercept a small fraction of the beam, the remainder of which will be deflected into a local beam dump. At zero degrees to the beam direction, intense beams (flux at $0^\circ \sim 6 \times 10^{12}$ n/sr-sec with 80 μA incident proton beam) of small energy spread (<10 MeV) can be produced. At angles of about 28°, to the incident beam direction, neutrons with polarizations in the neighborhood of 30% will be produced (Ch 67b).

For certain experiments beams of polarized neutrons are very advantageous. For example, in Section III-1, it was mentioned that the triple scattering spin-correlation parameter C_{nn} could be determined from a differential cross section measurement of a polarized beam scattered from a polarized target A_{xx}.

The neutron-proton situation in the 300-800 MeV energy range will now be reviewed very briefly (Si 68).

The neutron-proton data are very sparse indeed, consisting almost entirely of cross section and polarization data and approximately 10 data in the triple scattering category. However, there have been no spin-correlation experiments. Total cross section data, which are of fundamental importance in the interpretation of neutron-nucleus total cross sections, would be desirable.

Neutron-proton differential cross section and polarization measurements, particularly at small angles, are needed. The whole range of spin-correlation data is necessary over the entire range to uniquely determine the scattering matrix.

So far, what has been said applies to the elastic scattering data. The situation with regard to the inelastic processes is dismal by comparison. The two attractions of LAMPF are the copious neutron flux and the fact that the energy is easily variable. The copious flux has already been discussed. It, of course, allows measurements of triple scattering parameters which would not be feasible on other accelerators.

The variable energy feature is also of paramount importance in that it will allow the energy dependences of the observables to be measured. In the case of the nucleon-nucleon problem, for example, the transition from elastic scattering in the 400-MeV range to inelastic scattering in the 600-MeV range is not well understood. These regions will be mapped in detail.

So much for the neutron-nucleon problem. A few brief comments will now be made regarding the neutron-nucleus interactions (La 69c). Most of the work in this field consists of total cross section measurements. These cross sections, at first glance, are gratifying in their simplicity. They all have roughly the same shape with energy and the cross sections, as functions of A, are easily described by some simple formula at each energy.

The cross sections fall smoothly from about 150 MeV to 270 MeV, are flat to about 400 MeV, then rise slowly (10-20% total), due to the onset of pion production, to about 1 GeV, then drop slowly to their 300-MeV values again. It is really a fair guess to say that the cross sections do not vary with energy above 400 MeV.

A few of the simple expressions for the total cross sections are as follows:

E_n	Formula σ_T in $(\mathrm{fm})^2$	Reference
410 MeV	$\sigma_T = 2\pi R^2[1-\exp(-KR)]$ $R = 1.2A^{1/3}$, $K = 0.36$	(Ne 54)
10 GeV/c	$\sigma_T = 2\pi(1.3A^{1/3} - 0.6)^2$	(En 68)
27 GeV/c	$\sigma_T = 4.6\ A^{0.75}$	(Jo 68)

One rather interesting aspect of this work is in the investigation of the radii of the neutron and of the proton distributions in nuclei. The early experiments indicated that the radii of the distributions of protons and neutrons for light and medium weight nuclei coincided and for heavy nuclei the neutron distribution is insignificantly larger (perhaps 0.1 to 0.2 fm) than the proton distribution (Wi 55a, Wi 55b, El 61).

On the other hand, some recent work (Bu 67) indicates a substantial excess of neutrons on the nuclear surface, particularly for heavy nuclei. A recent report (Og 68) of a 1962 experiment on pion production by neutrons has been qualitatively interpreted as supporting this contention.

This result may or may not be correct. The whole field is in a very primative state. It is expected that the high-intensity machines, such as the one at LAMPF, will make great headway in unraveling the nature of nuclei.

IV. FUTURE

Neutron physics desperately needs an experimental breakthrough. We need the kind of boost that lithium-drifted germanium counters gave to gamma-ray work. This means new ideas--not brute force techniques.

Way down in importance come the projects that we know how to do. I see the frontiers of neutron physics spreading to higher energies, i.e., above 50 MeV. Also I am glad to see some penetration into the unexplored energy region between 8 and 14 MeV. To fill this void we really need more variable energy machines.

Except at the very highest energies we do not need survey experiments. We need very accurate measurements. Virtually anything that can be measured more accurately is worth doing.

Finally, I want to toss out a plaintive plea to spend more time standing back looking at the whole picture. It is all too obvious that many experiments are just chosen at random. On the other hand, it is not at all obvious that we are all working on the same problem, or problems, or indeed even what the problems are.

ACKNOWLEDGEMENTS

I am deeply indebted to many individuals throughout the world who have contributed so generously to this report. I particularly want to acknowledge the information, assistance, and encouragement of L. E. Agnew, Jr., S. J. Bame, H. H. Barschall, J. R. Beyster, M. Bormann, R. Bouchez, J. D. Brandenberger, G. Breit, H. Britt, P. S. Buchanan, B. L. Cohen, H. Condé, B. C. Diven, D. M. Drake, A. T. G. Ferguson, H. Feshbach, T. R. Fisher, D. G. Foster, Jr., W. R. Gibbs, W. S. Hogan, C. E. Hollandsworth, I. Halpern, J. Leroy, M. Kellogg, H. H. Knitter, R. O. Lane, G. Paić, F. Perey, C. LeRigoleur, I. L. Morgan, J. D. Seagrave, J. E. Simmons, A. B. Smith, W. Stein, Leona Stewart, J. Symonds, K. Tsukada, and J. E. Young.

REFERENCES

(Ab 64) A. Abragam and M. Borghini, Progress in Low Temperature Physics, Ed. by C. J. Gorter (North Holland Pub. Co., 1964) Vol. IV.

(Ag 63) A. Agodi and G. Pappalardo, Nucl. Phys. 47, 129 (1963).

(Al 56) Y. A. Aleksandrov and I. I. Bondarenko, Sov. Phys. JETP 4, 612 (1957).

(Al 57) Y. A. Aleksandrov, Sov. Phys. JETP, 6, 228 (1958).

(Al 66) Y. A. Aleksandrov, G. S. Samosvat, Sov. Phys. JETP Letters 4, 134 (1966).

(An 64) J. H. Anderson and D. Swann, Nucl. Inst. Meth. 30, 1 (1964).

(An 65) V. B. Anufrienko, B. V. Devkin, G. V. Kotelnikova, G. N. Lovchikova, O. A. Salnikov, L. A. Timohin, and N. J. Fetisov, International Conference on the Study of Nuclear Structure with Neutrons, Antwerp, July 19-23, 1965, EANDC-50-S (European-American Nuclear Data Committee, 1965) Vol. 2, p. 197.

(An 67) B. Antolković, G. Paić, P. Tomaš, and D. Rendić, Phys. Rev. 159, 777 (1967).

(Ar 66) U. R. Arifkhanov, N. A. Vlasov, V. V. Davydov, and L. N. Samoilov, Sov. J. Nucl. Phys. 2, 170 (1966).

(Ar 69) D. D. Armstrong and H. E. Wegner, Bull. Am. Phys. Soc. 14, 532 (1969).

(As 63) V. S. Ashby, H. C. Catron, M. D. Goldberg, R. W. Hill, J. M. LeBlanc, L. L. Newkirk, J. P. Stoering, C. J. Taylor, and M. A. Williamson, Phys. Rev. 129, 1771 (1963).

(As 66) J. B. Ashe, I. L. Morgan, and J. D. Hall, Rev. Sci. Instr. 37, 1559 (1966).

(Au 67) E. H. Auerbach and S. O. Moore, Phys. Rev. 163, 1124 (1967).

(Ba 52) H. H. Barschall, Phys. Rev. 86, 431 (1952).

(Ba 57) S. J. Bame, Jr., E. Haddad, J. E. Perry, Jr., and R. K. Smith, Rev. Sci. Instr. 28, 997 (1957).

(Ba 58) R. Batchelor and J. H. Towle, "Fast Neutron Time-of-Flight Spectrometer for the 6-MeV Van de Graaff Generator," AWRE Report NR/P-12/58 (1958).

(Ba 60a) S. J. Bame, Jr., E. Haddad, J. E. Perry, Jr., R. K. Smith, and B. Swartz, Rev. Sci. Instr. 31, 911 (1960).

(Ba 60b) H. H. Barschall, Nuclear Spectroscopy, Ed. by Fay Ajzenberg-Selove (Academic Press, New York, 1960) Part A, p. 451.

(Ba 61a) Helv. Phys. Acta, Suppl. VI, 436 (1961).

(Ba 61b) D. W. Barr, C. I. Browne, and J. S. Gilmore, Phys. Rev. 123, 859 (1961).

(Ba 61c) R. Batchelor, W. B. Gilboy, J. B. Parker, and J. H. Towle, Nucl. Inst. Meth. 13, 70 (1961).

(Ba 63) R. Batchelor and J. H. Towle, Nucl. Phys. 47, 385 (1963).

(Ba 65) H. H. Barschall, Proceedings of 2nd International Symposium on Polarization Phenomena of Nucleons, Karlsruhe, 1965 (Birkhauser Verlag Basel and Stutgart, 1966) p. 393.

(Ba 67) R. W. Bauer, J. D. Anderson, H. F. Lutz, C. Wong, J. W. McClure, and B. A. Pohl, Nucl. Phys. A93, 673 (1967).

(Ba 68a) E. Barnard, J. A. M. DeVilliers, C. A. Engelbrecht, and D. Reitmann, Nucl. Phys. A118, 321 (1968).

(Ba 68b) A. W. Barrows, R. C. Lamb, D. Vekley, and M. T. McEllistrem, Phys. Rev. A107, 153 (1968).

(Ba 68c) R. Batchelor, Proceedings of Conference on Neutron Cross Sections and Technology, Washington, D. C., 1968, D. T. Goldman, Ed. (NBS Pub. 299, 1968) p. 89.

(Be 63) B. A. Benetskij and I. M. Frank, Proceedings of the Conference on Direct Interactions and Nuclear Reaction Mechanisms, Padua, 1962 (Gordon & Breach, New York, 1963) p. 828.

(Be 64) L. Beckman, R. B. Jansson, and B. L. Nilsson, Research Institute of National Defence FOA 4-report A 4395-4262 (1964).

(Be 66) A. F. Behof, J. M. Hevezi, and G. Spalek, Nucl. Phys. 84, 290 (1966).

(Be 67a) P. L. Beach, R. W. Finlay, R. L. Cassola, and R. D. Koshel, Phys. Rev. 156, 1201 (1967).

(Be 67b) L. Beckman, J. Hansén, and R. Jansson, Nucl. Inst. Meth. 52, 157 (1967).

(Be 67c) R. W. Benjamin and I. L. Morgan, Phys. Rev. 163, 1252 (1967).

(Be 68) J. G. Beery, K. H. Harper, V. M. Stovall, and L. Rosen, Los Alamos Scientific Laboratory Report LA-3788 (1968).

(Be 69) J. R. Beyster, private communication (1969).

(Bl 52a) J. M. Blatt and V. F. Weisskopf, Theoretical Nuclear Physics (John Wiley and Sons, Inc., New York, 1952) p. 93.

(Bl 52b) J. M. Blatt and V. F. Weisskopf, Theoretical Nuclear Physics (John Wiley and Sons, Inc., New York, 1952) p. 367.

(Bl 52c) J. M. Blatt and V. F. Weisskopf, Theoretical Nuclear Physics (John Wiley and Sons, Inc., New York, 1952) p. 484.

(Bl 52d) J. M. Blatt and V. F. Weisskopf, Theoretical Nuclear Physics (John Wiley and Sons, Inc., New York, 1952) p. 533-535.

(Bo 62) D. Bodansky, Ann. Rev. Nucl. Sci. 12, 107 (1962).

(Bo 62) M. Bormann, Nucl. Phys. 65, 257 (1965).

(Bo 69a) B. E. Bonner, E. B. Paul, and G. C. Phillips, Nucl. Phys. A128, 183 (1969).

(Bo 69b) M. Bormann, private communication (1969).

(Br 59) G. Breit and M. L. Rustgi, Phys. Rev. 114, 830 (1959).

(Br 60) J. E. Brolley, Jr. and J. L. Fowler, Fast Neutron Physics, J. B. Marion and J. L. Fowler, Eds. (Interscience Pub. Inc., New York, 1960) Part I, p. 73.

(Br 63) D. M. Brink and R. O. Stephen, Phys. Letters 5, 77 (1963).

(Br 64) D. J. Bredin, Phys. Rev. 135, B412 (1964).

(Br 67a) G. Breit, R. E. Seaman, and K. A. Friedman, private communication (1967).

(Br 67b) Nuclear Standards for Neutron Measurements, Report of a Panel Sponsored by the IAEA, Brussels, 1967, IAEA Report-107.

(Br 68) C. N. Brown, Ph.D. Thesis, "An Experimental Test of the Impulse Approximation at 200 MeV," University of Rochester, New York (1968).

(Br 69a) J. D. Brandenberger, Nucl. Inst. Meth. 69, 271 (1969).

(Br 69b) W. K. Brown and G. A. Cowan, Los Alamos Scientific Laboratory Report LA-DC-10416 (April, 1969).

(Bu 57) S. T. Butler and O. H. Hittmair, Nuclear Stripping Reactions (Horwitz Pub., Inc., Sydney, 1957).

(Bu 64) S. G. Buccino, C. E. Hollandsworth, H. W. Lewis, and P. R. Bevington, Nucl. Phys. 60, 17 (1964).

(Bü 66) F. W. Büsser, F. Niebergall, G. Söhngen, and J. Christiansen, Nucl. Phys. 88, 593 (1966).

(Bu 67) E. H. S. Burhop, Nucl. Phys. B1, 438 (1967).

(Bu 68) P. G. Butler, N. Cohen, A. N. James, and J. P. Nicholson, Phys. Rev. Letters 21, 470 (1968).

(Bü 69) F. W. Büsser, H. Dubenkropp, F. Niebergall, and K. Sinram, Nucl. Phys. A129, 666 (1969).

(Ca 63) G. Calvi, R. Ricamo, A. Rubbino, and D. Zubice, Nucl. Phys. 48, 408 (1963).

(Ca 66) T. A. Cahill, Nucl. Inst. Meth. 42, 327 (1966).

(Ca 67) A. Carlson and H. Barschall, Phys. Rev. 158, 1142 (1967).

(Ch 52) G. F. Chew and G. C. Wick, Phys. Rev. 85, 636 (1952).

(Ch 63a) A. Chatterjee, Nucl. Phys. 47, 511 (1963).

(Ch 63b) A. Chatterjee, Nucl. Phys. 49, 686 (1963).

(Ch 64a) A. Chatterjee, Phys. Rev. 134, B374 (1964).

(Ch 64b) A. Chatterjee, Nucl. Phys. 60, 273 (1964).

(Ch 67a) D. Cheng, Rev. Mod. Phys. 39, 526 (1967).

(Ch 67b) D. Cheng, B. MacDonald, J. A. Helland, and P. M. Ogden, Phys. Rev. 163, 1470 (1967).

(Ch 68) K. C. Chung, D. E. Velkley, J. D. Brandenberger, and M. T. McEllistrem, Nucl. Phys. A115, 476 (1968).

(Ch 69) S. Chatterjee and A. Chatterjee, Nucl. Phys. A125, 593 (1969).

(Ci 66a) S. Cierjacks, P. Forti, L. Kropp, and H. Unseld, Seminar on Intense Neutron Sources, Santa Fe, September, 1966 (CONF-660925, European American Nuclear Data and Reactor Physics Committee).

(Ci 66b) N. Cindro, Rev. Mod. Phys. 38, 391 (1966).

(Ci 68) S. Cierjacks, P. Forti, D. Kopsch, L. Kropp, and J. Nebe, Proceedings of Conference on Neutron Cross Sections and Technology, Washington, D. C., 1968, D. T. Goldman, Ed. (NBS Special Pub. 299, 1968) Vol. 2, p. 743.

(Ci 69) S. Cierjacks, P. Forti, G. J. Kirovac, D. Kopsch, L. Kropp, and J. Nebe, Phys. Rev. Letters 23, 866 (1969).

(Cl 58) J. D. Clement, F. Boreli, S. E. Darden, W. Haeberli, and H. R. Stiebel, Nucl. Phys. 6, 177 (1958).

(Cl 69) P. J. Clements and A. Langsford, Phys. Letters 30B, 25 (1969).

(Co 60) J. H. Coon, Fast Neutron Physics, J. B. Marion and J. L. Fowler, Eds. (Interscience Pub., Inc., New Yokr, 1960) Part I, p. 677.

(Co 62) L. Colli, I. Iori, M. G. Marcazzan, and M. Milazzo, Phys. Letters 2, 12 (1962).

(Co 66) H. Condé, D. M. Drake, and J. C. Hopkins, "Conference on Neutron Cross Section Technology, Washington, D. C." CONF-660303 (March, 1966) p. 735.

(Co 67a) M. Coppola and H. H. Knitter (Euratom, Geel, Belgium) Kerntechnik 9, 459 (Oct. 1967).

(Co 67b) S. A. Cos, Nucl. Inst. Meth. 56, 245 (1967).

(Co 68a) B. L. Cohen, E. C. May, T. M. O'Keefe, C. L. Fink, and B. Rosner, Phys. Rev. Letters 21, 226 (1968).

(Co 68b) B. L. Cohen, E. C. May, T. M. O'Keefe, C. L. Fink, and B. Rosner, Phys. Rev. Letters 21, 226 (1968).

(Co 68c) S. A. Cox, Neutron Cross Sections and Technology Conference, Washington, D. C., 1968 (NBS Pub. 229, 1968) p. 701.

(Co 69) B. L. Cohen, private communication (1969).

(Cr 59) L. Cranberg and J. Levin, Los Alamos Scientific Laboratory Report LA-2177, Appendices I and II (1959).

(Cr 61) L. Cranberg, R. A. Fernold, F. S. Hahn, and E. F. Shrader, Nucl. Inst. Meth. 12, 335 (1961).

(Cr 63a) L. Cranberg, C. D. Zafiratos, J. S. Levin, and T. A. Oliphant, Phys. Rev. Letters 11, 341 (1963).

(Cr 63b) A. H. Cromer and E. H. Thorndike, Phys. Rev. 131, 1680 (1963).

(Cr 67) L. Cranberg, T. A. Oliphant, J. Levin, and C. D. Zafiratos, Phys. Rev. 159, 969 (1967).

(Cs 66) J. Csikai and G. Petö, Phys. Letters 20, 52 (1966).

(Cz 64) J. B. Czirr, D. R. Nygren, and C. D. Zafiratos, Nucl. Inst. Meth. 31, 226 (1964).

(Cz 68) J. B. Czirr, private communications via C. D. Bowman (1968).

(Cz 69) T. Czibók, Gy. Hrehuss, I. Kovacs, L. Nagy, and I. Vinnay, Phys. Letters 29B, 105 (1969).

(Da 61) W. Daehnick and R. Sherr, Rev. Sci. Instr. 32, 666 (1961).

(Da 64) D. Dandy and D. P. Hammond, Nucl. Inst. Meth. 30, 23 (1964).

(Da 68a) J. C. Davis and H. H. Barschall, Phys. Letters 27B, 636 (1968).

(Da 68b) J. C. Davis and F. T. Nodu, Proceedings of Conference on Neutron Cross Sections and Technology, Washington, D. C., 1968, D. T. Goldman, Ed. (NBS Pub. 299, 1968) p. 177.

(De 63) W. Deuchars, J. L. Perkin, and R. Batchelor, Nucl. Inst. Meth. 23, 305 (1963).

(De 66) A. De-Shalit, Preludes in Theoretical Physics, A. De-Shalit, et al. Eds. (North Holland, 1966) p. 35.

(Di 67) W. C. Dickinson and C. D. Bowman, Rev. Mod. Phys. 39, 592 (1967).

(Di 69) J. K. Dickens and F. G. Perey, Nucl. Sci. Eng. 36, 280 (1969).

(Dr 62) D. M. Drake, "A Study of Neutron Evaporation in 42-MeV Alpha Particle Bombardments of Several Elements," Ph.D. Thesis, University of Washington (1962) unpublished.

(Dr 69a) D. M. Drake, Nucl. Phys., to be published (1969).

(Dr 69b) D. M. Drake, J. C. Hopkins, C. S. Young, H. Condé, and A. Sattler, Nucl. Phys. A128, 209 (1969).

(Dr 69c) L. Drigo, C. Manduchi, G. Moschini, M. T. R. Manduchi, G. Tornielli, and G. Zannoni, Nuovo Cim. Letters 1, 237 (1969).

(Ed 66) J. A. Edgington and B. Rose, Nucl. Phys. 89, 523 (1966).

(El 61) L. R. B. Elton, Nucl. Phys. 23, 681 (1961).

(El 62) A. J. Elwyn and R. O. Lane, Nucl. Phys. 31, 78 (1962).

(El 64) A. J. Elwyn, R. O. Lane, A. Langsdorf, Jr., and J. E. Monahan, Phys. Rev. 133, B80 (1964).

(El 66) A. J. Elwyn, J. E. Monahan, R. O. Lane, A. Langsdorf, Jr., and F. P. Mooring, Phys. Rev. 142, 758 (1966).

(El 69) A. J. Elwyn and J. E. Monahan, Nucl. Phys. A123, 33 (1969).

(En 63) C. E. Engelke, R. E. Benenson, E. Melkonian, and J. M. Lebowitz, Phys. Rev. 129, 326 (1963).

(En 68) J. Engler, K. Horn, J. König, F. Mönnig, P. Schludecker, H. Schopper, P. Sievers, H. Ullrich, and K. Runge, Phys. Letters 28B, 64 (1968).

(Er 60a) T. Ericson, Phys. Rev. Letters 5, 430 (1960).

(Er 60b) T. Ericson, Phil. Mag. Suppl. 9, 425 (1960).

(Er 60c) T. Ericson, Adv. in Phys. IX, 425 (1960).

(Er 63) T. Ericson, Ann. Phys. (New York) 23, 390 (1963).

(Fa 62) U. Facchini, E. Saetta Menichella, and F. Tonolini, Phys. Letters 1, 209 (1962).

(Fa 64) U. Facchini, Nucl. Phys. 51, 460 (1964).

(Fa 66) U. Fasoli, D. Tonolo, and G. Zago, Il Nuovo Cim. XIIIV B, 455 (1966).

(Fe 67a) H. Feshbach, A. K. Kerman, and R. H. Lemmer, Ann. of Phys. 41, 230 (1967).

(Fe 67b) P. Fessenden and D. R. Maxson, Phys. Rev. 158, 948 (1967).

(Fi 67) T. R. Fisher, R. S. Safrata, E. G. Shelley, J. McCarthy, S. M. Austin, and R. C. Barrett, Phys. Rev. 157, 1149 (1967).

(Fi 69a) T. R. Fisher, D. C. Healey, and J. S. McCarthy, Nucl. Phys. A130, 609 (1969).

(Fi 69b) T. R. Fisher, private communication (1969).

(Fo 63) R. Fox, Nucl. Phys. 43, 110 (1963).

(Fo 64) D. B. Fossan and M. Walt, Phys. Rev. Letters 12, 672 (1964).

(Fo 65) D. G. Foster, Jr., and D. W. Glasgow, Nucl. Inst. Meth. 36, 1 (1965).

(Fo 66) D. B. Fossan, R. A. Chalmers, S. R. Salisbury, and F. J. Vaughn, Phys. Rev. 152, 980 (1966).

(Fo 69) D. G. Foster, Jr., private communication (1969).

(Fr 66) V. Franco and R. J. Glauber, Phys. Rev. 142, 1195 (1966); and V. Franco, private communication.

(Ga 60) J. Gammel, Fast Neutron Physics (Interscience Pub., Inc., New York, 1960) Part II, Chap. VI, p. 2185.

(Ga 64) D. G. Gardner and Yu-Wen Yu, Nucl. Phys. 60, 49 (1964).

(Gi 65a) W. R. Gibbs, "The Interpretation of Nuclear Excitation Functions at High Energy: Ericson Fluctuations," Los Alamos Scientific Laboratory Report LA-3266 (1965).

(Gi 65b) W. R. Gibbs, Phys. Rev. 139 B1185 (1965).

(Gi 65c) A. Gilbert and A. G. W. Cameron, Can. J. Phys. 43, 1446 (1965).

(Gi 65d) W. B. Gilboy and J. H. Towle, Nucl. Phys. 64, 130 (1965).

(Gi 67) W. R. Gibbs, Phys. Rev. 153, 1206 (1967).

(Gl 69) D. W. Glasgow and D. G. Foster, Jr., Phys. Rev. Letters 22, 139 (1969).

(Go 61) M. D. Goldberg, J. D. Anderson, J. P. Stoering, and C. Wong, Phys. Rev. 122, 1510 (1961).

(Go 67) G. V. Gorlov, N. S. Lebedeva, and V. M. Morozov, Sov. Phys. JETP Letters 5, 106 (1967).

(Gr 65) L. Grodzins, P. H. Rose, and R. J. Van de Graaff, Nucl. Inst. Meth. 36, 202 (1965).

(Gr 69) S. M. Grimes, Nucl. Phys. A124, 369 (1969).

(Ha 52) W. Hauser and H. Feshbach, Phys. Rev. 87, 366 (1952).

(Ha 63a) W. Haeberli, Fast Neutron Physics, J. B. Marion and J. L. Fowler, Eds. (Interscience Pub., Inc., New York, 1963) Vol. II, p. 1379.

(Ha 63b) W. Haeberli, Fast Neutron Physics, J. B. Marion and J. L. Fowler, Eds. (Interscience Pub., Inc., New York, 1963) Part II, p. 1423.

(Ha 64) I. Hall, Phys. Letters 10, 199 (1964).

(Ha 65) R. P. Haddock, R. M. Salter, Jr., M. Zeller, J. B. Czirr, and D. R. Nygren, Phys. Rev. Letters 14, 318 (1965).

(Ha 66) R. P. Haddock and R. J. Wagner, Proceedings of the International Conference on Polarized Targets and Ion Sources, Saclay, France, 1966 (CENF, Saclay) p. 381-385.

(Ha 67) M. L. Halbert, F. E. Durham and A. van der Woude, Phys. Rev. 162, 899 (1967).

(Ha 69) W. Haeberli, Conference on the Three-Body System, Birmingham, 1969 (North Holland Pub. Co., Amsterdam) to be published.

(He 64) L. Heller, P. Signell, and N. R. Yoder, Phys. Rev. Letters 13, 577 (1964).

(He 66a) A. Hemmendinger, Conference on Nuclear Data - Microscopic Cross Sections and Other Data Basic for Reactors, Paris, October, 1966, STI/PUB/140 (IAEA, Vienna, 1967) Vol. II, p. 219.

(He 66b) E. M. Henley and L. K. Morrison, Phys. Rev. 141, 1489 (1966).

(He 67) L. Heller, Rev. Mod. Phys. 39, 584 (1967).

(He 68) A. Hemmendinger, B. C. Diven, W. K. Brown, A. Ellis, A. Furnish, E. R. Shunk, and R. R. Fullwood, Los Alamos Scientific Laboratory Report LA-3478 (1968).

(He 69) L. Heller and M. Bolsterli, private communication (1969).

(Hi 68) P. Hille, Nucl. Phys. A107, 49 (1968).

(Ho 63) P. E. Hodgson, The Optical Model of Elastic Scattering (Oxford University Press, Oxford, 1963).

(Ho 66) B. Hoop, Jr. and H. H. Barschall, Nucl. Phys. 83, 65 (1966).

(Ho 67a) B. Holmqvist, B. Gustavsson, and T. Wiedling, Arkiv Fysik 34, 481 (1967).

(Ho 67b) R. Honecker and H. Grässler, Nucl. Inst. Meth. 46, 282 (1967).

(Ho 67c) J. C. Hopkins, Los Alamos Scientific Laboratory Report LA-DC-8781 (1967).

(Ho 67d) J. C. Hopkins, Proceedings of the Symposium on Light Nuclei, Few Body Problems, and Nuclear Forces, Brela, Jugoslavia, 1967 (Gordon & Breach, New York, 1969) p. 337.

(Ho 67e) J. C. Hopkins, J. T. Martin, and J. D. Seagrave, Nucl. Inst. Meth. 56, 175 (1967).

(Ho 68a) B. Holmqvist, Arkiv för Fysik Bd 38, nr 25, 403 (1968).

(Ho 68b) J. C. Hopkins and D. M. Drake, Nucl. Phys. A107, 139 (1968).

(Ho 68c) J. C. Hopkins, D. M. Drake, and H. Condé, Nucl. Phys. A107, 139 (1968).

(Ho 68d) T. L. Houk and R. Wilson, Rev. Mod. Phys. 39, 546 (1967); and Erratum 40, 672 (1968).

(Ho 69a) W. S. Hogan and R. G. Seyler, Phys. Rev. 177, 1706 (1969).

(Ho 69b) W. S. Hogan, private communication (1969).

(Ho 69c) M. Holmberg and J. Hansén, Nucl. Phys. A129, 305 (1969).

(Ho 69d) J. C. Hopkins and G. Breit, to be published.

(Hr 69) Gy, Hrehuss and T. Czibók, Phys. Letters 28B, 585 (1969).

(Hu 53) P. Huber and D. E. Baumgartner, Helv. Phys. Acta 26, 420 (1953).

(Hu 65a) P. Huber and H. Schopper, Eds. Proceedings of the 2nd International Symposium on Polarization Phenomena of Nucleons, Karlsruhe, 1965 (Birkhäuser Verlag Basel and Stuttgart, 1966).

(Hü 65b) J. Hüfner and A. De-Shalit, Phys. Letter 15, 52 (1965).

(Je 63) C. D. Jeffries, Dynamic Nuclear Orientation (John Wiley and Sons, Inc., New York, 1963).

(Jo 67) C. H. Johnson and J. L. Fowler, Phys. Rev. 162, 890 (1967).

(Jo 68) L. W. Jones, M. J. Longo, J. R. O'Fallon, and M. N. Kreisler, Phys. Letters 27B, 328 (1968).

(Ká 68) J. Károlyi, J. Csikai, and G. Petö, Nucl. Phys. A122, 234 (1968).

(Ke 65) G. R. Keepin, Physics of Nuclear Kinetics (Addison-Wesley Pub. Co., Inc., Reading, Mass., 1965).

(Ke 69) M. P. Kellogg, private communication (1969).

(Kn 67) H. H. Knitter and M. Coppola, Zeit. Phys. 207, 56 (1967).

(Ko 67) P. F. M. Koehler, K. N. Rothe, and E. H. Thorndike, Phys. Rev. Letters 18, 933 (1967).

(Ko 68) P. F. M. Koehler, K. N. Rothe, and E. H. Thorndike, Phys. Rev. 168, 1536 (1968).

(Ku 61) A. F. Kuckes, R. Wilson, and P. F. Cooper, Ann. Phys. 15, 193 (1961).

(Ku 64) P. Kulišić, V. Ajdačić, N. Cindro, B. Lalović, and P. Strohal, Nucl. Phys. 54, 17 (1964).

(Ku 68) F. T. Kuchnir, A. J. Elwyn, J. E. Monahan, A. Lagsdorf, Jr., and F. P. Mooring, Phys. Rev. 176, 1405 (1968).

(La 54) J. M. B. Lang and K. J. LeCouteur, Proc. Phys. Soc. (London) A67, 586 (1954).

(La 60) R. R. Larsen, Nuovo Cimento, X 18, 1039 (1960).

(La 62) R. O. Lane and W. F. Miller, Nucl. Inst. Meth. 16, 1 (1962).

(La 64a) R. O. Lane, A. J. Elwyn, and A. Langsdorf, Jr., Phys. Rev. 136, B1710 (1964).

(La 64b) R. O. Lane, A. J. Elwyn, and A. Langsdorf, Jr., Phys. Rev. 133, B409 (1964).

(La 67) A. Langsford, P. H. Bowen, G. C. Cox, P. E. Dolley, R. A. J. Riddle, and M. J. M. Saltmarsh, Nucl. Phys. A99, 246 (1967).

(La 69a) R. O. Lane, private communication (1969).

(La 69b) R. O. Lane, R. D. Koshel, and J. E. Monahan, to be published; and private communication via R. O. Lane (1969).

(La 69c) R. O. Lane, J. E. Simmons, and J. C. Hopkins, unpublished (1969).

(Le 57a) I. I. Levintov, A. V. Miller, and V. N. Shamshev, Sov. Phys. JETP 5, 258 (1957).

(Le 57b) I. I. Levintov, A. V. Miller, E. Z. Tarumov, and V. N. Shamshev, Nucl. Phys. 3, 237 (1957).

(Le 67) J. L. Leroy, Nuclear Standards for Neutron Measurements, Brussels, 1967, IAEA Report 107.

(Le 69) J. S. Levin, M. P. Kellogg, R. B. Perkins, and E. T. Ritter, Conference on Computer Systems in Experimental Nuclear Physics, Skytop, Pa., March, 1969 (Proceedings to be published).

(Li 65) H. Liskien and A. Paulsen, Nucl. Phys. 63, 393 (1965).

(Li 67) R. H. Lindsay and J. J. Veit, Phys. Rev. 157, 933 (1967).

(Li 69a) H. Liskien, G. Nastri, and A. Paulsen, Efficiency Calculations for a Recoil Proton Counter with Collimator, to be published (1969).

(Li 69b) H. Liskien and A. Paulsen, Nucl. Inst. Meth. 69, 70 (1969).

(Lu 68) S. Lulić, P. Strohal, B. Antolković, and G. Paić, Nucl. Phys. A119, 517 (1968).

(Ly 68) J. E. Lynn, "Structure in Sub-Threshold Fission Modes," AERE Report R-5891 (1968).

(Ma 63) T. H. May, R. L. Walter, and H. H. Barschall, Nucl. Phys. 45, 17 (1963).

(Ma 65) F. Manero, Nucl. Phys. 65, 419 (1965).

(Ma 66a) J. J. Malanify, P. J. Bendt, T. R. Roberts, and J. E. Simmons, Phys. Rev. Letters 17, 481 (1966); and J. E. Simmons, private communication.

(Ma 66b) J. B. Marion, Rev. Mod. Phys. 38, 660 (1966).

(Ma 67) S. C. Mathur, P. S. Buchanan, and I. L. Morgan, Phys. Rev. 160, 816 (1967).

(Ma 68a) M. H. MacGregor, R. A. Arndt, and R. M. Wright, UCRL-71279 (1968); and Phys. Rev. 179, 1624 (1969).

(Ma 68b) M. H. MacGregor, R. A. Arndt, and R. M. Wright, Phys. Rev. 173, 1272 (1968).

(Ma 68c) E. Magneco, and J. Theobald, Nucl. Phys. A112, 602 (1968).

(Ma 68d) H. Marshak, A. Langsford, C. Y. Wong, and T. Tamura, Phys. Rev. Letters 20, 554 (1968).

(Ma 68e) J. Martin, D. T. Stewart, and W. M. Currie, Nucl. Phys. A113 564 (1968).

(Ma 69a) M. Maruyama, Nucl. Phys., in press (1969).

(Ma 69b) S. C. Mathur, P. S. Buchanan, and I. L. Morgan, Phys. Rev., to be published (1969).

(Mc 67) K. W. McVoy, Ann. of Phys. 43, 91 (1967).

(Mc 68) J. S. McCarthy, T. R. Fisher, E. G. Shelley, R. S. Safrata, and D. Healey, Phys. Rev. Letters 20, 502 (1968).

(Me 66a) D. F. Measday, Nucl. Inst. Meth. 40, 213 (1966); Phys. Letters 21, 66 (1966).

(Me 66b) D. F. Measday and J. N. Palmieri, Nucl. Phys. 85, 142 (1966).

(Mi 68a) A. Michaudon, Proceedings of Washington, D. C. Conference on Neutron Cross Section and Technology, 1968, D. T. Goldman, Ed. (NBS Special Pub. 299) p. 427.

(Mi 68b) D. Miljanić, G. Paić, B. Antolković, and P. Tomaš, Nucl. Phys. A106, 401 (1968).

(Mi 68c) D. Miljanić, M. Furić, and V. Valković, Nucl. Phys. A119, 379 (1968).

(Mi 69) T. G. Miller and J. A. Biggerstaff, Nucl. Phys. A124, 637 (1969).

(Mo 52) R. C. Mobley, Phys. Rev. 88, 360 (1952).

(Mo 63) M. J. Moravcsik, The Two-Nucleon Interaction (Clarendon Press, Oxford, 1963) p. 9.

(Mo 64a) P. A. Moldauer, C. A. Engelbrecht, and G. J. Duffy, Argonne National Laboratory Report No. 6978 (1964) unpublished.

(Mo 64b) J. E. Monahan and A. J. Elwyn, Phys. Rev. 136, B1678 (1964).

(Mo 64c) M. J. Moravcsik, Phys. Rev. 136, B624 (1964).

(Mo 67) J. E. Monahan and A. J. Elwyn, Phys. Rev. 153, 1148 (1967).

(Mo 68a) J. Monahan and A. Elwyn, Phys. Rev. Letters 20, 1119 (1968).

(Mo 68b) G. L. Morgan and R. L. Walter, Phys. Rev. 168, 1114 (1968).

(Mo 69) I. L. Morgan, private communication (1969).

(Mu 63) C. O. Muehlhause, Paper I-3, "International Conference on Nuclear Physics with Reactor Neutrons" (Oct 15-17, 1963) p. 21, ANL-6797; and private communication.

(Ne 54) V. A. Nedzel, Phys. Rev. 94, 174 (1954).

(Ne 60a) H. C. Newns, Proc. Phys. Soc. 76, 489 (1960).

(Ne 60b) H. W. Newson and J. H. Gibbons, Fast Neutron Physics, J. B. Marion and J. L. Fowler, Eds. (Interscience Publishers, New York, 1960) Part II, Ch. VL.

(Ni 63) T. Niewodniczanski and M. P. Steiger, Proceedings of the Conference on Direct Interactions and Nuclear Reaction Mechanisms, Padua, 1962 (Gordon & Breach, New York, 1963) p. 828.

(Ni 66) D. B. Nichols, B. D. Kern, and M. T. McEllistrem, Phys. Rev. 151, 879 (1966).

(Ni 68) D. B. Nichols and M. T. McEllistrem, Phys. Rev. 166, 1074 (1968).

(No 63) H. P. Noyes, Phys. Rev. 130, 2025 (1963).

(No 65) H. P. Noyes, Nucl. Phys. 74, 508 (1965).

(No 68a) H. P. Noyes, SLAC-PUB-409 (1968).

(No 68b) H. P. Noyes, private communication (1968).

(Og 68) K. O. Oganesyan, Sov. Phys. JETP 27, 679 (1968).

(Or 68) V. J. Orphan, A. D. Carlson, and C. G. Hoot, Proceedings of Conference on Neutron Cross Sections and Technology, Washington, D. C., 1968 (NBS Pub. 299, Sept. 1968) p. 139.

(Or 69) V. J. Orphan, C. G. Hoot, A. D. Carlson, J. John, and J. R. Beyster, Nucl. Inst. Meth. 72, 254 (1969).

(Ow 68) R. O. Owens, and J. H. Towle, Nucl. Phys. A112, 337 (1968).

(Pa 58) P. J. Pasma, Nucl. Phys. 6, 141 (1958).

(Pa 61) J. B. Parker, J. H. Towle, D. Sams, and P. G. Jones, Nucl. Inst. Meth. 14, 1 (1961).

(Pa 64a) G. Pappalardo, Phys. Letters 13, 320 (1964).

(Pa 64b) J. B. Parker, J. H. Towle, D. Sams, W. B. Gilboy, A. D. Purnell, and H. J. Stevens, Nucl. Inst. Meth. 30, 77 (1964).

(Pa 66) Proceedings of the Paris Conference on Nuclear Data for Reactors, 1966 (IAEA, Vienna, 1967).

(Pa 67) G. Paić, D. Rendić, and P. Tomaš, Nucl. Phys. A96, 476 (1967).

(Pa 69) A. Paulsen and H. Liskien, Phys. Letters 29B, 562 (1969).

(Pe 61) R. B. Perkins and J. E. Simmons, Phys. Rev. 124, 1153 (1961).

(Pe 62a) F. Perey and B. Buck, Nucl. Phys. 32, 353 (1962).

(Pe 62b) J. M. Peterson, Phys. Rev. 125, 955 (1962).

(Pe 64) R. B. Perkins and C. Glashausser, Nucl. Phys. 60, 433 (1964).

(Pe 68) F. G. Perey, private communication (1968).

(Pe 69a) F. G. Perey, WASH-1127 (1969) Reports to the NCSAC.

(Pe 69b) C. Perrin, J. C. Gondrand, M. Durand, S. Desreumaux, and R. Bouchez, International Conference on the Three-Body Problem in Nuclear and Particle Physics, Birmingham, July 1969 (to be published by North Holland).

(Ph 67) G. C. Phillips, Proceedings of the Symposium on Light Nuclei, Few Body Problems, and Nuclear Forces, Brela, Jugoslavia, 1967 (Gordon & Breach, New York, 1969) p. 887.

(Po 56) C. E. Porter and R. G. Thomas, Phys. Rev. 104, 483 (1956).

(Re 67a) J. D. Reber and J. D. Brandenberger, Phys. Rev. 163, 1077 (1967).

(Re 67b) D. Rendić, Nucl. Phys. A91, 604 (1967).

(Re 67c) D. Rendić, Proceedings of the Symposium on Light Nuclei, Few-Body Problems, and Nuclear Forces, Brela, Jugoslavia, 1967 (Gordon and Breach, New York, 1968) p. 485.

(Re 68a) D. Rendić, B. Antolković, G. Paić, M. Turk, and P. Tomaš, Nucl. Phys. A117, 113 (1968).

(Re 68b) J. T. Reynolds, C. J. Slavik, C. R. Lubitz, and N. C. Francis, Phys. Rev. 176, 1213 (1968).

(Ri 62) M. E. Rickey, and R. Smythe, Nucl. Inst. Meth. 18, 67 (1962).

(Ri 65) R. A. J. Riddle, A. Langsford, P. H. Bowen, and G. C. Cox, Nucl. Phys. 61, 457 (1965).

(Ro 59) L. S. Rodberg, Nucl. Phys. 15, 72 (1959).

(Ro 64) M. L. Roush, M. A. Wilson, and W. F. Hornyak, Nucl. Inst. Meth. 31, 112 (1964).

(Ro 65a) L. Rosen, Proceedings of the International Conference on the Study of Nuclear Structure with Neutrons, Antwerp (july 19-23, 1965) p. 379.

(Ro 65b) L. Rosen, J. G. Beery, A. S. Goldhaber, and E. H. Auerbach, Ann. Phys. (New York) 34, 96 (1965).

(Ro 66) L. Rosen, Phys. Today 19, 21 (1966).

(Ro 69a) L. Rosen, Science J. 5A, 39 (1969).

(Ro 69b) L. N. Rothenberg, Bull. Am. Phys. Soc. 14, 511 (1969).

(Sa 53) G. R. Satchler, Proc. Phys. Soc. (London) A66, 1081 (1953).

(Sa 54) G. R. Satchler, Phys. Rev. 94, 1304 (1954).

(Sa 56a) J. T. Sample, Can. J. Phys. 34, 36 (1956).

(Sa 56b) G. R. Satchler, Phys. Rev. 104, 1198 (1956).

(Sa 58) G. R. Satchler, Phys. Rev. 111, 1747 (E) (1958).

(Sa 68) J. R. Sawers, Jr., G. L. Morgan, L. A. Schaller, and R. L. Walter, Phys. Rev. 168, 1102 (1968).

(Sc 48) J. Schwinger, Phys. Rev. 73, 407 (1948).

(Sc 63) J. P. Scanlon, G. H. Stafford, J. J. Thresher, and P. H. Bowen, Nucl. Phys. 41, 401 (1963).

(Sc 68) R. B. Schwartz, R. A. Schrack, and H. T. Heaton, II, Proceedings of Conference on Neutron Cross Sections and Technology, Washington, D. C., 1968, D. T. Goldman, Ed. (NBS Special Pub. 299, 1968) p. 771.

(Sc 69) R. B. Schwartz, R. A. Schrack, and H. T. Heaton, II., Phys. Letters 30B, 36 (1969).

(Se 64a) J. D. Seagrave, J. E. Brolley, and J. G. Beery, Rev. Sci. Instr. 35, 1290 (1964).

(Se 64b) K. K. Seth, R. M. Wilenzick, and T. A. Griffy, Phys. Letters 11, 308 (1964).

(Se 65) K. K. Seth, Phys. Letters 16, 306 (1965).

(Se 66) K. Seth, Nucl. Data 2A, 299 (1966).

(Se 67) J. D. Seagrave, Proceedings of the Symposium on Light Nuclei, Few-Body Problems, and Nuclear Forces, Brela, Jugoslavia, 1967 (Gordon and Breach, New York, 1968) p. 485.

(Se 69a) J. D. Seagrave, Proceedings of the Conference on the Three-Body Problem in Nuclear and Particle Physics, Birmingham, July, 1969 (North Holland, Amsterdam) to be published.

(Se 69b) J. D. Seagrave, private communication (1969).

(Sh 63) E. Sheldon, Rev. Mod. Phys. 35, 795 (1963).

(Sh 65) F. L. Shapiro, International Conference on the Study of Nuclear Structure with Neutrons, Antwerp, July 19-23, 1965 (North Holland, Amsterdam, 1966) p. 223.

(Sh 66) E. Sheldon and D. M. van Patter, Rev. Mod. Phys. 38, 143 (1966).

(Sh 69) E. F. Shrader, WASH-1127 (1969) Reports to the NCSAC.

(Si 66) P. P. Singh, P. Hoffman-Pinther, and D. W. Lang, Phys. Letters 23, 255 (1966).

(Si 68) J. E. Simmons, "Some Physics Uses of LAMPF," 1968 Summer Study Group at Los Alamos Scientific Laboratory, LA-4089 (1968) p. 33.

(Si 69) J. E. Simmons, private communication (1969).

(Sl 67a) Ivo Šlaus, Rev. Mod. Phys. 39, 575 (1967).

(Sl 67b) I. Šlaus and G. Paić, Conference on Solid State Physics, Nuclear Physics, and Particle Physics, Santiago, 1967 (W. A. Benjamin, Inc., New York, 1968) p. 473.

(Sl 68) R. J. Slobodrian, Phys. Rev. Letters 21, 438 (1968).

(Sm 67) A. B. Smith, P. Guenther, R. Larsen, C. Nelson, P. Walker, and J. F. Whalen, Nucl. Inst. Meth. 50, 277 (1967).

(Sm 68) A. B. Smith, P. T. Guenther, and J. F. Whalen, Phys. Rev. 168, 1344 (1968).

(Sm 69) A. B. Smith, J. F. Whalen, and K. Takeuchi, to be published (1969).

(St 62) P. Strohal, N. Cindro, and B. Eman, Nucl. Phys. 30, 49 (1962).

(St 65) L. Stewart, Los Alamos Scientific Laboratory Report LA-3270 (1965).

(St 67) V. M. Strutinsky, Nucl. Phys. A95, 420 (1967).

(St 68) V. M. Strutinsky and S. Bjørnholm, International Symposium on Nuclear Structure, Dubna, July 4-11, 1968 (IAEA, Vienna, 1968) p. 431.

(Ta 68) S. Tanaka, K. Tsukada, M. Maruyama, and Y. Tomita, JAERI Memo 2949 (1968); and K. Tsukada, private communication.

(Th 59) R. M. Thaler, Phys. Rev. 114, 827 (1959).

(Th 63) D. B. Thomson, Phys. Rev. 129, 1649 (1963).

(Th 64a) T. D. Thomas, Nucl. Phys. 53, 558 (1964).

(Th 64b) T. D. Thomas, Nucl. Phys. 53, 577 (1964).

(Th 67) E. H. Thorndike, Rev. Mod. Phys. 39, 513 (1967).

(Th 68) A. R. Thomas, D. Spalding, and E. H. Thorndike, Phys. Rev. 167, 1240 (1968).

(To 62) J. H. Towle and W. B. Gilboy, Nucl. Phys. 32, 610 (1962).

(Tr 59) C. C. Trail and S. Raboy, Rev. Sci. Instr. 30, 425 (1959).

(Tr 68) G. E. Tripard, L. F. C. Monier, B. L. White, and P. W. Martin, Nucl. Inst. Meth. 66, 261 (1968).

(Ts 64) K. Tsukada and T. J. Lee, Phys. Letters 11, 141 (1964).

(Ts 66) K. Tsukada, S. Tanaka, M. Maruyama, and Y. Tomita, Nucl. Phys. 78, 369 (1966).

(Ts 69) K. Tsukada, S. Tanaka, Y. Tomita, and M. Maruyama, Nucl. Phys. A125, 641 (1969).

(Tu 68) W. E. Tucker, Texas Nuclear Corporation (Austin, Texas) Annual Progress Report ORO-2791-27 (1968).

(Tu 69) W. E. Tucker, private communication (1969).

(Va 60) R. Vandenbosch and J. R. Huizenga, Phys. Rev. 120, 1313 (1960).

(Va 67a) V. Valković, I. Šlaus, P. Tomaš, and M. Cerineo, Nucl. Phys. A98, 305 (1967).

(Va 67b) W. T. H. van Oers and K. W. Brockman, Nucl. Phys. A92, 561 (1967).

(Va 67c) W. T. H. van Oers and I. Slaus, Phys. Rev. 160, 853 (1967).

(Ve 69) D. E. Velkley, K. C. Chung, A. Mittler, J. D. Brandenberger, and M. T. McEllistrem, Phys. Rev. 179, 1090 (1969).

(Vi 69) Vienna Conference on Physics and Chemistry of Fission, July, 1969 (IAEA Program SM-122) to be published.

(Vo 56) R. G. P. Voss and R. Wilson, Phil. Mag. 1, 175 (1956).

(Vo 64) H. K. Vonach, R. Vandenbosch, and J. R. Huizenga, Nucl. Phys. 60, 70 (1964).

(Vo 68) E. Vogt, Advances in Nuclear Physics, Ed. by Michael Baranger and Erich Vogt (Plenum Press, New York, 1968) Vol. 1, p. 261.

(Vo 69) V. A. Voitenko, G. A. Prokopets, V. I. Strizhak, I. Fiz. (Sov. J. Nucl. Phys.) 9, 9 (1969).

(Wa 62) R. L. Walter, W. Benenson, P. S. Dubbeldam, and T. H. May, Nucl. Phys. 30, 292 (1962).

(Wa 65a) R. Wagner, P. D. Miller, T. Tamura, and H. Marshak, Phys. Rev. 139, B29 (1965).

(Wa 65b) M. Walt and D. B. Fossan, Phys. Rev. 137, B629 (1965).

(Wa 68) Proceedings of Washington, D. C. Conference on Neutron Cross Section and Technology, 1968, D. T. Goldman, Ed. (NBS Special Pub. 299).

(We 65) B. E. Wenzel and M. F. Stener, Phys. Rev. 137, B80 (1965).

(Wh 66) J. F. Whalen, R. Roge, and A. B. Smith, Nucl. Inst. Meth. 39, 185 (1966).

(Wi 55a) R. W. Williams, Phys. Rev. 98, 1387 (1955).

(Wi 55b) R. W. Williams, Phys. Rev. 98, 1393 (1955).

(Wi 61) W. E. Wilson, R. L. Walter, and D. B. Fossan, Nucl. Phys. 27, 421 (1961).

(Wi 62) C. E. Wiegand, T. Elioff, W. B. Johnson, L. B. Auerbach, J. Lach, and T. Ypsilantis, Rev. Sci. Instr. 33, 526 (1962).

(Wi 63) R. Wilson, The Nucleon-Nucleon Interaction (Interscience, Wiley and Sons, New York, 1963) p. 44.

(Wi 65) R. M. Wilenzick, K. K. Seth, P. R. Bevington, and H. W. Lewis, Nucl. Phys. 62, 511 (1965).

(Wo 54) R. D. Woods and D. S. Saxon, Phys. Rev. 92, 577 (1954).

(Wo 56) L. Wolfenstein, Ann. Rev. Nucl. Sci. 6, 43 (1956).

(Wr 68) S. C. Wright, D. Shawn, L. Pondrom, S. Olsen, and R. Handler, Phys. Rev. 175, 1704 (1968).

(Wu 62) T. Wu and T. Ohmura, Quantum Theory of Scattering (Prentice-Hall, Englewood Cliffs, N. J., 1962).